

THE ELECTRONIC SPECTRA OF THE OXALYL HALIDES

THE ELECTRONIC SPECTRA
OF THE OXALYL HALIDES

by

WALTER JOSEPH BALFOUR, B.Sc.

A Thesis

Submitted to the Faculty of Graduate Studies
in Partial Fulfillment of the Requirements
for the Degree
Doctor of Philosophy

McMaster University

September 1967

DOCTOR OF PHILOSOPHY (1967)
(Chemistry)

McMASTER UNIVERSITY
Hamilton, Ontario

TITLE: The Electronic Spectra of the Oxalyl Halides.

AUTHOR: Walter Joseph Balfour, B.Sc. (Aberdeen University),

SUPERVISOR: Dr. G. W. King

NUMBER OF PAGES: xiii;210;a.22

SCOPE AND CONTENTS:

The near-ultraviolet vapour-phase absorption spectra of oxalyl fluoride, oxalyl chloride and oxalyl bromide have been investigated under low, medium and high resolution. Two discrete spectral systems have been observed for each of these molecules. The transitions responsible for the electronic spectra have been identified as singlet-singlet and singlet-triplet transitions associated with $n \rightarrow \pi^*$ orbital electron promotion. The vibrational and rotational structures accompanying these transitions have been analyzed and are in general agreement with theoretical predictions. The molecules remain planar and trans in their excited states.

DEDICATION

To my Mother, whose love and self-sacrifice have made this possible.

ACKNOWLEDGEMENTS

I wish to express my sincere thanks to Dr. G. W. King for his continued advice and encouragement throughout the course of this research and thesis preparation.

I am indebted to the following persons: my research colleagues Dr. J. L. Hencher, Dr. V. A. Job, Mr. K. G. Kidd, Mrs. H. E. Lock, Mr. J. O. P. McBride, Dr. D. C. Moule, Dr. A. W. Richardson, Mr. S. P. So, Mr. K. I. Srikameswaran and Mr. C. H. Warren for experimental and theoretical assistance; Dr. J. E. Parkin and Dr. D. J. Kenworthy for advice in computing; and Drs. M. Adelhelm, F. A. Miller and R. E. Kagarise for the communication of results prior to publication.

Thanks are also due to Mrs. J. Stewart whose skill in typing the manuscript at short notice has been most valuable.

Finally, this research was made possible through generous financial assistance from Canadian Industries Limited (1963-64) and the National Research Council of Canada (1964-67).

TABLE OF CONTENTS

| | Page |
|--|------|
| <u>CHAPTER 1</u> | |
| Introduction | 1 |
| <u>CHAPTER 2</u> | |
| Experimental | 20 |
| <u>CHAPTER 3</u> | |
| Theory of Electronic Spectra | 33 |
| <u>CHAPTER 4</u> | |
| Theory of Electronic-Vibrational Spectra | 67 |
| <u>CHAPTER 5</u> | |
| Vibrational Analyses of the First ${}^1A_u \leftarrow$ ${}^1A_g \ n \rightarrow \pi^*$ Systems of the Oxalyl Halides | 89 |
| <u>CHAPTER 6</u> | |
| Vibrational Analyses of the First ${}^3A_u \leftarrow {}^1A_g \ n \rightarrow \pi^*$ Systems of the Oxalyl Halides | 144 |
| <u>CHAPTER 7</u> | |
| Rotational Band Envelopes for Asymmetric Molecules | 182 |
| <u>CHAPTER 8</u> | |
| Conclusions | 202 |

Page

| | |
|-------------------------------|-----|
| <u>BIBLIOGRAPHY</u> | 204 |
| <u>APPENDIX</u> | 210 |

LIST OF TABLES

| | Page | |
|-----------|--|----|
| Table 1.1 | Molecular Parameters for some Acetyl Compounds | 12 |
| 1.2 | Molecular Parameters for the Oxalyl Halides | 14 |
| 1.3 | Van der Waals' Radii | 19 |
| 3.1 | The Character Table for the Point Group C_{2h} | 36 |
| 3.2 | The Character Table for the Point Group C_{2v} | 36 |
| 3.3 | The Character Table for the Point Group C_s | 37 |
| 3.4 | The Character Table for the Point Group C_2 | 37 |
| 3.5 | Direct Product Table for the Point Group C_s | 37 |
| 3.6 | Direct Product Table for the Point Group C_{2h} | 38 |
| 3.7 | Correlation of Symmetry Species for the Point Groups C_{2h} and C_s . . . | 38 |
| 3.8 | Expected Low-lying Transitions for (COX) ₂ Molecules | 49 |

| | | |
|-----------|---|----|
| Table 3.9 | (n, π^*) Singlet Triplet Energy Separation in Carbonyl Compounds . | 49 |
| 3.10 | Oscillator Strengths for some $n \rightarrow \pi^*$ Transitions in Carbonyl Compounds | 54 |
| 3.11 | Origin Bands for the First n, π^* Transitions in the Oxalyl Halides | 57 |
| 3.12 | Weak, Diffuse Absorption Systems in the Near-Ultraviolet | 57 |
| 4.1 | The Ground State Fundamental Frequencies of Oxalyl Fluoride . . | 74 |
| 4.2 | The Ground State Fundamental Frequencies of Oxalyl Chloride . . | 75 |
| 4.3 | The Ground State Fundamental Frequencies of Oxalyl Chloride Fluoride | 76 |
| 4.4 | Raman Frequencies for Oxalyl Bromide | 77 |
| 4.5 | Relative Intensities of Carbonyl Progression in Oxalyl Chloride . . | 85 |
| 4.6 | Carbonyl Bond Length Changes in I ${}^1A_u \leftarrow {}^1A_g$ System of $(COCl)_2$. . | 86 |
| 4.7 | Changes in Carbonyl Bond Lengths in the I ${}^1A_u \leftarrow {}^1A_g$ Systems of Some Oxalyl Compounds | 88 |

| | Page | |
|-----------|--|-----|
| Table 5.1 | The I ${}^1A_u \leftarrow {}^1A_g$ Absorption Spectrum of $(CO^{35}Cl)_2$ | 101 |
| 5.1a | The I ${}^1A_u \leftarrow {}^1A_g$ Absorption Spectrum of $CO^{35}ClCO^{37}Cl$ | 107 |
| 5.1b | The I ${}^1A_u \leftarrow {}^1A_g$ Absorption Spectrum of $(CO^{37}Cl)_2$ | 109 |
| 5.2 | The I ${}^1A_u \leftarrow {}^1A_g$ Absorption Spectrum of Oxalyl Bromide | 115 |
| 5.3 | The I ${}^1A_u \leftarrow {}^1A_g$ Absorption Spectrum of Oxalyl Fluoride | 129 |
| 5.4 | Observed Bands in II $A_u \leftarrow A_g$ System of Oxalyl Fluoride | 133 |
| 5.5 | The I ${}^1A'' \leftarrow {}^1A'$ Absorption Spectrum of Oxalyl Chloride Fluoride | 136 |
| 5.6 | Torsional Sequences in Singlet- Singlet $n \rightarrow \pi^*$ Systems of Some Conjugated Ketones | 141 |
| 6.1 | Spin-Orbit Coupling Between Triplet and Singlet States | 146 |
| 6.2 | The I ${}^3A_u \leftarrow {}^1A_g$ Absorption Spectrum of $(CO^{35}Cl)_2$ | 153 |
| 6.2a | The I ${}^3A_u \leftarrow {}^1A_g$ Absorption Spectrum of $CO^{35}ClCO^{37}Cl$ | 157 |
| 6.2b | The I ${}^3A_u \leftarrow {}^1A_g$ Absorption Spectrum of $(CO^{37}Cl)_2$ | 159 |

| | Page |
|-----------|---|
| Table 6.3 | The I ${}^3A_u \leftarrow {}^1A_g$ Absorption Spectrum of Oxalyl Bromide 162 |
| 6.4 | The I ${}^3A_u \leftarrow {}^1A_g$ Absorption Spectrum of Oxalyl Fluoride 171 |
| 6.5 | The I ${}^3A'' \leftarrow {}^1A'$ Absorption Spectrum of Oxalyl Chloride Fluoride 175 |
| 6.6 | The a_g Vibrations of Oxalyl Bromide 179 |
| 6.7 | The a_g Vibrations of Oxalyl Chloride 179 |
| 6.8 | The a_g Vibrations of Oxalyl Fluoride 180 |
| 6.9 | The a' Vibrations of Oxalyl Chloride Fluoride 180 |
| 6.10 | Sequence Intervals in the I ${}^1A_u \leftarrow {}^1A_g$ Systems of the Oxalyl Halides . . . 181 |
| 6.11 | Sequence Intervals in the I ${}^3A_u \leftarrow {}^1A_g$ Systems of the Oxalyl Halides . . . 181 |
| 7.1 | Classification of the Levels of Submatrices 186 |
| 7.2 | Correlation between Axes (x,y,z) and the Principal Axes (a,b,c) 186 |
| 7.3 | Selection Rules for Asymmetric Rotors 191 |

LIST OF FIGURES

| | | Page |
|------------|--|------|
| Figure 1.1 | Rotational Isomers of the Oxalyl Halides | 7 |
| 1.2 | Steric Interaction in <u>Cis</u> - and <u>Trans</u> - Oxalyl Fluoride and Oxalyl Chloride Fluoride | 16 |
| 1.3 | Steric Interaction in <u>Cis</u> - and <u>Trans</u> - Oxalyl Chloride and Oxalyl Bromide | 17 |
| 1.4 | The Formal Charge Distribution in Oxalyl Chloride | 18 |
| 2.1 | Apparatus for the Preparation of the Oxalyl Fluorides | 21 |
| 2.2 | Gas Injection Apparatus for Vapour-Phase Chromatography | 24 |
| 2.3 | A Sample Gas-Chromatogram | 26 |
| 3.1 | The Symmetry Elements of the Oxalyl Dihalides | 34 |
| 3.2 | Basis Atomic Orbitals | 40 |
| 3.3 | Molecular Orbitals for the Oxalyl Halides | 44 |
| 3.4 | Near Ultraviolet Spectrum of Oxalyl Fluoride | 58 |

| | Page |
|---|------|
| Figure 3.5 | |
| Near Ultraviolet Spectrum of Oxalyl Chloride | 59 |
| 3.6 | |
| Near Ultraviolet Spectrum of Oxalyl Bromide | 60 |
| 3.7 | |
| A Schematic Representation of Predissociation in the Spectra of the Oxalyl Halides | 63 |
| 4.1 | |
| Progressions and Sequences | 80 |
| 4.2 | |
| The Franck-Condon Effect | 82 |
| 5.1 | |
| The Chlorine Vibrational Isotope Effect in the I ${}^1A_u \leftarrow {}^1A_g$ System of Oxalyl Chloride | 94 |
| 5.2 | |
| The Chlorine Vibrational Isotope Effect in the I ${}^1A_u \leftarrow {}^1A_g$ System of Oxalyl Chloride | 95 |
| 5.3 | |
| The ${}^1A_u \leftarrow {}^1A_g$ Absorption Spectrum of $(COCl)_2$ in the Region 3710- 3590 Å | 100 |
| 5.4 | |
| The ${}^1A_u \leftarrow {}^1A_g$ Absorption Spectrum of $(COBr)_2$ in the Region 3960- 3840 Å | 114 |
| 5.5 | |
| The ${}^1A_u \leftarrow {}^1A_g$ Absorption Spectrum of $(COF)_2$ in the Region 3100- 2970 Å | 120 |

| | | |
|------------|---|-------|
| Figure 5.6 | A Section of the ${}^1A'' \leftarrow {}^1A'$ Spectrum of COFCOCl under Low Resolution . . . | 134 |
| 6.1 | The Chlorine Vibrational Isotope Effect in the I ${}^3A_u \leftarrow {}^1A_g$ System of Oxalyl Chloride | 150 |
| 6.2 | The ${}^3A_u \leftarrow {}^1A_g$ Absorption Spectrum of $(\text{COCl})_2$ in the Region 4120-4000 Å | 152 |
| 6.3 | The ${}^3A_u \leftarrow {}^1A_g$ Absorption Spectrum of $(\text{COBr})_2$ in the Region 4380-4250 Å | 162a. |
| 6.4 | The ${}^3A_u \leftarrow {}^1A_g$ Absorption Spectrum of $(\text{COF})_2$ in the Region 3370-3250 Å | 170 |
| 7.1 | A-type Near-Oblate | 194 |
| 7.2 | B-type Near-Oblate | 195 |
| 7.3 | The Origin Bands of Oxalyl Fluoride | 197 |
| 7.4 | Prolate C-type Contours for Oxalyl Fluoride | 199 |
| 7.5 | O_o^o (${}^1A_u \leftarrow {}^1A_g$) Band of Oxalyl Fluoride | 200 |

CHAPTER 1
INTRODUCTION

1.1 Theoretical Introduction.

If the energy due to translation is neglected, the non-relativistic Hamiltonian operator, \mathcal{H} , for an isolated molecule, can be expressed as a sum of terms due to the kinetic and potential energies of the electrons and the kinetic and potential energies of the nuclei.

$$\mathcal{H} = -\frac{\hbar^2}{2m_e} \sum_i \nabla_i^2 - \sum_\alpha \frac{\hbar^2}{2M_\alpha} \nabla_\alpha^2 - \sum_{\alpha,i} \frac{Z_\alpha e^2}{r_{\alpha i}} + \sum_{i>j} \frac{e^2}{r_{ij}} + \sum_{\alpha>\beta} \frac{Z_\alpha Z_\beta e^2}{r_{\alpha\beta}} \quad (1.1)$$

where i, j, \dots are subscripts referring to electrons

α, β, \dots are subscripts referring to nuclei

\hbar is Planck's constant divided by 2π

e is the charge on the electron

∇^2 is the Laplacian operator

m_e and M_α are the respective masses of the electron
and nucleus α

Z_α is the atomic number of nucleus α and

r_{ab} is the distance between particles a and b .

This quantum mechanical Hamiltonian operator, \mathcal{H} , has eigenfunctions $\psi_T(r,s)$ and eigenvalues E_T which satisfy the time-independent Schrödinger wave equation

$$\mathcal{H} \psi_T(r,s) = E_T \psi_T(r,s) \quad (1.2)$$

The electronic coordinates are designated collectively by r and the nuclear coordinates by s .

Born and Oppenheimer¹ in 1927 showed that, to a good approximation, the energy of a system of electrons and nuclei is defined and measurable for each nuclear configuration even when the nuclei are in motion. Consequently we may write

$$\psi_T(r,s) = \psi_E(r,s) \psi_N(s) \quad (1.3)$$

where the ψ_E are eigenfunctions of the electronic Hamiltonian, \mathcal{H}_E .

$$\mathcal{H}_E \psi_E(r,s) = E_E \psi_E(r,s) \quad (1.4)$$

For a fixed nuclear configuration,

$$\mathcal{H}_E = -\frac{\hbar^2}{2m_e} \sum_i \nabla_i^2 - \sum_{\alpha,i} \frac{Z_\alpha e^2}{r_{\alpha i}} + \sum_{i>j} \frac{e^2}{r_{ij}} \quad (1.5)$$

We may consider the energy E_E , for this fixed position of the nuclei, to be part of the potential energy of the nuclei.

$$(\mathcal{H}_N + E_E) \psi_N(s) = E_T \psi_N(s) \quad (1.6)$$

where

$$\mathcal{H}_N = - \sum_{\alpha} \frac{\hbar^2}{2M_{\alpha}} \nabla_{\alpha}^2 + \sum_{\alpha > \beta} \frac{Z_{\alpha} Z_{\beta} e^2}{r_{\alpha\beta}} \quad (1.7)$$

Since the potential governing the motion of the nuclei is a function of the nuclear separation, it is usual to consider nuclear energies relative to the value for the nuclei at their equilibrium positions. This position corresponds to a minimum value, E_e , of the electronic energy.

$$E_T = E_e + E_N \quad (1.8)$$

The nuclear energy E_N consists of vibrational and rotational contributions. In general, interactions (e.g. Coriolis effects) between vibrations and rotations are very small and, to a good approximation, the nuclear wave function ψ_N may be expressed as a product of a vibrational and rotational wave function.

$$\psi_N(s) = \psi_V(s) \psi_R(s) \quad (1.9)$$

Thus
$$\psi_T(r,s) = \psi_e(r,s) \psi_V(s) \psi_R(s) \quad (1.10)$$

and
$$E_T = E_e + E_V + E_R \quad (1.11)$$

1.2 Interaction of Light with Matter.

Classically, an electromagnetic wave may be generated by an electric charge in motion. For a body consisting of many charges, a wave is generated if the body has a varying electric dipole moment $\vec{\mu}$.

$$\vec{\mu} = \mu_x \vec{i} + \mu_y \vec{j} + \mu_z \vec{k} \quad (1.12)$$

where $\mu_x = \sum_i e_i x_i$; $\mu_y = \sum_i e_i y_i$;

$$\mu_z = \sum_i e_i z_i \quad (1.13)$$

and x_i, y_i, z_i are the cartesian coordinates of the i^{th} charge, with respect to any axis system (x, y, z) within the molecule. \vec{i}, \vec{j} and \vec{k} are unit vectors along the x, y and z directions, respectively. Radiation may be absorbed by a molecule if the oscillating electric or magnetic field of the incident wave is able to generate an oscillating dipole of the same frequency within the molecule.

Quantum mechanically, the problem is to determine the probability of a transition between two stationary states of a molecule, under the perturbing influence of a light wave. If the initial state is described by a wave function ψ_{I}'' and the final state by a wave function ψ_{I}' then the probability of a transition between these two states can be shown² to be proportional to the square of

the transition moment \vec{R} , where

$$\vec{R} = \int \psi_{\text{T}}'^* \vec{\mu} \psi_{\text{T}}'' d\tau \quad (1.14)$$

Arguments based on the symmetry of the eigenfunctions readily indicate whether or not the integral \vec{R} is non-zero and selection rules, governing the allowed changes in quantum numbers, can be derived.

The energy difference between the lower state described by ψ_{T}'' and the upper state (ψ_{T}') gives the energy of the transition. This is usually expressed in wavenumbers.

$$\sigma (\text{cm}^{-1}) = \frac{E_{\text{T}}' - E_{\text{T}}''}{hc} \quad (1.15)$$

E_{T}' and E_{T}'' are the upper and lower state eigenvalues, respectively, h is Planck's constant and c the velocity of light in a vacuum.

1.3 Rotational, Vibrational and Electronic Spectral Transitions.

In practice, it is found that the electronic energy of a molecule is usually very much greater than the energy of vibration and the latter is, in turn, very much greater than the energy for pure rotation.

Rotational energy changes for a few very light molecules produce spectra in the far infrared but the

majority of pure rotational spectra occur in the micro-wave region, say from 0.1 cm^{-1} to 10 cm^{-1} (3000 Mc/sec. to 30,000 Mc/sec.).

The vibrations of polyatomic molecules give rise to absorption in the infrared part of the electromagnetic spectrum. Most vibrational frequencies lie between 100 cm^{-1} and $4,000 \text{ cm}^{-1}$. Each vibrational quantum state has rotational quantum states associated with it so that absorption of a quantum of vibrational energy often occurs with a simultaneous change in rotational energy, resulting in a vibration-rotation spectrum.

Electronic states are usually widely separated in energy and promotion of an electron leads to absorption of visible or ultraviolet light ($14,000 \text{ cm}^{-1}$ - $100,000 \text{ cm}^{-1}$). The electronic transition may be accompanied by both vibrational and rotational energy changes.

1.4 Historical.

The oxalyl halides belong to a group of organic molecules called α -diketones and have the molecular formula COX-COY where X and Y are both halogen atoms. The molecules studied in this thesis are oxalyl fluoride (X=Y=F), oxalyl chloride (X=Y=Cl), oxalyl bromide (X=Y=Br), and oxalyl chloride fluoride (X=F, Y=Cl).

There are three possible rotational isomers for the oxalyl halides, planar-cis, planar-trans and non-planar. (Figure 1.1.) Since the planar-trans isomer has no permanent dipole moment, it will not possess a rotational spectrum. No microwave absorption has ever been reported in the literature for these halides in the gas phase.

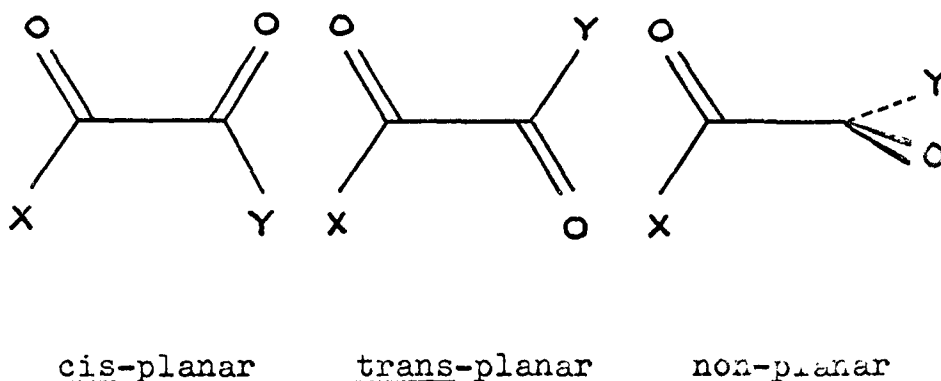


Figure 1.1. Rotational Isomers of the Oxalyl Halides.

A number of physical methods have been employed to investigate the ground state structure in an attempt to decide which form or forms are stable. Wierl³ and later LuValle⁴ examined oxalyl chloride vapour using electron diffraction. Rough estimates of bond lengths and bond angles were obtained but no definite conclusions could be drawn regarding its molecular conformation.

X-ray studies of the crystalline states of oxalyl chloride⁵ and oxalyl bromide^{5,6} revealed a centrosymmetric arrangement in both cases. (The space groups are P_{bca} for oxalyl chloride and $P_{2_1/C}$ for oxalyl bromide.). The molecules of oxalyl chloride and oxalyl bromide were shown to be trans. For oxalyl bromide the molecules were shown to be, at least, very nearly planar but there is evidence that the molecules of oxalyl chloride are not strictly planar in the crystal.

The infrared and Raman spectra of the oxalyl halides, especially oxalyl chloride, have received considerable attention⁷⁻¹⁵. In the case of oxalyl chloride two differing interpretations have been proposed, one favouring a mixture of cis- and trans-planar species, the other requiring only the trans-planar species. Bencher and King¹⁶ critically re-examined the evidence and were able to explain satisfactorily all features of both the infrared and Raman spectra of oxalyl chloride on the assumption that the molecule is planar and trans in the gas phase. Their investigation of the infrared and Raman spectra of oxalyl fluoride¹⁷ and the infrared spectrum of oxalyl chloride fluoride¹⁷ showed that these molecules are also planar and trans. Kanda et al.¹⁸ have briefly reported an analysis of the Raman spectrum of oxalyl bromide based on a trans-planar structure but

no information has appeared in the literature on the infrared spectrum of this molecule.

Both oxalyl chloride¹⁹ and oxalyl bromide²⁰ have been shown to absorb radiation in the near ultraviolet. Vibrational structure in the absorption spectrum of oxalyl chloride was first noted by Saksena and Kagarise²¹ and partial vibrational analyses were proposed by Sidman²² and by Saksena and Jauhri²³. These workers concluded, although for entirely different reasons, that a mixture of cis and trans molecules was present. Recently Kanda and coworkers¹⁸ have re-examined, under low resolution, the near ultraviolet vapour phase absorption spectra of oxalyl chloride and oxalyl bromide. They have also studied the phosphorescence spectra in cyclohexane at 90° K and conclude that these molecules are exclusively planar and trans. Photodecomposition in the spectral region of absorption in oxalyl chloride¹⁹ and oxalyl bromide²⁰ has been studied by Rollefson. Thermal decomposition has also been observed for these molecules^{24,20}.

Oxalyl chloride has been found²⁵ to possess a non-zero dipole moment in benzene solution. ($\mu_{\text{dipole}} = 0.92 \text{ D.}$). Although this value is not inconsistent with that expected for oscillation about a stable trans position, it has been suggested²⁶ that the non-zero

dipole moment is due to complex formation between oxalyl chloride and benzene. The related molecule biacetyl, $\text{CH}_3\text{COCOCH}_3$, has been shown²⁷ by infrared and Raman spectroscopy to be planar and trans. Negative results from a search for the microwave spectrum²⁸ of this molecule support the postulated structure yet a gas phase dipole moment of 1.05 D^{29} has been measured.

Thus, despite speculation to the contrary over the years, it now seems well established that the only ground state form existing in measurable quantities in the vapour phase is the planar-trans species. Since this is in complete accord with the findings presented in this thesis, we shall assume throughout that only this species is present in the gas phase.

1.5 The Ground State Geometry of the Oxalyl Halides.

The molecules glyoxal (HCOCHO), acetaldehyde (CH_3CHO) and the acetyl halides (CH_3COX) are related in chemical structure to the oxalyl halides. Accurate bond lengths and bond angles have been obtained recently for these other molecules by spectroscopic methods. However, no reliable molecular dimensions are available for the oxalyl halides. For this reason, molecular parameters were initially estimated by transferring values from the above-mentioned molecules.

Paldus and Ramsay³⁰ have analyzed the rotational structure of the (0,0) band in the $\pi^* \leftarrow n$, $\tilde{A}(^1A_u) \leftarrow \tilde{X}(^1A_g)$, system of glyoxal and its two deuterated derivatives. Although they were unable to obtain a complete solution to the structural problem they derived a very accurate value for the sum of the CO and CC bond lengths in the ground state.

$$r''_{CO} + r''_{CC} (\text{glyoxal}) = 2.73 \pm 0.01 \text{ \AA}.$$

This value is remarkably close to that observed in a microwave study of acetaldehyde³¹, where the C-CH=O group is also present.

$$r''_{CO} + r''_{CC} (\text{acetaldehyde}) = 2.716 \pm 0.007 \text{ \AA}.$$

Values for the $r''_{CO} + r''_{CC}$ distance in the oxalyl halides were taken from the microwave values reported for the corresponding acetyl halides. The relevant data for the acetyl compounds are listed in Table 1.1. The methyl carbon and the carbon of the carbonyl group are numbered 1 and 2, respectively.

A carbonyl bond length of 1.18 Å has been obtained for both acetyl fluoride and formyl fluoride³⁵ and it is reasonable to assume this same value for oxalyl fluoride. In addition, a length of 1.34 Å is reasonable for a CF bond when adjacent to a carbonyl group^{32,35,36}. The bond

Table 1.1

Molecular Parameters for some Acetyl Compounds³¹⁻³⁶.(i) CH_3CHO

$$r_{\text{C}_1\text{C}_2} = 1.2155 \pm 0.0020 \text{ \AA}$$

$$\widehat{\text{C}_1\text{C}_2\text{O}} = 123^\circ 55' \pm 6'; \quad r_{\text{C}_2\text{O}} = 1.5005 \pm 0.0050 \text{ \AA}$$

(ii) CH_3COF

$$r_{\text{C}_1\text{C}_2} = 1.181 \pm 0.01 \text{ \AA}$$

$$\widehat{\text{C}_1\text{C}_2\text{O}} = 128^\circ 21' \pm 2^\circ; \quad r_{\text{C}_2\text{O}} = 1.503 \pm 0.003 \text{ \AA}$$

$$\widehat{\text{C}_1\text{C}_2\text{F}} = 110^\circ 18' \pm 1^\circ; \quad r_{\text{C}_2\text{F}} = 1.348 \pm 0.015 \text{ \AA}$$

(iii) CH_3COCl

$$r_{\text{C}_1\text{C}_2} = 1.192 \pm 0.010 \text{ \AA}$$

$$\widehat{\text{C}_1\text{C}_2\text{O}} = 127^\circ 5' \pm 10'; \quad r_{\text{C}_2\text{O}} = 1.499 \pm 0.010 \text{ \AA}$$

$$\widehat{\text{C}_1\text{C}_2\text{Cl}} = 112^\circ 39' \pm 30'; \quad r_{\text{C}_2\text{Cl}} = 1.789 \pm 0.005 \text{ \AA}$$

angles are more difficult to estimate. Values of 123° for \widehat{CCO} and 114° for \widehat{CCCl} in oxalyl chloride are reported by Allen and Sutton⁴ and the corresponding angles in acetyl chloride are 127° and 112° . A similar fall in the \widehat{CCO} from acetaldehyde (124°) to glyoxal (121°) is observed. Since the \widehat{CCO} in acetyl fluoride is 128° a value of 125° was assumed for this angle in oxalyl fluoride. The \widehat{CCF} in acetyl fluoride is 3° less than the \widehat{CCCl} in acetyl chloride. On the assumption of a similar change of angle in the oxalyl series, a value of 111° was taken for \widehat{CCF} in oxalyl fluoride.

The parameters for oxalyl chloride and oxalyl chloride fluoride were arrived at using similar arguments while those for oxalyl bromide were taken from reference 6. The adopted geometry is given in Table 1.2.

1.6 Factors governing the Conformation of the Oxalyl Halides.

The most important single factors that restrict the freedom of rotation about the C-C bond are conjugation, steric interaction, and dipole-dipole repulsion. If the two carbonyls of the oxalyl group are coplanar, the π -electrons will be delocalized over the whole O=C-C=O system. This delocalization increases the stability of this geometry.

Table 1.2

Molecular Parameters for the Oxalyl Halides.

a) Oxalyl fluoride.

$$r_{\text{CO}} = 1.18 \text{ \AA}; \quad r_{\text{CC}} = 1.50 \text{ \AA}; \quad r_{\text{CF}} = 1.34 \text{ \AA}$$

$$\widehat{\text{CCO}} = 125^\circ; \quad \widehat{\text{CCF}} = 111^\circ$$

b) Oxalyl chloride

$$r_{\text{CO}} = 1.19 \text{ \AA}; \quad r_{\text{CC}} = 1.50 \text{ \AA}; \quad r_{\text{CCl}} = 1.78 \text{ \AA}$$

$$\widehat{\text{CCO}} = 123^\circ; \quad \widehat{\text{CCCl}} = 112^\circ$$

c) Oxalyl chloride fluoride $\text{C}_1\text{OClC}_2\text{OF}$

$$r_{\text{C}_1\text{O}} = 1.19 \text{ \AA}; \quad r_{\text{C}_2\text{O}} = 1.18 \text{ \AA}; \quad r_{\text{CC}} = 1.50 \text{ \AA}$$

$$r_{\text{CF}} = 1.34 \text{ \AA}; \quad r_{\text{CCl}} = 1.78 \text{ \AA}; \quad \widehat{\text{C}_1\text{C}_2\text{O}} = 125^\circ$$

$$\widehat{\text{C}_2\text{C}_1\text{O}} = 123^\circ; \quad \widehat{\text{CCCl}} = 112^\circ; \quad \widehat{\text{CCF}} = 111^\circ$$

d) Oxalyl bromide

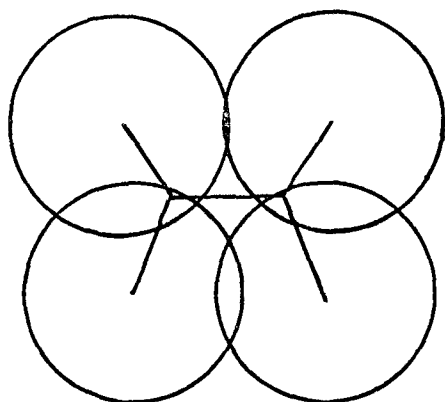
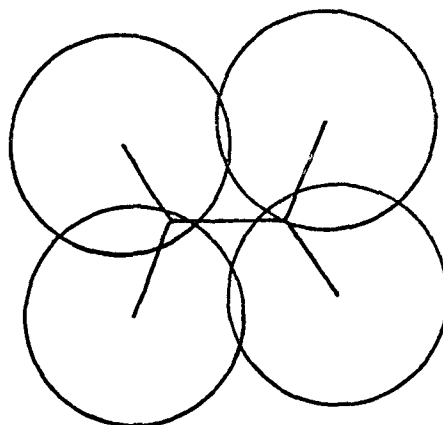
$$r_{\text{CO}} = 1.17 \text{ \AA}; \quad r_{\text{CC}} = 1.56 \text{ \AA}; \quad r_{\text{CBr}} = 1.84 \text{ \AA}$$

$$\widehat{\text{CCO}} = 122.3^\circ; \quad \widehat{\text{CCBr}} = 109.4^\circ$$

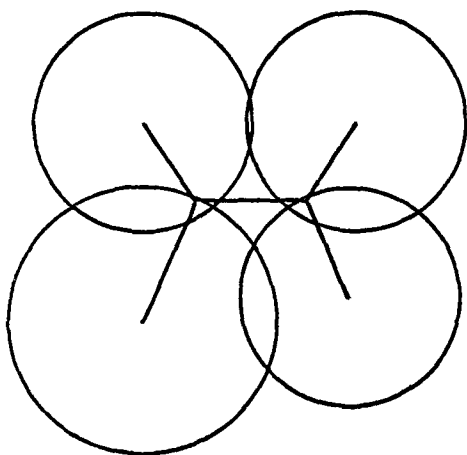
When the electron shells of the non-bonded atoms of a molecule come very close together, repulsive forces of the Van der Waals type are important. Figures 1.2 and 1.3 show scale drawings of the oxalyl halides using the Van der Waals' radii in Table 1.3 and the assumed geometry in Table 1.2.

From Figures 1.2 and 1.3 it can be seen that steric interaction is greater in the cis configuration than in the trans. The same kind of Van der Waals repulsive forces arise between pairs of electrons in different atoms or bonds within a molecule as between different molecules. These repulsive forces between bonds on adjacent atoms are expected to be greater for π -bonds than for σ -bonds. The trans structure will have less bond-bond interaction than the cis, as in the latter, the π -electrons of the C=O groups are eclipsed.

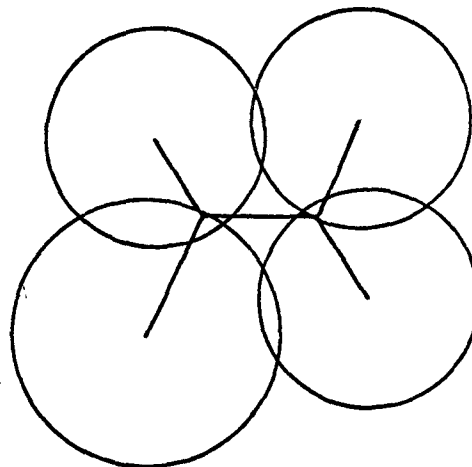
The formal charge distributions for oxalyl chloride in both cis and trans conformations have been evaluated by Soundarajan and Raman³⁸. Their calculation indicates that the C=O bond is quite polar. Dipole-dipole repulsion will be less in the trans configuration than in the cis. Figure 1.4 shows the calculated charge distribution for the trans isomer.

cis - (COF)₂TRANS - (COF)₂

0 1 2 3 Å

 A horizontal scale bar with tick marks at 0, 1, 2, and 3 Å.


cis - COFCOCl



TRANS - COFCOCl

FIGURE 1.2 STERIC INTERACTION IN CIS- AND TRANS -
OXALYL FLUORIDE AND OXALYL CHLORIDE FLUORIDE.

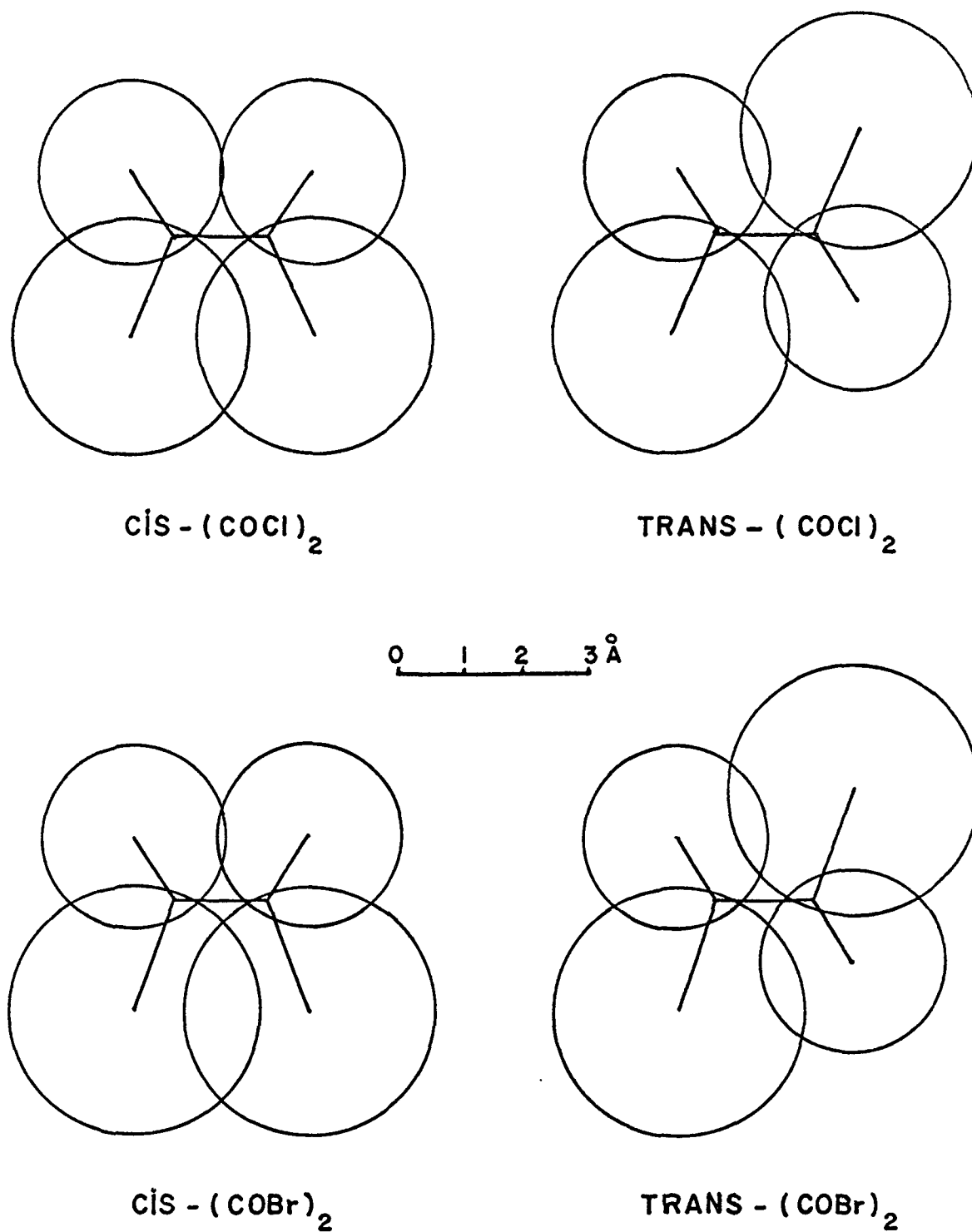


FIGURE 1.3. STERIC INTERACTION IN CIS- AND TRANS-
OXALYL CHLORIDE AND OXALYL BROMIDE.

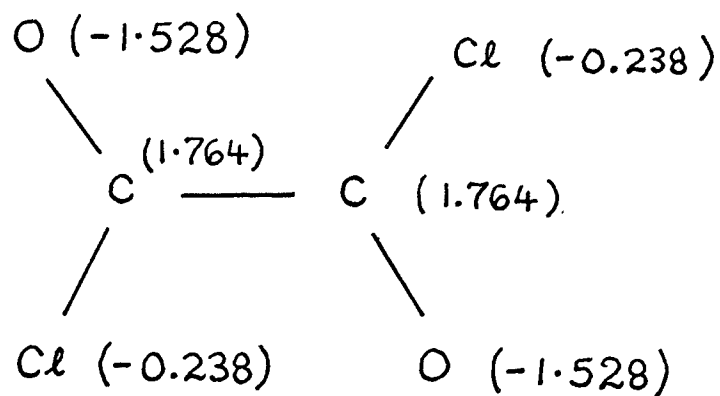


Figure 1.4. The Formal Charge Distribution
in Oxalyl Chloride.

Table 1.3
Van der Waals' Radii³⁷ (Å)

| | | | |
|-----------------|------|----|------|
| H | 1.20 | F | 1.35 |
| O | 1.40 | Cl | 1.80 |
| CH ₃ | 2.00 | Br | 1.95 |

CHAPTER 2
EXPERIMENTAL

2.1 Preparation of Oxalyl Fluoride and Oxalyl Chloride Fluoride.

Oxalyl chloride and oxalyl bromide are commercially available. Tullock and Coffman³⁹ have described a general method for the fluorination of carboxylic acid chlorides by means of a suspension of sodium fluoride in a non-aqueous, polar solvent. They obtained 60% conversion of oxalyl chloride to oxalyl fluoride by carrying out the reaction in tetramethylene sulphone (tetrahydrothiophene-1,1-dioxide) for three hours at $\sim 100^{\circ}$ C. If the reaction is allowed to proceed at room temperature, without reflux, and for longer periods of time, a small amount of oxalyl chloride fluoride is obtained in addition to the major product, oxalyl fluoride. This modified method due to Hencher⁴⁰ was used to prepare the samples of both oxalyl fluoride and oxalyl chloride fluoride. A diagram of the apparatus used for the preparation of the oxalyl fluorides is shown in Figure 2.1.

Powdered, dry sodium fluoride (52 g) was placed in a two-necked, 500 ml, round-bottomed flask and kept

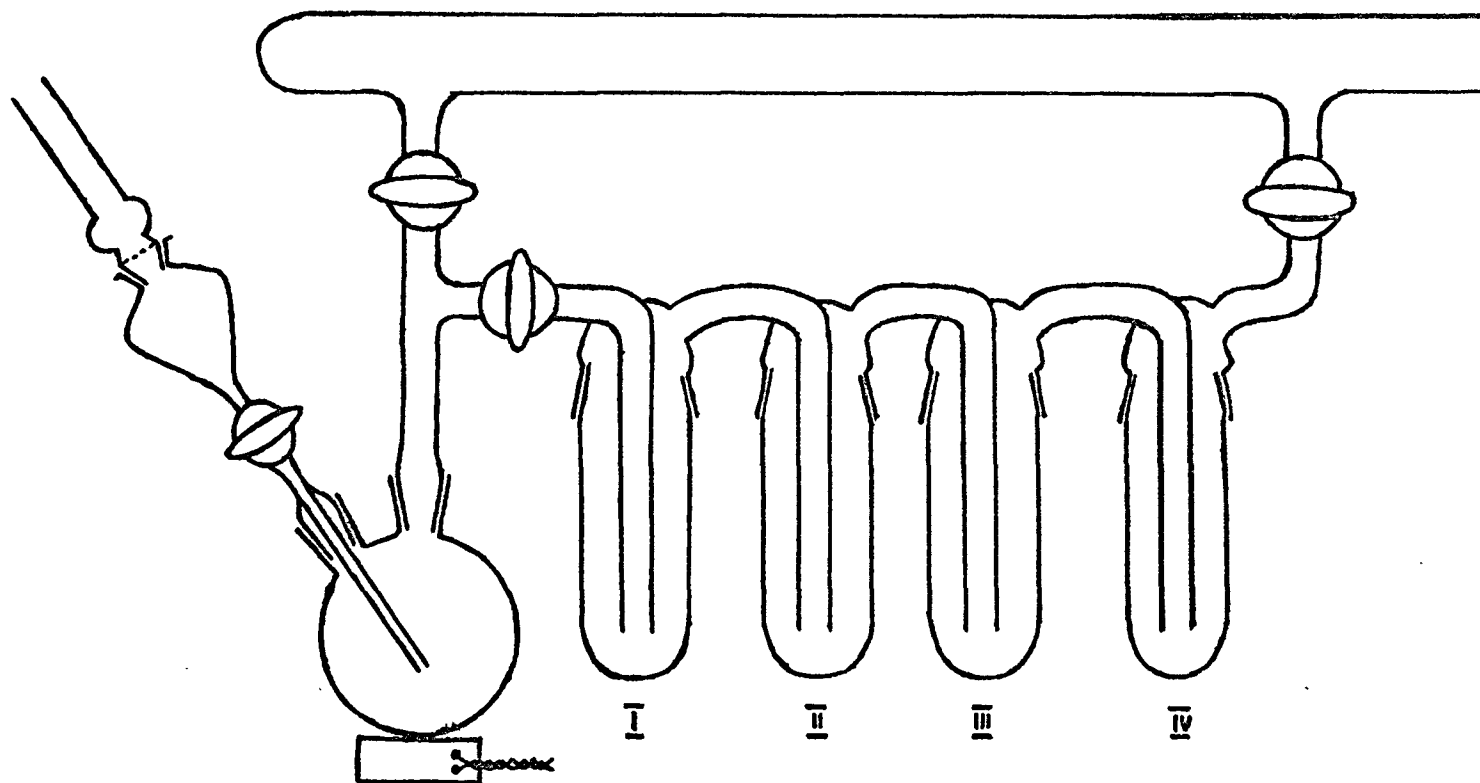


FIGURE 2.1

APPARATUS FOR THE PREPARATION
OF THE OXALYL FLUORIDES

at 200° C under vacuum overnight to remove all traces of moisture. Air was admitted through a drying tube containing anhydrous calcium sulphate. Dry tetramethylene sulphone (100 g; Matheson, Coleman and Bell), a liquid at room temperature, was added. The mixture was stirred magnetically while oxalyl chloride (21 ml) was added through a dropping funnel fitted with a drying tube. The oxalyl chloride was introduced dropwise, so that the reaction vessel never showed any appreciable rise in temperature during the addition.

The reaction was allowed to proceed for about twelve hours at atmospheric pressure then Dewar flasks containing a mixture of dry ice and acetone (-78° C) were placed round traps I and II and Dewars with liquid nitrogen (-196° C) round traps III and IV. The volatile products were pumped off slowly through the traps and collected. The oxalyl fluorides together with some unreacted oxalyl chloride were trapped out in I and II while the more volatile decomposition products such as carbon monoxide, carbon dioxide, and carbonyl fluoride were trapped out in III and IV. Finally, the reaction vessel was heated with a hot-air blower to about 60° C to drive over any remaining products.

The Dewar flasks were taken away from traps III and IV and the contents of these traps discarded. Most

of the oxalyl chloride (b.p. 64° C) was removed by trap-to-trap distillation before the desired products, oxalyl chloride fluoride (b.p. 25° C) and oxalyl fluoride (b.p. 1° C) were distilled, under vacuum, into a storage tube.

2.2 Purification of the Oxalyl Fluorides.

The mixture of oxalyl fluoride and oxalyl chloride fluoride, containing some oxalyl chloride, was separated by vapour-phase chromatography. A Perkin-Elmer model 154 vapour fractometer was used with a bypass device which allowed only a small fraction of the sample to pass through the detector.

The apparatus employed to inject samples into the fractometer is shown in Figure 2.2. The pressure stopcocks A, B, C and D were capable of withstanding internal pressures of three to four atmospheres. A and B were two-way stopcocks such that in one position the carrier gas could bypass the sample in E (---->) while in the other position the carrier has swept out the sample from E.

The storage tube containing the crude products from the preparation was attached with tygon tubing to the limb at stopcock C and a vacuum pump was connected at D. Dry nitrogen was used as carrier gas at a pressure such that the column reading was 13 p.s.i. To ensure a

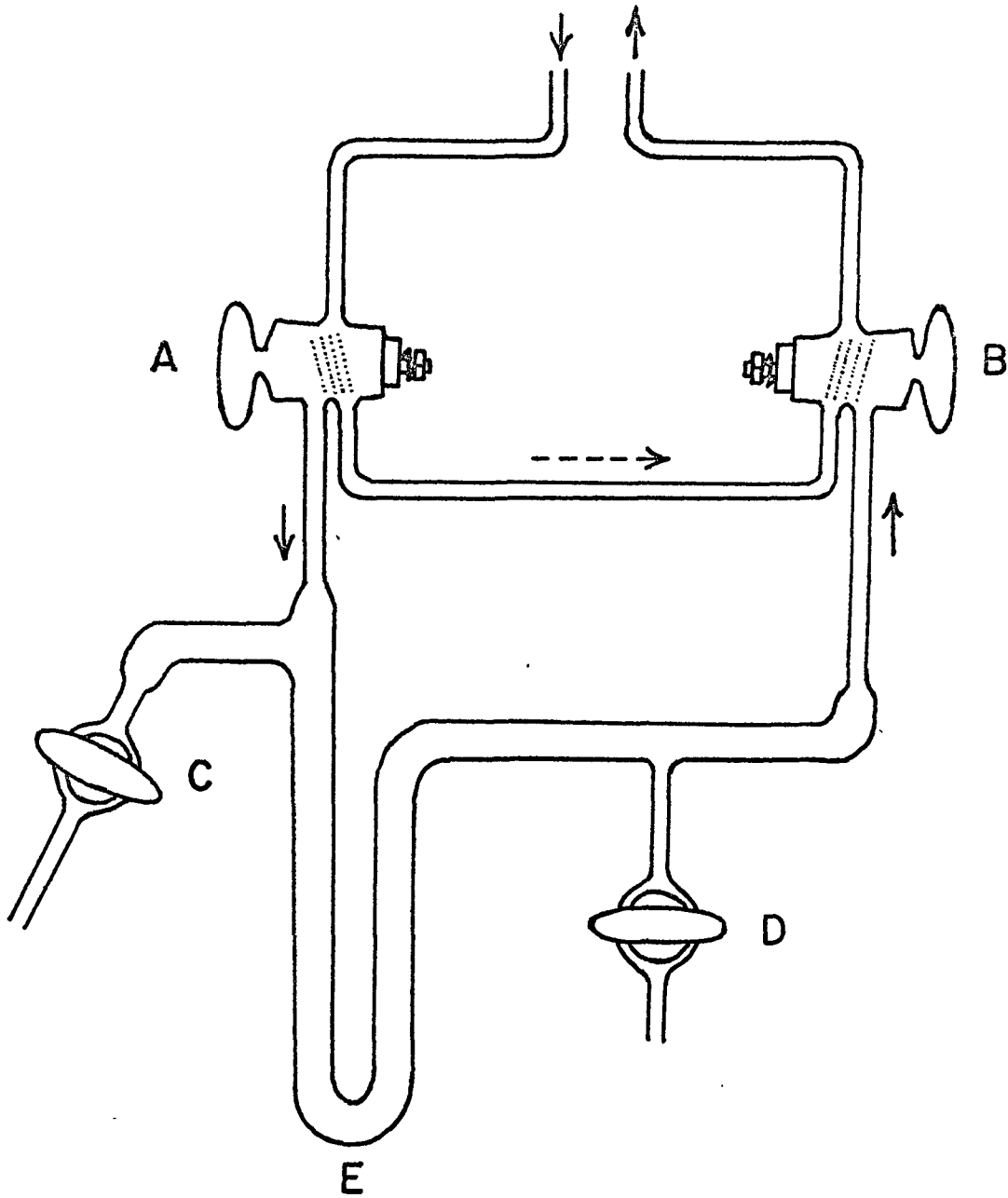


FIGURE 2.2 GAS INJECTION APPARATUS FOR VAPOUR - PHASE CHROMATOGRAPHY

clean separation of the components of the mixture, the carrier gas was allowed to sweep out the sample from tube E for just twenty seconds.

A column two metres long and 2 cm in diameter was used at room temperature. The column packing was prepared by mixing dry Chromasorb P (Johns-Manville 30/60 mesh) with a saturated solution of fluorolube grease (40% by weight of packing) in sodium-dried ether. The ether was stripped off on a rotary evaporator and the packing spread out thinly and evenly on a glass tray. The tray and contents were heated for four hours at 110° C in an oven.

With maximum flow rate, the oxalyl fluoride fraction passed the detector from ~3 to ~6 minutes after initial injection and the oxalyl chloride fluoride fraction from ~9 to ~14 minutes after injection. The oxalyl chloride took over twenty minutes to pass through the column and gave a weak, broad peak. A sample chromatogram is shown in Figure 2.3.

The oxalyl halides, especially oxalyl chloride, readily attack most vacuum lubricants¹⁹. The stopcocks used here were greased with fluorolube. All stopcocks had to be freshly greased every three or four days to prevent "freezing".

Sensitivity :

x 64 for 0 to 9 min.

x 8 for 9 to 18 min.

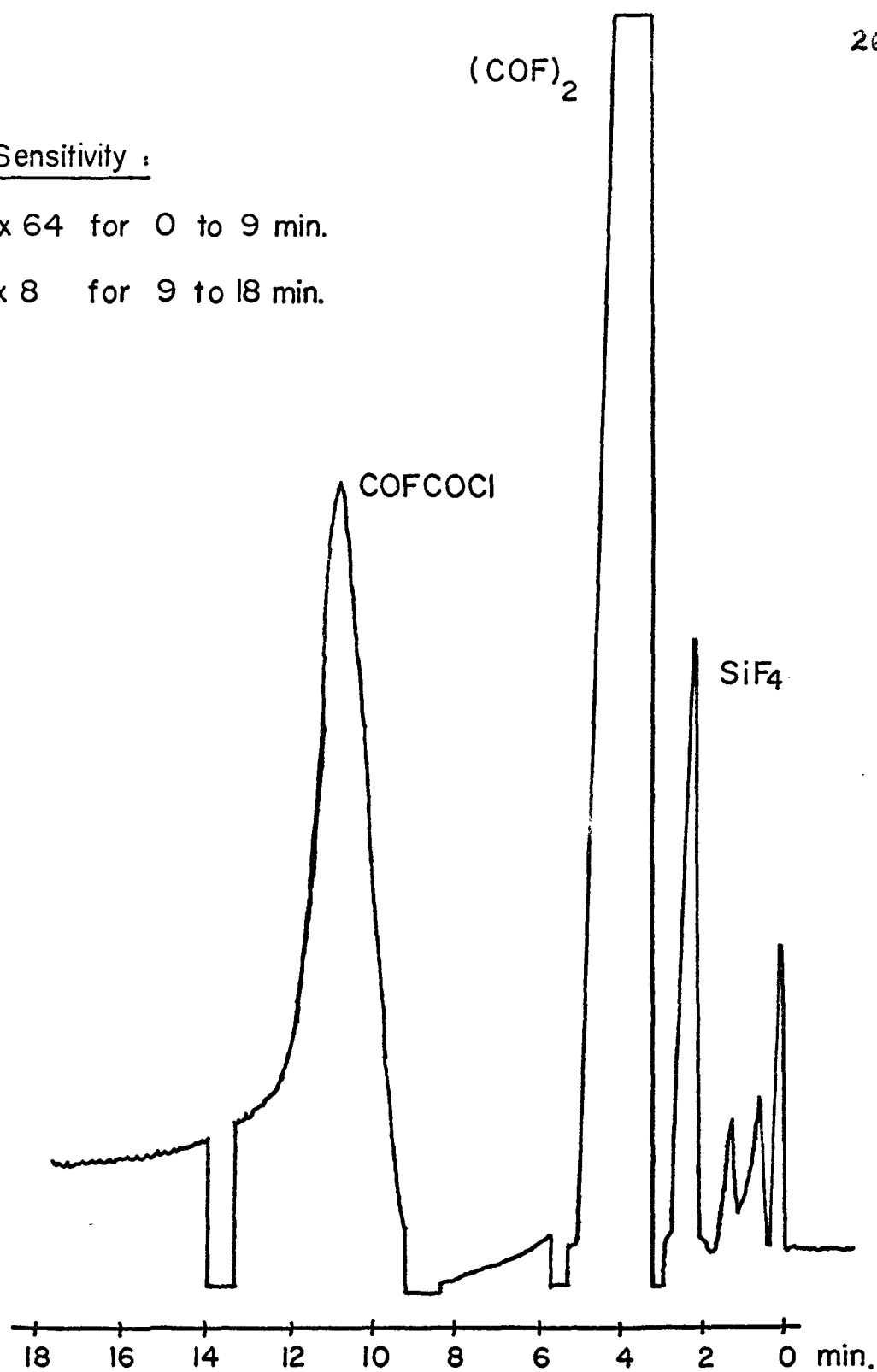


FIGURE 2-3 A SAMPLE GAS - CHROMATOGRAM

2.3 Identification and Purity of the Samples.

As mentioned earlier, detailed vibrational analyses of the infrared spectra of oxalyl fluoride and oxalyl chloride fluoride have been proposed by Hencher and King¹⁷. The frequencies they report for oxalyl fluoride are in good agreement with those of Tullock⁴¹. Haszeldine and Nyman⁴², who prepared oxalyl chloride fluoride by an alternative route to that described above, identified their product from molecular weight determination and elemental analysis. They reported the same infrared spectrum as Hencher and King. The spectra of the compounds currently prepared were also identical with those reported previously. The ¹³C-F nuclear magnetic resonance spectra⁴³ of oxalyl fluoride and oxalyl chloride fluoride have been observed and these confirm the identification of the compounds.

The purity of the sample of oxalyl fluoride was also checked by infrared spectroscopy; no impurities were detectable up to vapour pressures of 300 mm Hg in a 10 cm cell. In the ultraviolet spectrum neither the strong 27189 cm⁻¹ band of oxalyl chloride nor the strong band of oxalyl chloride fluoride at 30004 cm⁻¹ were detected in a pressure path length of 3 m. atm. of oxalyl fluoride.

The sample of oxalyl chloride fluoride was less

pure than that of oxalyl fluoride. Some strong bands of both oxalyl chloride and oxalyl fluoride appeared weakly in the ultraviolet spectrum at pressure path lengths in excess of $\frac{1}{2}$ m. atm. However, these bands could easily be identified by comparison with the spectra of pure oxalyl fluoride and chloride.

The preparation and purification yielded altogether about 10 ml of oxalyl fluoride and ~ 0.5 ml of oxalyl chloride fluoride. The chromatographic separation was very tedious, but did give pure samples of oxalyl fluoride. Because only a small amount of oxalyl chloride fluoride was obtained it was not possible to carry out as complete a spectral investigation on this compound as on the other oxalyl halides. (The synthesis of large quantities of "mixed" halides is currently being attempted as a separate research project by Mr. K. G. Kidd.)

2.4 Experimental Ultraviolet Spectroscopy.

(a) Low Resolution.

The gas phase absorption spectra of the oxalyl halides were investigated under low resolution, between 7000 Å and 2000 Å, using Hilger medium and large quartz spectrographs, a Cary model 14 recording spectrophotometer and a Bausch and Lomb 1.5 m grating spectrograph, model 11. The majority of the low resolution spectra were

photographed, using a 10 micron slit, in the first and second orders of the Bausch and Lomb spectrograph. Either the first order region, from 3700 Å to 7400 Å, or the second order region, from 1850 Å to 3700 Å can be recorded on this instrument with a single exposure. The plate dispersions for these two orders are 14.8 Å/mm and 7.4 Å/mm respectively and the corresponding theoretical resolving powers are 35,000 and 70,000. Because there is no region of the spectrum where both orders can be observed with this spectrograph, it was not possible to compare directly the intensities of absorption bands above 3700 Å with those below 3700 Å. The banded absorption of the oxalyl halides extends from ~4400 Å to ~2900 Å and so intensities were compared from plates taken on the Hilger quartz spectrographs.

(b) High Resolution.

The high resolution absorption spectra of the oxalyl halides were photographed in the first and second orders of a 20 foot Ebert grating spectrograph⁴⁴. Spectra of the mercury multiplet at 2537 Å show that the actual resolving power of this instrument is very close to the theoretical, second order value of 300,000. For the first order, the plate dispersion at 4000 Å is 0.67 Å/mm.

The stronger absorption bands of the molecules studied were observed with vapour pressures of 20 mm Hg in a 50 cm quartz cell. However, to detect weaker bands, path lengths up to 75 metres and pressures from 5 mm to 220 mm Hg (oxalyl fluoride) were found necessary. The long path lengths were attained with a 1.85 m. multiple pass absorption cell of the White type. The construction and alignment of such a cell have been described by Bernstein and Herzberg⁴⁵. When the mirrors for the cell had been freshly aluminized it was possible to obtain 48 traversals of the cell with a 450 watt, 115 v. D.C. high pressure Xenon source. Aluminum is slowly attacked by the vapours of the oxalyl halides and the mirrors were re-aluminized every two or three days when in use.

The vapours of oxalyl chloride and oxalyl bromide were exposed to ultraviolet light only when it was necessary (i.e., when taking spectra) in order to minimize photodecomposition.

2.5 Photography and Calibration of Spectra.

Kodak spectrum analysis #1 and Ilford Q.1 (thin glass) plates were used on the Hilger quartz spectrographs. Spectra were photographed on the grating spectrographs with Kodak spectrum analysis #1 and Ilford FP3 35 mm film. The plates and films were developed for four minutes at

18° C in neat Kodak D19 developer. After development the plates were fixed in an acid fixer, washed for twenty to thirty minutes in cold running water and allowed to dry in a dust-free place.

The light source normally used was a 450 watt Osram XBO high pressure xenon lamp. A striking potential of about 40 Kv, from a Siemens-Schuckert starter was applied momentarily across the electrodes of the lamp in order to ignite it.

For calibration purposes, an iron emission spectrum from a Pfund arc or from a neon-filled iron hollow cathode lamp, was recorded adjacent to the absorption spectrum. Accurate wavelengths in air for the iron lines were obtained from the M.I.T. wavelength tables⁴⁶ and these were readily converted to vacuum values using correction tables due to Edlén⁴⁷.

The positions of the sharp band heads observed in the absorption spectra of the oxalyl halides were measured off the first order films taken on the Ebert spectrograph, using a travelling microscope with a precision of ~ 0.001 mm. The wavelengths of these band heads were determined by comparison with the standard iron spectrum according to a procedure described by Robinson⁴⁸. The frequencies are estimated to be accurate to $\pm 0.2 \text{ cm}^{-1}$. Some sharp bands which were too weak to

locate accurately in the microscope were measured off photographic enlargements. The frequencies of a few very diffuse bands at high frequencies in the spectra were estimated from traces made on a Joyce-Loebl Mk III C double-beam recording microdensitometer.

CHAPTER 3
THEORY OF ELECTRONIC SPECTRA

3.1 Symmetry of the Oxalyl Halides.

The symmetry elements of the oxalyl halides $(COX)_2$ are shown in Figure 3.1 for both planar-trans and planar-cis configurations. Usually the symmetry operators which interchange identical nuclei in a molecule are described by the same symbols as those given to the corresponding symmetry elements. For the trans configuration, these symmetry operators are, with coordinate axes as shown in the Figure,

- (i) E, the identity operator which leaves the molecule unchanged;
- (ii) $C_2(z)$, the operation of two-fold rotation about the z-axis;
- (iii) σ_h , reflection in the plane containing the atoms of the molecule;
- (iv) i, the operation of inversion through the centre of symmetry of the molecule.

These four symmetry operators comprise the molecular point group, C_{2h} .⁺

⁺ In this chapter an elementary knowledge of group theory will be assumed^{49,50}.

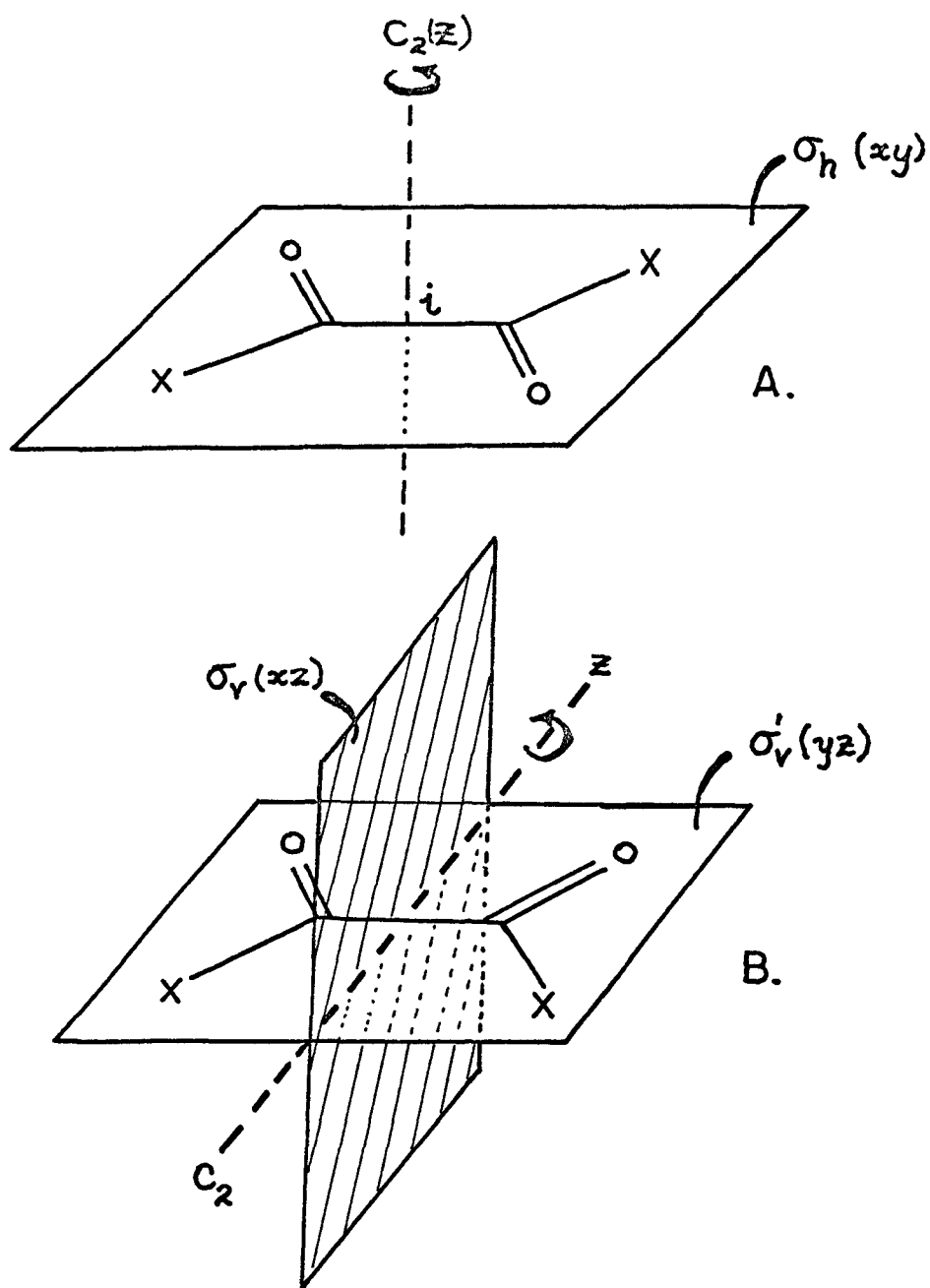


FIGURE 3.1 THE SYMMETRY ELEMENTS OF THE OXALYL DIHALIDES .

- A. Planar - trans , C_{2h} .
 B. Planar - cis , C_{2v} .

The symmetry operations of the cis configuration, E , C_2 , σ_v and σ'_v form the molecular point group C_{2v} . In the non-planar oxalyl halide molecules, there are only two symmetry elements, E and $C_2(z)$. The point group C_2 formed by the operators E and $C_2(z)$ is a subgroup of C_{2v} and C_{2h} .

When the two halogen atoms in the molecule are different, the cis and trans conformers each have the same symmetry elements, the identity E and the plane of the molecule, σ_h . The point group formed from the operators E and σ_h is called C_s which is also a subgroup of C_{2v} and C_{2h} .

Tables 3.1 to 3.4 contain character tables for the point groups C_{2h} , C_{2v} , C_s and C_2 . Multiplication tables for C_{2h} and C_s are given in Tables 3.5 and 3.6.

3.2 Molecular Orbitals for the Oxalyl Halides.

As was first suggested by Mulliken⁵¹, the transition of lowest energy in carbonyl compounds involves the excitation of an essentially non-bonded electron, localized largely on oxygen, to an antibonding π -orbital extending over several atomic centres. Such a transition has been designated $n \rightarrow \pi^*$ by Kasha⁵² and, for aldehydes and ketones, usually gives rise to weak absorption in the $25,000 \text{ cm}^{-1}$ to $33,000 \text{ cm}^{-1}$ region. The transitions

TABLE 3.1
THE CHARACTER TABLE FOR THE POINT GROUP C_{2h}

| | C_{2h} | E | $C_2(z)$ | $\sigma_h(x,y)$ | i |
|------------|----------|---|----------|-----------------|----|
| R_z | A_g | 1 | 1 | 1 | 1 |
| T_z | A_u | 1 | 1 | -1 | -1 |
| R_x, R_y | B_g | 1 | -1 | -1 | 1 |
| T_x, T_y | B_u | 1 | -1 | 1 | -1 |

TABLE 3.2
THE CHARACTER TABLE FOR THE POINT GROUP C_{2v}

| | C_{2v} | E | $C_2(z)$ | $\sigma_v(xz)$ | $\sigma'_v(yz)$ |
|------------|----------|---|----------|----------------|-----------------|
| T_z | A_1 | 1 | 1 | 1 | 1 |
| R_z | A_2 | 1 | 1 | -1 | -1 |
| T_x, R_y | B_1 | 1 | -1 | 1 | -1 |
| T_y, R_x | B_2 | 1 | -1 | -1 | 1 |

TABLE 3.3

THE CHARACTER TABLE FOR THE POINT GROUP C_s

| | C_s | E | $\sigma_h(xy)$ |
|-----------------|-------|---|----------------|
| T_x, T_y, R_z | A' | 1 | 1 |
| T_z, R_x, R_y | A'' | 1 | -1 |

TABLE 3.4

THE CHARACTER TABLE FOR THE POINT GROUP C_2

| | C_2 | E | $C_2(z)$ |
|----------------------|-------|---|----------|
| T_z, R_z | A | 1 | 1 |
| T_x, T_y, R_x, R_y | B | 1 | -1 |

TABLE 3.5

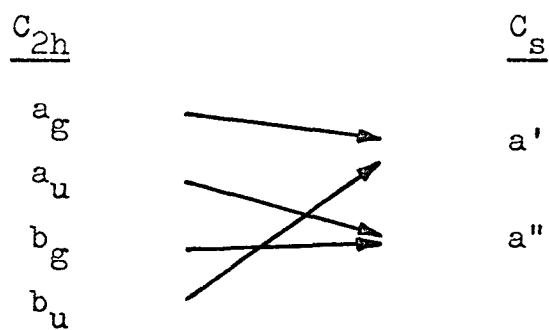
DIRECT PRODUCT TABLE FOR THE POINT GROUP C_s

| C_s | A' | A'' |
|-------|-----|-----|
| A' | A' | A'' |
| A'' | A'' | A' |

TABLE 3.6
DIRECT PRODUCT TABLE FOR THE POINT GROUP C_{2h}

| C_{2h} | A_g | A_u | B_g | B_u |
|----------|-------|-------|-------|-------|
| A_g | A_g | A_u | B_g | B_u |
| A_u | A_u | A_g | B_u | B_g |
| B_g | B_g | B_u | A_g | A_u |
| B_u | B_u | B_g | A_u | A_g |

TABLE 3.7
CORRELATION OF SYMMETRY SPECIES FOR
THE POINT GROUPS C_{2h} AND C_s

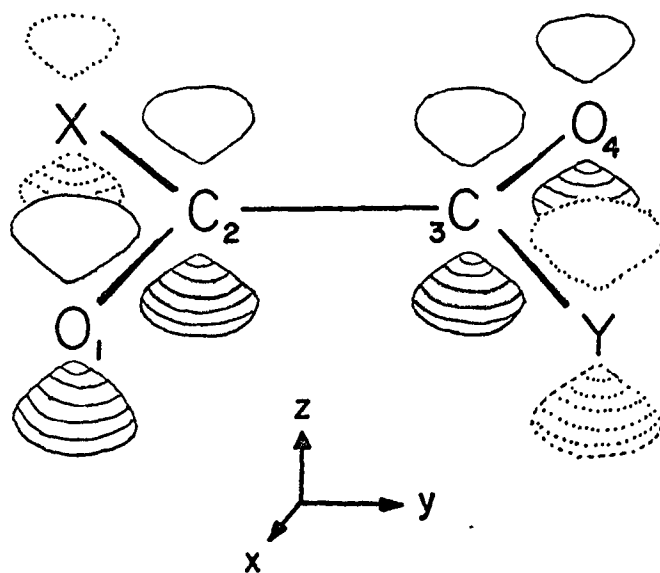


observed at these energies for the oxalyl halides are undoubtedly of the $n \rightarrow \pi^*$ type.

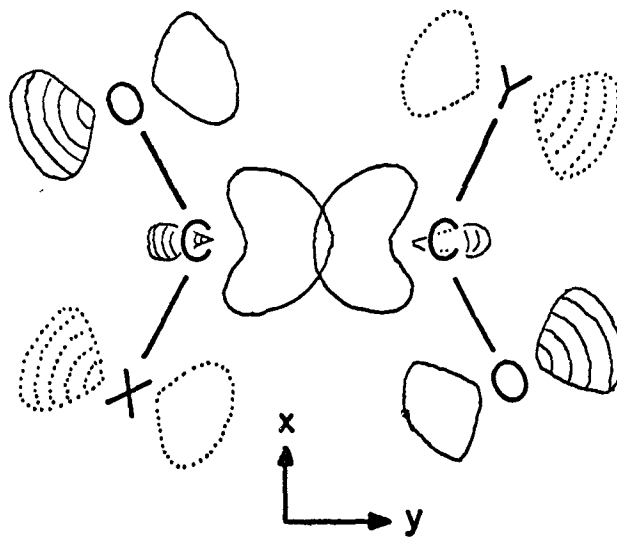
The molecular orbitals for the $(\text{COX})_2$ oxalyl halides may be constructed by taking appropriate linear combinations of atomic orbitals (LCAO/MO). The molecular orbitals can be divided into three types, σ -orbitals, π -orbitals and n-orbitals. Basis atomic orbitals, from which the molecular orbitals are constructed, are shown in Figure 3.2.

(a) σ -orbitals: These orbitals form the inner core of the molecule. The electrons within these orbitals are tightly bound to the nuclei and are not excited during a spectroscopic transition of the type studied in this thesis and so will not be considered further.

(b) π -orbitals: Each carbon and each oxygen atom has one electron in a p_z orbital perpendicular to the molecular plane. (Any contribution from the halogen atomic orbitals is ignored in this simple approximation.) If we let the four p_z atomic orbitals of the $\text{O}_1\text{-C}_2\text{-C}_3\text{-O}_4$ system be labelled ϕ_1 , ϕ_2 , ϕ_3 and ϕ_4 , then the four orthogonal LCAO/MO's, which must transform as irreducible representations of the molecular point group, are given by



a. π -electron atomic orbitals



b. σ - and n -electron atomic orbitals

FIGURE 3.2 BASIS ATOMIC ORBITALS.

$$\begin{aligned}
 \psi_1 &= c_{11} \phi_1 + c_{12} \phi_2 + c_{13} \phi_3 + c_{14} \phi_4 \\
 \psi_2 &= c_{21} \phi_1 + c_{22} \phi_2 - c_{23} \phi_3 - c_{24} \phi_4 \\
 \psi_3 &= c_{31} \phi_1 - c_{32} \phi_2 - c_{33} \phi_3 + c_{34} \phi_4 \\
 \psi_4 &= c_{41} \phi_1 - c_{42} \phi_2 + c_{43} \phi_3 - c_{44} \phi_4
 \end{aligned} \tag{3.1}$$

where all the c_{ij} 's are positive and, for $(\text{COX})_2$ -type molecules

$$\left. \begin{aligned}
 c_{i1} \phi_1 &= c_{i4} \phi_4 \\
 c_{i2} \phi_2 &= c_{i3} \phi_3
 \end{aligned} \right\} i = 1, \dots, 4 \tag{3.2}$$

By applying the symmetry operations of the C_{2h} point group to each of the ψ_i 's in turn, we find that ψ_1 transforms as the symmetry species a_u , ψ_2 belongs to the irreducible representation b_g , ψ_3 to a_u and ψ_4 to b_g .

(c) n-orbitals: After both the σ -electrons of the core and the π -electrons of the conjugated system have been considered, there still remains a doubly-occupied, in-plane 2p orbital on each of the oxygen atoms.

Linear combinations of these "non-bonding" orbitals,

$$\begin{aligned}
 \psi_{n_+} &= \frac{1}{\sqrt{2}} (\phi_{1n} + \phi_{4n}) \\
 \psi_{n_-} &= \frac{1}{\sqrt{2}} (\phi_{1n} - \phi_{4n})
 \end{aligned} \tag{3.3}$$

give two molecular orbitals. ψ_{n_+} transforms as b_u and ψ_{n_-} as a_g .

Similar molecular orbitals can be constructed for COX-COY - type molecules. However, because of the lower symmetry, the molecular orbitals must be classified under the point group C_s . We readily see from the correlation table 3.7 that, for oxalyl chloride fluoride, all the π -orbitals transform as a'' while the in-plane σ - and n-orbitals belong to the a' representation.

3.3 Electronic Configurations for the Oxalyl Halides.

In the oxalyl halides we have bonding, non-bonding and anti-bonding molecular orbitals; antibonding molecular orbitals being distinguished from bonding ones by an asterisk, e.g. σ^* , π^* . Among the π -orbitals⁺, π_1 and π_2 orbitals, which have no nodes and one node respectively, are relatively bonding orbitals as in other related molecules. These are occupied in the ground state, each with two electrons of opposed spins. The unoccupied orbitals π_3^* (2 nodes) and π_4^* (3 nodes) are relatively antibonding and are used in formulating

⁺ Here π_i represents the π -orbital described by ψ_i and n_+ the n-orbital described by ψ_{n_+} etc.

wave functions for the excited states.

It is generally accepted that the π -orbital energies increase with increasing number of nodes. Thus, energywise,

$$\pi_1 < \pi_2 < \pi_3^* < \pi_4^* .$$

If there is no interaction between atomic orbitals

ϕ_{1n} and ϕ_{4n} , n_+ and n_- will both have the same energy: that of an atomic $2p_n$ orbital on oxygen. For small, but finite interaction, the bonding combination n_+ is expected to be lower in energy than the antibonding one n_- . In any event, the two n-type molecular orbitals (both filled in the ground state) are predicted to be very nearly equal in energy.

The two n-orbitals, because they are essentially non-bonding, will lie in energy between the filled π -orbitals, π_1 and π_2 , and the unoccupied π^* -orbitals, π_3^* and π_4^* . The complete ordering with respect to energy is then

$$\pi_1 < \pi_2 < n_+ \leq n_- < \pi_3^* < \pi_4^* .$$

The σ -orbitals lie below π_1 and the σ^* -orbitals lie above π_4^* . (Figure 3.3.)

The lowest electron configuration, and the state it gives rise to, are

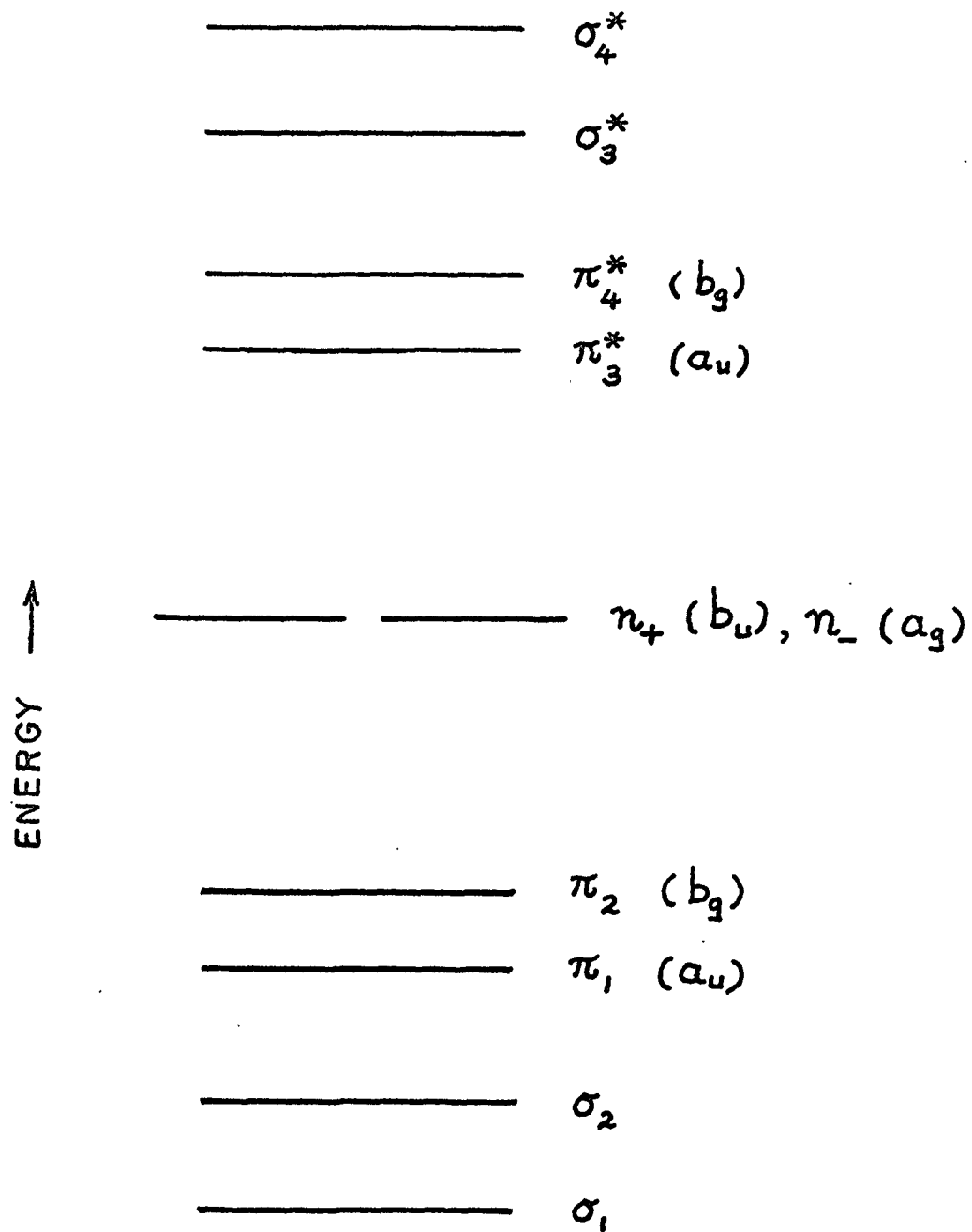
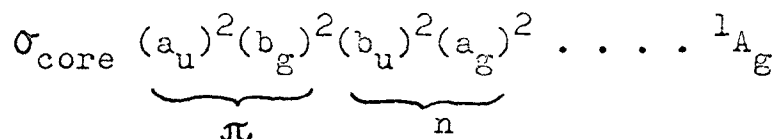
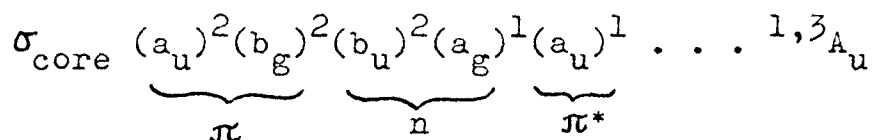


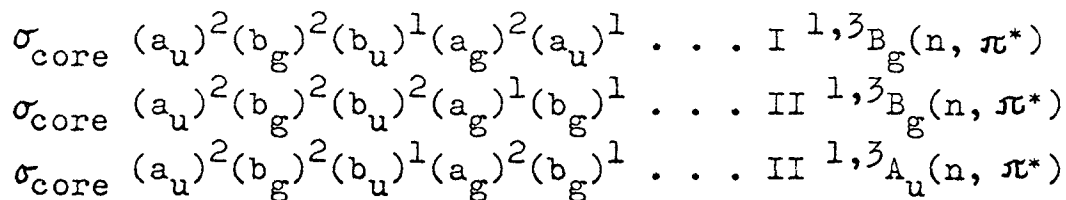
FIGURE 3·3 MOLECULAR ORBITALS
FOR THE OXALYL HALIDES.



As is found experimentally for most molecules where $n \rightarrow \pi^*$ transitions can occur, the electronic excitation requiring least energy is that for the promotion of an electron from a non-bonding orbital to π^* . For the first excited state:



This configuration gives rise to two (n, π^*) states, 3A_u and 1A_u , depending on whether the spins of the unpaired electrons in the singly-occupied orbitals are parallel or antiparallel. Excited states are distinguished from others of the same symmetry but higher energy by Roman numerals as prefixes. So the first excited states of the oxalyl halides are I ${}^3A_u(n, \pi^*)$ and I ${}^1A_u(n, \pi^*)$. The configurations for other possible excited states of higher energy are, in increasing order of probable energy,



$$\begin{aligned} \sigma_{\text{core}} & (a_u)^2(b_g)^1(b_u)^2(a_g)^2(a_u)^1 \dots \text{I } ^1,^3B_u(\pi, \pi^*) \\ \sigma_{\text{core}} & (a_u)^2(b_g)^1(b_u)^2(a_g)^2(b_g)^1 \dots \text{I } ^1,^3A_g(\pi, \pi^*) \end{aligned}$$

Under the lower symmetry of C_s , the ground state of the oxalyl halides is $^1A'$ and the excited states corresponding to the above respective configurations are,

$$\begin{aligned} & \text{I } ^1,^3A''(n_-, \pi_3^*), \text{ II } ^1,^3A''(n_+, \pi_3^*), \text{ III } ^1,^3A''(n_-, \pi_4^*), \\ & \text{IV } ^1,^3A''(n_+, \pi_4^*), \text{ I } ^1,^3A'(\pi_2, \pi_3^*) \text{ and II } ^1,^3A'(\pi_2, \pi_4^*). \end{aligned}$$

It should be noted that, throughout this discussion we have assumed that both the ground and excited states belong to the same point group. The vibrational and rotational analyses of the discrete absorption spectra of the oxalyl halides studied here show that the geometry of the molecules in the excited states involved remains planar-trans.

3.4 Selection Rules for Electronic Transitions.

The intensity of an electric dipole transition between states with wave functions ψ_T'' and ψ_T' is proportional to the square of the transition moment \vec{R} , where

$$\vec{R} = \int \psi_T' \vec{\mu} \psi_T'' d\tau \quad (3.4)$$

The transition moment is a scalar quantity and must remain invariant under all the symmetry operations of the point group of the molecule. This leads to the rule

that the integral in equation (3.4) will be different from zero if, and only if, the direct product

$$\Gamma(\psi'_e) \otimes \Gamma(\psi''_e) = \Gamma\vec{\mu} \quad (3.5)$$

where Γ stands for an irreducible representation of the molecular point group.

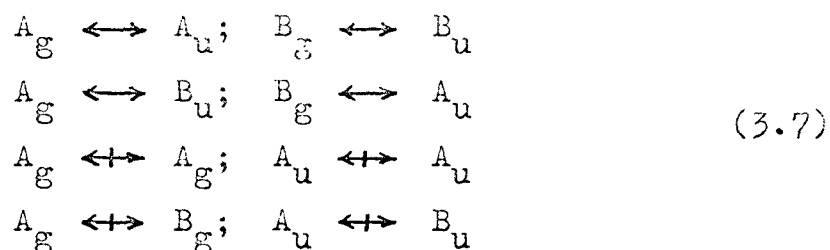
Since the electric dipole moment operator $\vec{\mu}$ is a polar vector⁺, its x, y and z components transform like the cartesian coordinates.

$$\Gamma\mu_x = \Gamma T_x; \quad \Gamma\mu_y = \Gamma T_y; \quad \Gamma\mu_z = \Gamma T_z. \quad (3.6)$$

An electric dipole transition between states with wave functions ψ'_e and ψ''_e is said to be symmetry allowed if $\Gamma(\psi'_e) \otimes \Gamma(\psi''_e)$ transforms like one of ΓT_x , ΓT_y or ΓT_z . The irreducible representations to which the general vectors T_x , T_y , and T_z belong, for the point groups C_{2h} , C_{2v} , C_s and C_2 , can be found by referring to Tables 3.1 to 3.4.

On application of the above to the point group C_{2h} , we find the following electronic selection rules for electric dipole radiation.

⁺ Polar vectors change sign under the parity operation, i. The angular momentum vectors do not change under such an operation and are axial vectors.



The z-direction in the trans molecule is defined as the direction perpendicular to the molecular plane (xy). Therefore, for planar, trans (COX)₂, an electronic transition, from the ground state A_g to an excited state of symmetry A_u, is symmetry allowed by the perpendicular component of the electric dipole moment. Such a transition is termed perpendicular or, alternatively, said to be perpendicularly polarized. A transition is also allowed from the ground state to an excited state of symmetry B_u. In this case, we can simply say that the transition is polarized in the plane of the molecule.

A summary of the symmetry allowed, electric dipole transitions expected in the absorption spectra of the (COX)₂ oxalyl halides is given in Table 3.8. The transitions are listed in increasing order of energy.

3.5 n → π* Singlet-Singlet and Singlet-Triplet Transitions.

n → π* absorptions are always weak in intensity (f ~ 10⁻² - 10⁻⁴) even when the transition is formally allowed by symmetry. Platt⁵³ suggested that their low

TABLE 3.8
 EXPECTED LOW-LYING TRANSITIONS
 FOR $(\text{COX})_2$ MOLECULES

| <u>Ground State</u> | <u>Excited State</u> | <u>Polarization</u> |
|---------------------|----------------------|---------------------|
| A_g | I $A_u(n, \pi^*)$ | perpendicular |
| A_g | II $A_u(n, \pi^*)$ | perpendicular |
| A_g | I $B_u(\pi, \pi^*)$ | in-plane |

TABLE 3.9
 (n, π^*) SINGLET TRIPLET ENERGY SEPARATION
 IN CARBONYL COMPOUNDS (cm^{-1})

| <u>Compound</u> | <u>Singlet (n, π^*) State</u> | <u>Triplet (n, π^*) State</u> | <u>ΔE</u> | <u>Reference</u> |
|---------------------------|--|--|------------------------------|------------------|
| formaldehyde [‡] | 28196 | 25194 | 3002 | 56,57 |
| propynal | 26163 | 24127 | 2035 | 58,59 |
| glyoxal | 21973 | 19197 | 2776 | 60,61 |
| biacetyl ⁺⁺ | 22873 | 19806 | 3067 | 62 |

[‡] to O^+ of inversion doublet

⁺⁺ crystal at 4°K

intensity is a result of a difference in spatial properties of the n - and π^* -orbitals. We may write the transition moment for a single electron promotion from orbital n to orbital π^*

$$\vec{R}_{n, \pi^*} = \int n(i) \vec{\mu}(i) \pi^*(i) d\tau \quad (3.8)$$

where the electron involved is labelled by i .

According to El Sayed and Robinson⁵⁴, we cannot expect the electron in the π^* -orbital to achieve much delocalization, even in conjugated systems. In the limit of complete localization of the n and π^* electrons on the same atom, the $2p_n \rightarrow 2p_{\pi^*}$ transition should have zero probability because of the atomic selection rule⁵⁵,

$$\Delta l = \pm 1 \quad (3.9)$$

However, because the π^* -electron is delocalized to some extent over other atoms, and also because the n -orbital can acquire some s -character from hybridization,

\vec{R}_{n, π^*} is non-zero, but usually small.

It was mentioned in paragraph 3.3 that the configuration resulting from the excitation of an electron from a non-bonding orbital to an antibonding π -orbital should give rise to two terms, singlet and triplet. It has been found experimentally that the triplet (n, π^*) excited state lies lower in energy than the corresponding

singlet state by between 2000 and 3000 cm^{-1} for carbonyl compounds. Some typical singlet-triplet energy separations are given in Table 3.9. The origin of the energy separation between singlet and triplet states has been discussed by Pople⁶³ who showed that the difference in energies of the two states is

$$\begin{aligned} \mathcal{E}\{^1(n, \pi^*)\} - \mathcal{E}\{^3(n, \pi^*)\} \\ = 2 \iint n(i) \pi^*(j) \left(\frac{e^2}{r_{ij}} \right) \pi^*(i) n(j) d\tau_i d\tau_j \end{aligned} \quad (3.10)$$

Since the exchange integral in equation (3.10) is positive⁶⁴, the singlet state is higher in energy than the corresponding triplet.

In our discussion of electronic selection rules and symmetry properties of electronic states, we have concentrated on the spatial part of the wave function. It now becomes necessary to introduce a wave function ψ_s for the total electron spin of the molecule. The spin of a state is characterized by a spin quantum number s given by the equation

$$\mathcal{S}^2 \psi_s = s(s+1)\hbar^2 \psi_s \quad (3.11)$$

where \mathcal{S} is the total spin angular momentum operator. The number $2s + 1$, which represents the spin degeneracy of the state with spin s is called the multiplicity of the state.

The complete wave function for a molecule may be expressed as a product of spatial and spin wave functions.

$$\Psi = \psi_T \psi_S \quad (3.12)$$

For an electronic transition, the transition moment, including electron spin, is given by

$$\vec{R}_{es} = \iint \psi_e'^* \psi_s'^* \vec{\mu} \psi_e'' \psi_s'' d\tau_e d\tau_s \quad (3.13)$$

To a first approximation, we may ignore spin-orbit interaction and separate the double integral into two parts, one involving spatial coordinates (τ_e) and the other only the spin coordinates (τ_s).

$$\vec{R}_{es} = \int \psi_e'^* \vec{\mu} \psi_e'' d\tau_e \int \psi_s'^* \psi_s'' d\tau_s \quad (3.14)$$

Now, since

$$\int \psi_s'^* \psi_s'' d\tau_s = \delta_{s's''} \quad (3.15)$$

where s'' and s' are the spin quantum numbers of the ground and excited states respectively and δ is the Krönecker delta symbol, we have a spin selection rule

$$\Delta s = 0 \quad (3.16)$$

This means that, in the absence of spin-orbit interaction, transitions involving a change of multiplicity are unallowed. However, because the magnetic moment

associated with the orbital motion of the electron can couple with the spin magnetic moment, the above spin selection rule breaks down and singlet-triplet transitions are observed. The intensities of singlet-triplet absorption spectra are typically weaker than the corresponding singlet-singlet spectra by a factor of $\sim 10^4$ for $n \rightarrow \pi^*$ transitions⁵². Some experimentally determined $n \rightarrow \pi^*$ oscillator strengths for carbonyl compounds are given in Table 3.10.

3.6 Identification of the Observed Spectral Systems in the Oxalyl Halides.

Each of the oxalyl halides studied shows two distinct regions of absorption in the near ultraviolet⁺.

These are

- (i) discrete absorption with complex band structure which becomes increasingly diffuse with increasing frequency;
- (ii) a continuous absorption at higher frequencies with few observed vibrational features.

⁺ The spectral region beyond 1900 Å has not been investigated.

TABLE 3.10
OSCILLATOR STRENGTHS FOR SOME
 $n \rightarrow \pi^*$ TRANSITIONS IN CARBONYL
COMPOUNDS (FROM REFERENCE 65)

| <u>Compound</u> | <u>Oscillator Strength Singlet-Singlet</u> | <u>Oscillator Strength Singlet-Triplet</u> |
|-----------------|--|--|
| benzoquinone | 0.34×10^{-3} | 6.3×10^{-7} |
| benzaldehyde | 0.55×10^{-3} | 1.8×10^{-7} |
| acetophenone | 0.84×10^{-3} | 1.3×10^{-7} |
| benzophenone | 2.1×10^{-3} | 0.6×10^{-7} |

(a) The discrete spectra:

The vibrationally discrete spectrum of oxalyl bromide extends from $\sim 4400 \text{ \AA}$ to $\sim 3200 \text{ \AA}$ and that of oxalyl fluoride from $\sim 3400 \text{ \AA}$ to beyond 2800 \AA . The corresponding spectra for oxalyl chloride and oxalyl chloride fluoride lie within this wavelength range.

It is apparent from the observed rotational structure of the bands and from the vibrational patterns found in the spectra, that each oxalyl halide has two electronic transitions within the discrete absorption region. The origin bands of these two systems, which are both symmetry allowed transitions, differ in energy by about 2500 cm^{-1} . They also differ in intensity with the lower energy spectra being about 100 times weaker than the corresponding systems to higher energy, so that the former becomes "swamped" by the latter at higher frequencies. Since the above evidence strongly suggests that the transitions lead to singlet and triplet (n, π^*) states, it is reasonable to assign the banded absorption spectra of the $(\text{COX})_2$ molecules to the electronic transitions $I \ ^1A_u \leftarrow \ ^1A_g$ and $I \ ^3A_u \leftarrow \ ^1A_g$. (For COXCOY molecules the corresponding transitions are $I \ ^1A'' \leftarrow \ ^1A'$ and $I \ ^3A'' \leftarrow \ ^1A'$.) The observed vibrational and rotational structure of the spectra are in complete agreement with that expected for such

transitions and leave little doubt that the assignment is correct. The recent work of Borkman and Kearns⁶⁶ on oxalyl bromide lends further support to this interpretation.

Detailed analyses of the vibrational and rotational structure of these spectra are discussed in subsequent chapters of this thesis. The assigned origin bands of the discrete spectral systems are listed in Table 3.11.

(b) The continuous absorption:

The spectra of oxalyl fluoride, oxalyl chloride and oxalyl bromide were recorded on a Cary model 14 spectrophotometer in the region from 7000 Å to 1900 Å. Portions of these spectra are reproduced in Figures 3.4, 3.5 and 3.6. Unfortunately, a sufficient quantity of oxalyl chloride fluoride was not available for studies on the Cary spectrometer.

The banded absorption which, for the oxalyl halide molecules, is observed in the 4000 Å to 3000 Å region, gradually becomes diffuse towards higher energies and eventually all vibrational details disappear into the rising background continuum. This weak, continuous absorption in oxalyl fluoride reaches a maximum around 2465 Å while at still shorter wavelengths some broad vibrational features can be detected extending from

TABLE 3.11
 ORIGIN BANDS FOR THE FIRST n, π^*
 TRANSITIONS IN THE OXALYL HALIDES (cm^{-1})

| Compound | Transition | Singlet- Singlet | Singlet- Triplet | Energy Separation |
|-------------------|------------------------|---------------------|---------------------|----------------------|
| $(\text{COBr})_2$ | I $A_u \leftarrow A_g$ | 25370.5 | 22938.0 | 2432.5 |
| $(\text{COCl})_2$ | I $A_u \leftarrow A_g$ | 27192.4 | 24370.2 | 2822.2 |
| COFCOCl | I $A'' \leftarrow A'$ | 28724.2 | 25827.4 | 2895.8 |
| $(\text{COF})_2$ | I $A_u \leftarrow A_g$ | 32445.0 | 29941.9 | 2503.1 |

TABLE 3.12
 WEAK, DIFFUSE ABSORPTION SYSTEMS IN
 THE NEAR ULTRAVIOLET

| Compound | Region |
|-------------------|---------------|
| $(\text{COBr})_2$ | 3000 - 2400 Å |
| $(\text{COCl})_2$ | 2900 - 2400 Å |
| COFCOCl | 2700 Å - ? |
| $(\text{COF})_2$ | 2700 - 2300 Å |

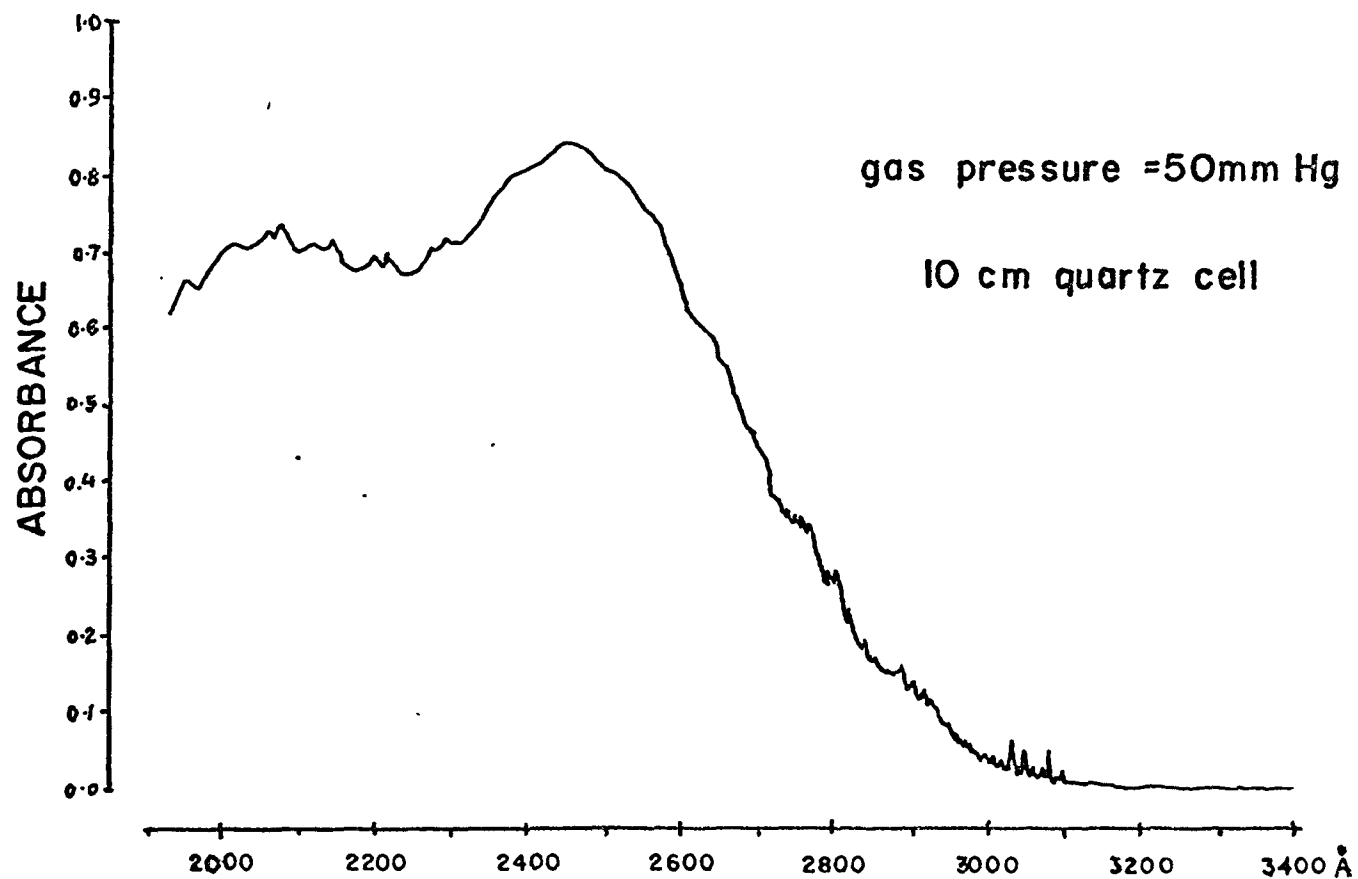


FIGURE 3.4 NEAR ULTRAVIOLET SPECTRUM OF OXALYL FLUORIDE

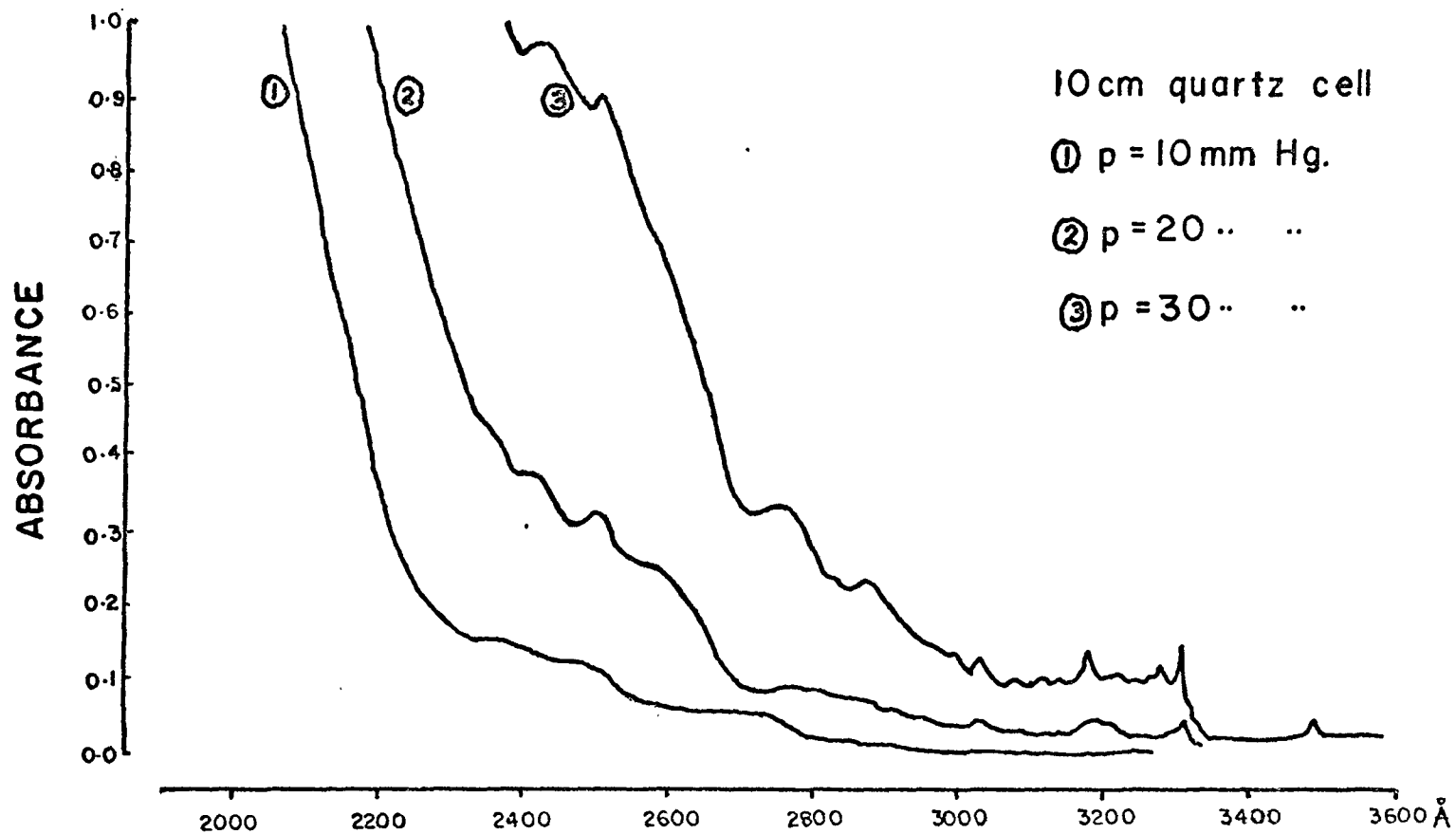


FIGURE 3·5 NEAR ULTRAVIOLET SPECTRUM OF OXALYL CHLORIDE

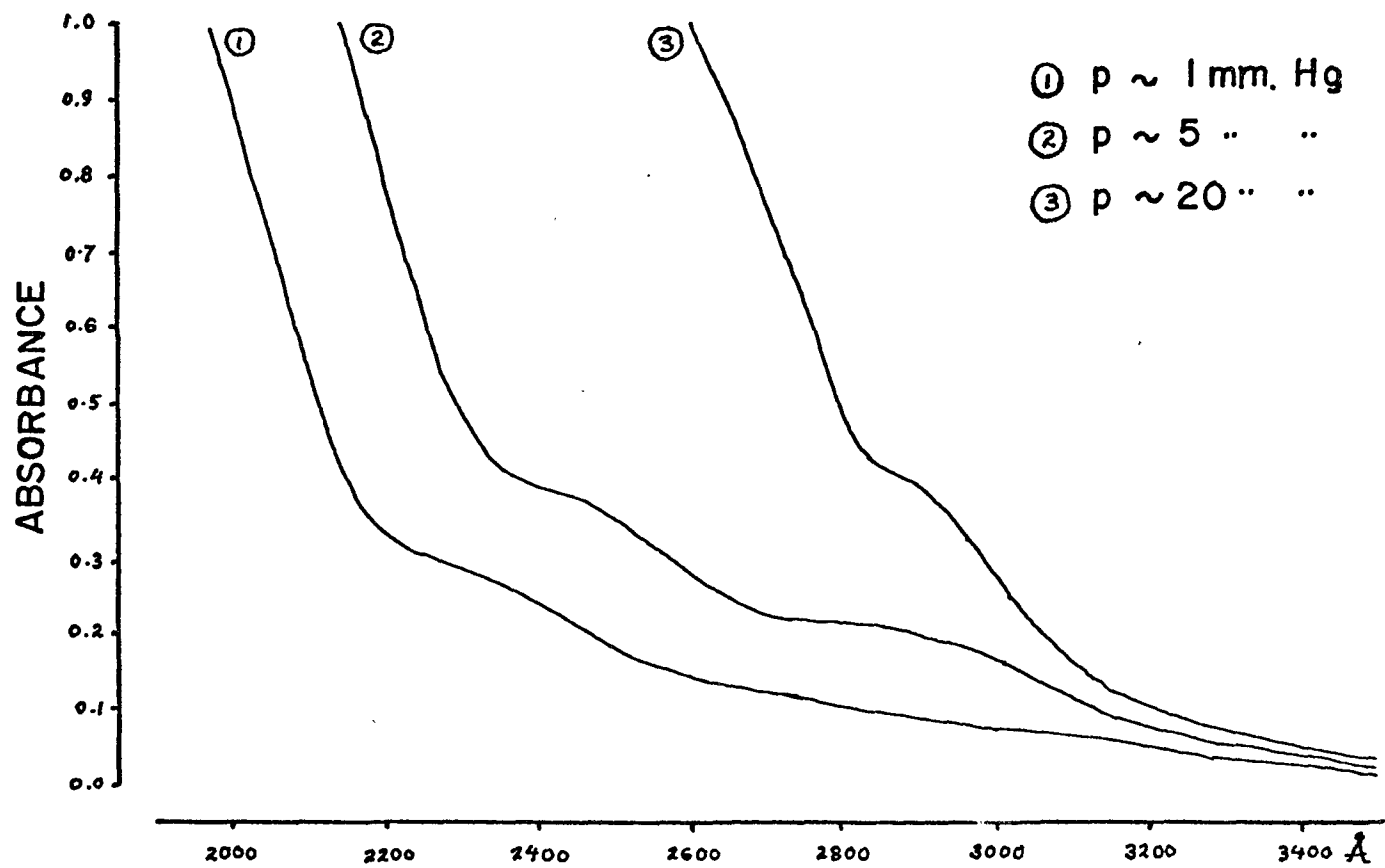


FIGURE 3·6 NEAR ULTRAVIOLET SPECTRUM OF OXALYL BROMIDE

2300 Å to the vacuum ultraviolet. A few, broad, diffuse maxima are found in the corresponding continuous absorption system of oxalyl chloride in the region from ~2900 Å to 2400 Å. There is strong absorption for oxalyl chloride from 2300 Å to the vacuum ultraviolet. A continuous spectrum similar to that of oxalyl chloride is observed in the case of oxalyl bromide where there is weak, featureless absorption from ~3000 Å to ~2400 Å and strong absorption from 2400 Å to beyond 1900 Å.

A summary of the regions of weak, continuous absorption found in the near ultraviolet, for the oxalyl compounds, is shown in Table 3.12.

Systems analogous to the weak, diffuse absorptions in the oxalyl halides have been reported for both glyoxal⁶⁷, (3200 - 2300 Å), and biacetyl⁶⁸, (2800 - 2500 Å). Walsh⁶⁷ assigned these spectra to the $II A_u \leftarrow A_g$ transition associated with a second $n \rightarrow \pi^*$ promotion. There are several good reasons for thinking that this interpretation is correct.

(i) Intensity: The absorptions are much weaker than those expected for transitions of either $n \rightarrow \sigma^*$ or $\pi \rightarrow \pi^*$ types.

(ii) Diffuseness: The continuous nature of the absorption, together with the evidence from photodecomposition^{19,20} studies with 2500 Å radiation, strongly suggests

that the upper state involved in the transition is dissociative.



Such a fragmentation of the molecule is to be expected from a transition of the $n \rightarrow \pi_4^*$ (b_g) type since this upper π^* -orbital has a node across the carbon-carbon bond.

(iii) Predissociation of the discrete absorption systems: As mentioned earlier, the sharp vibrational structure of the I ${}^1A_u \leftarrow {}^1A_g$ system becomes increasingly diffuse towards shorter wavelengths. This phenomenon, known as predissociation, is not uncommon in the spectra of polyatomic molecules and arises when two potential surfaces, one of which is dissociative, come close enough to each other to interact. To a good approximation, predissociation is possible only between electronic states of the same symmetry species and therefore, in the oxalyl halides, a dissociative state of symmetry A_u must lie close in energy to the I $A_u(n, \pi^*)$ state. A schematic diagram of the interaction between the two A_u states is given in Figure 3.7 where the dashed curves represent the potential surfaces before perturbation.

The transitions in oxalyl chloride and oxalyl bromide which give rise to strong absorption below

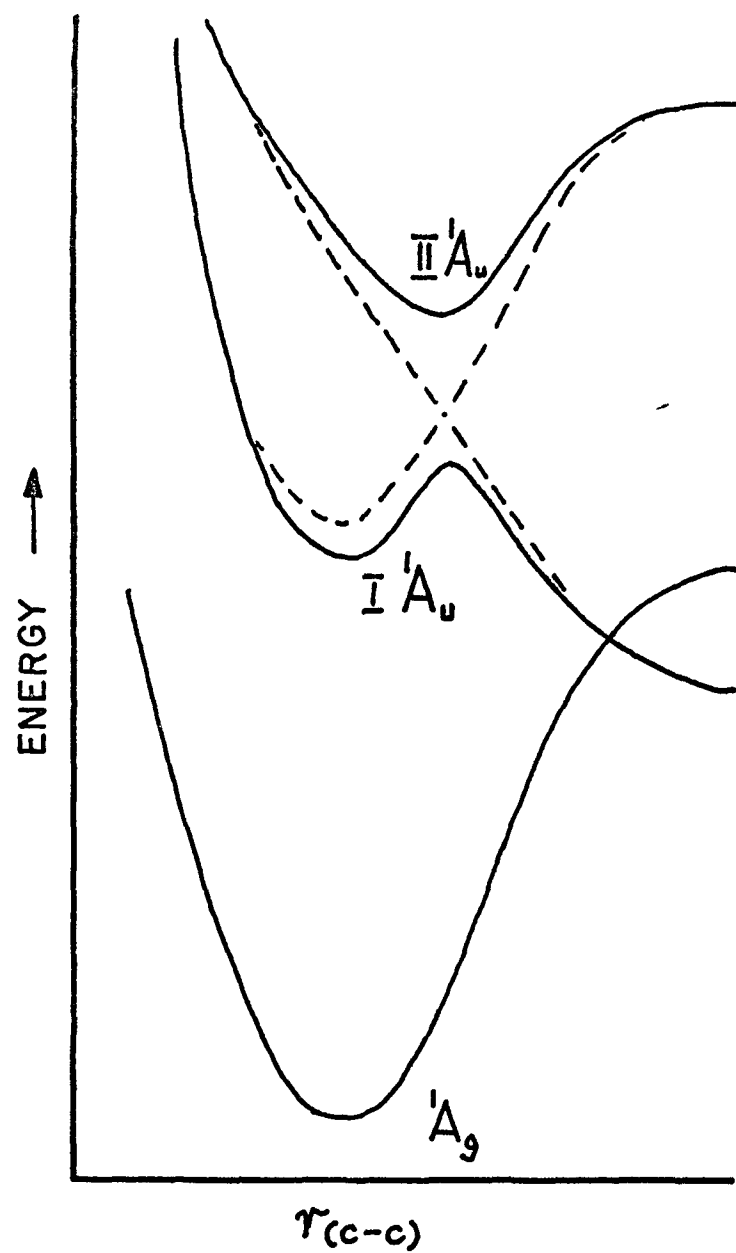


FIGURE 3.7 A SCHEMATIC REPRESENTATION OF PREDISSOCIATION IN THE SPECTRA OF THE OXALYL HALIDES.

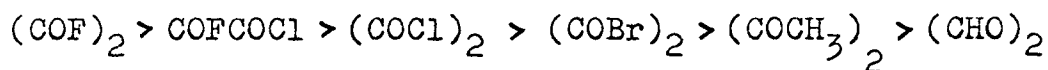
2200 Å are probably of the $n \rightarrow \sigma^*$ type. (The corresponding transition in oxalyl fluoride has not been located at wavelengths greater than 2000 Å.) The $n \rightarrow \sigma^*$ transitions of several aldehydes and ketones have been identified by Walsh⁶⁷ in the 1750 - 2100 Å region. Since an $n \rightarrow \sigma^*$ transition does not involve electrons or levels affected by conjugation, we should expect the energy of the $n \rightarrow \sigma^*$ transition in the oxalyl compounds to be approximately the same as that found for non-conjugated carbonyl compounds.

3.7 Discussion of the Near Ultraviolet Spectra.

Sidman²², in his low resolution investigation of the near ultraviolet spectrum of oxalyl chloride, concluded that the discrete spectrum was due to absorption by molecules in the trans conformation while the continuum underlying the sharp structure was a result of absorption by the cis isomer. He drew support for his conclusions from his observation that this continuum is temperature dependent in the discrete spectral region. However, if we assume that the continuum in this region arises from transitions to the dissociative II $A_u(n, \pi^*)$ upper electronic state from vibrationally excited levels of the ground state, then the temperature dependence can be explained simply in terms of the Maxwell-Boltzmann

distribution law. It is probable that most of the continuum on the low frequency side is due to extended progressions of "hot" bands.

Because of conjugation, the first $n \rightarrow \pi^*$ discrete absorption in the oxalyl halides appears at considerably longer wavelengths than this absorption in the corresponding carbonyl halides. In terms of energy, the frequencies of the spectra of the oxalyl compounds follow a similar ordering to that observed in the formaldehyde series⁶⁹.



This blue shift of the carbonyl absorption on going from glyoxal to oxalyl fluoride may be due either to

- a) a raising of the π^* -orbital energy through interaction with the halogen p_π system;
- b) greater stabilization of the n-orbital on oxygen through interaction with the n-orbital on the neighbouring halogen; or
- c) a combination of both a) and b).

In difluorodiazirine⁷⁰, where the fluorine atoms do NOT lie in the n-orbital plane, but rather in the π^* -orbital overlap region, the $n \rightarrow \pi^*$ absorption occurs at lower energies than in diazirine itself.

Empirically, the sharpness of the observed bands in the first $n \rightarrow \pi^*$ system of the oxalyl halides decreases in the order $F \rightarrow Cl \rightarrow Br$. We expect that the greater the energy separation between the two lowest π^* levels the less that the upper (n, π^*) state can predissociate the lower one. It is probable that, due to its greater electron-withdrawing power (-I effect), the fluorine is more effective than either chlorine or bromine in raising the energy of the higher π^* level relative to that of the lower π^* level.

CHAPTER 4
THEORY OF ELECTRONIC-VIBRATIONAL SPECTRA

4.1 Harmonic Molecular Vibrations.

Our model for a discussion of molecular vibrations consists of N point masses (atoms) held together at their equilibrium positions by harmonic restoring forces. $3N$ mass-weighted cartesian displacement coordinates η_i , (3 for each atom) describe the system at a given time t . The classical expressions for the kinetic and potential energies in terms of these coordinates are given by equations (4.1) and (4.2), respectively.

$$2T = \sum_{i=1}^{3N} \dot{\eta}_i^2 \quad (4.1)$$

$$2V = \sum_{i,j=1}^{3N} b_{ij} \eta_i \eta_j \quad (4.2)$$

where the b_{ij} 's are constants. When these expressions are substituted into the Lagrangian equations of motion, non-trivial solutions are obtained which are given by the determinantal equation

$$| b_{ij} - \lambda \delta_{ij} | = 0 \quad (i,j=1, \dots, 3N) \quad (4.3)$$

λ is a constant and δ_{ij} is the Krönecker delta symbol. There are $3N-6$ non-zero values of λ for a non-linear molecule, each value of λ corresponding to one normal mode of vibration of the molecule. λ is related to the frequency of simple harmonic oscillation by

$$\lambda = 4\pi^2\nu^2 \quad (4.4)$$

It is possible to define a new set of coordinates Q_i , linearly related to η_i , such that the expressions for the kinetic and potential energies are sums of only squared terms.

$$2T = \sum_{i=1}^{3N} \dot{Q}_i^2 \quad (4.5)$$

$$2V = \sum_{i=1}^{3N} \lambda_i Q_i^2 \quad (4.6)$$

Since the Q_i , called normal coordinates, are orthogonal, the vibrational wave function ψ_v may be written as a product

$$\psi_v = \prod_{i=1}^{3N-6} \psi_i(Q_i) \quad (4.7)$$

Thus we may separate the total vibrational wave equation

$$-\frac{1}{2} \sum_{i=1}^{3N-6} \left(\hbar^2 \frac{\partial^2}{\partial Q_i^2} - \lambda_i Q_i^2 \right) \psi_v = E_v \psi_v \quad (4.8)$$

into $3N-6$ vibrational wave equations, one for each normal coordinate.

$$-\frac{\hbar^2}{2} \frac{\partial^2}{\partial Q_i^2} \psi_i(Q_i) + \frac{\lambda_i}{2} Q_i^2 \psi_i(Q_i) = E_i \psi_i(Q_i) \quad (4.9)$$

($i=1, \dots, 3N-6$)

where

$$E_v = \sum_{i=1}^{3N-6} E_i \quad (4.10)$$

Equation (4.9) is simply that for a linear harmonic oscillator and has eigenvalues

$$E_i = h\nu_i(v_i + \frac{1}{2}) \quad v_i=0,1,2,\dots \quad (4.11)$$

and eigenfunctions which are of the form

$$\psi_i(Q_i) = \mathcal{N}_i^0 \mathbb{H}_{v_i}(\zeta) \exp\left\{-\frac{1}{2} \zeta_i^2\right\} \quad (4.12)$$

where \mathcal{N}_i^0 is a normalizing factor, \mathbb{H}_{v_i} is the Hermite polynomial of degree v_i and

$$\zeta_i = Q_i (\lambda_i^{1/2} / \hbar)^{1/2}.$$

Therefore

$$E_v = (v_1 + \frac{1}{2})h\nu_1 + (v_2 + \frac{1}{2})h\nu_2 + \dots + (v_{3N-6} + \frac{1}{2})h\nu_{3N-6} \quad (4.13)$$

and

$$\psi_v = \mathcal{N}_v H_{v_1}^{(Q_1)} H_{v_2}^{(Q_2)} \dots H_{v_{3N-6}}^{(Q_{3N-6})} \times \exp \left\{ -\frac{1}{2} (\xi_1^2 + \xi_2^2 + \dots + \xi_{3N-6}^2) \right\} \quad (4.14)$$

4.2 Symmetry and Selection Rules.

When we operate on a set of cartesian displacement coordinates ξ_i with some symmetry operator \mathcal{R} the new coordinates ξ'_i which we obtain, will be some linear combination of the original coordinates. In matrix notation,

$$[\xi'] = [R][\xi] \quad (4.15)$$

The character χ for the coordinate representation under the operation \mathcal{R} is simply the trace of the matrix $[R]$.

$$\chi(\Gamma_{3N})_{\mathcal{R}} = \sum_{i=1}^{3N} r_{ii} \quad (4.16)$$

For the oxalyl halides under the point group, C_{2h} , we have

| | | | | |
|---------------------|----|-------|------------|---|
| | E | C_2 | σ_h | i |
| $\chi(\Gamma_{3N})$ | 18 | 0 | 6 | 0 |

The character for vibration may be obtained from $\chi(\Gamma_{3N})$ by subtracting the characters of the representations to which the three translations, T_x , T_y and T_z , and the

three rotations, R_x , R_y and R_z , belong. We find

$$\chi(\Gamma_{\text{vib.}}) \quad \begin{array}{cccc} E & C_2 & \sigma_h & i \\ 12 & 2 & 6 & 0 \end{array}$$

which decomposes to give the direct sum:

$$\Gamma_{\text{vib.}} = 5a_g \oplus 2a_u \oplus b_g \oplus 4b_u \quad (4.17)$$

A similar treatment for the oxalyl halides under the point group C_s gives

$$\Gamma_{\text{vib.}} = 9a' \oplus 3a'' \quad (4.18)$$

The vibrational ground state wave function will transform as a totally symmetric representation of the molecular point group and, in the point groups C_{2h} and C_s , the Hermite polynomials of even degree are all totally symmetric while those of odd degree transform as the normal coordinate Q_i .

In order to derive selection rules for vibrational transitions, we must consider whether or not the appropriate transition moment is zero. What is important in vibration is the change in dipole moment as the molecule vibrates.

$$\mu_x = (\mu_x)_0 + \sum_i \left(\frac{\partial \mu_x}{\partial Q_i} \right)_0 Q_i + \dots \quad (4.19)$$

The transition moment $\int \psi_v'^* \mu_x \psi_v'' d\tau_v$ is non-zero, and thus a transition is allowed with the absorption of infrared radiation provided there is a change of dipole moment with vibration. In addition, within the harmonic approximation, changes in vibrational quantum numbers are governed by the selection rules,

$$\Delta v_i = \pm 1, \quad \Delta v_j = 0 \quad \text{for all } j, j \neq i \quad (4.20)$$

In molecules which possess a centre of symmetry, there is no change of dipole moment during any vibration that is symmetric with respect to inversion and, therefore, vibrations belonging to the symmetry species a_g and b_g of the point group C_{2h} are unallowed in the infrared spectrum.

A similar application of theory to the Raman effect shows that a Raman transition is allowed from the vibrationless ground state (a_g in C_{2h}) to vibrational levels of symmetry a_g and b_g only. These are precisely the symmetry species which are inactive in the infrared spectrum. This mutual exclusion, where "g"-type vibrations are active only in the Raman spectrum and "u"-type vibrations only in the infrared spectrum, is found for all centrosymmetric molecules.

Studies by Hencher and King on the vibrational spectra of oxalyl chloride¹⁶ and oxalyl fluoride¹⁷

failed to show any strong Raman lines that corresponded to frequencies intense in the infrared. This observation may be taken as strong evidence in favour of a centrosymmetric structure for these molecules. The fundamental frequencies found by these authors for oxalyl fluoride and oxalyl chloride are given in Tables 4.1 and 4.2, respectively. The frequencies of the fundamental vibrations observed in the infrared¹⁷ and Raman⁷¹ spectra of oxalyl chloride fluoride are listed in Table 4.3. The infrared spectrum of oxalyl bromide has not been analyzed. The Raman displacements reported for this molecule by Kanda *et al.*¹⁸ are shown in Table 4.4.

The effect of introducing anharmonicity is to modify equation (4.11) for the energy levels to give

$$E_i = (v_i + \frac{1}{2})h\nu_i - x_i(v_i + \frac{1}{2})^2h\nu_i \quad (4.21)$$

The anharmonicity constant x_i is usually small. A second consequence of anharmonicity is that weak bands, where $\Delta v = \pm 2, \pm 3, \dots$, are observed in addition to the harmonic selection rule $\Delta v = \pm 1$. The infrared spectrum will therefore consist of harmonics or overtones, combination and difference bands as well as the fundamental bands.

The derivation of selection rules for vibration when accompanying an allowed electronic transition,

TABLE 4.1

THE GROUND STATE FUNDAMENTAL FREQUENCIES
OF OXALYL FLUORIDE¹⁷

| | <u>Fundamental</u> | | <u>cm⁻¹</u> | <u>Activity</u> |
|----------------|--------------------|------------|------------------------|-----------------|
| a _g | CO stretch | ν_1 | 1872 | R |
| | CF stretch | ν_2 | 1286 | R |
| | CC stretch | ν_3 | 809 | R |
| | CCO scissors | ν_4 | 565 | R |
| | CCO rock | ν_5 | 292 | R |
| a _u | CF wag | ν_6 | 422 ⁺ | IR |
| | CC torsion | ν_7 | 127 ⁺⁺ | IR |
| b _g | CF wag | ν_8 | 420 | R |
| b _u | CO stretch | ν_9 | 1870 | IR |
| | CF stretch | ν_{10} | 1098 | IR |
| | CCO scissors | ν_{11} | 672 | IR |
| | CCO rock | ν_{12} | 255 | IR |

⁺ estimated from Fermi doublet.

⁺⁺ estimated from combination bands.

R = Raman IR = infrared

TABLE 4.2

THE GROUND STATE FUNDAMENTAL FREQUENCIES
OF OXALYL CHLORIDE¹⁶

| | <u>Fundamental</u> | | <u>cm⁻¹</u> | <u>Activity</u> |
|----------------|--------------------|------------|------------------------|-----------------|
| a _g | CO stretch | ν_1 | 1778 | R |
| | CC stretch | ν_2 | 1078 | R |
| | CCl stretch | ν_3 | 619 | R |
| | CCO scissors | ν_4 | 465 | R |
| | CCO rock | ν_5 | 276 | R |
| a _u | CCl wag | ν_6 | 360 | IR |
| | CC torsion | ν_7 | 159 ⁺ | IR |
| b _g | CCl wag | ν_8 | 201 | R |
| b _u | CO stretch | ν_9 | 1790 | IR |
| | CCl stretch | ν_{10} | 778 | IR |
| | CCO scissors | ν_{11} | 520 | IR |
| | CCO rock | ν_{12} | 210 ^{+,++} | IR |

⁺ calculated from combination frequencies.

⁺⁺ observed by R. E. Kagarise (205 cm⁻¹) and F. A. Miller (198 ± 2 cm⁻¹) (private communications, 1966).

TABLE 4.3

THE GROUND STATE FUNDAMENTAL FREQUENCIES
OF OXALYL CHLORIDE FLUORIDE^{17,71}

| | <u>Fundamental</u> | | <u>IR cm⁻¹</u> | <u>R cm⁻¹</u> |
|-----|--------------------|------------|---------------------------|--------------------------|
| a' | CO stretch | ν_1 | 1858 | 1856 |
| | CO stretch | ν_2 | 1790 | 1784 |
| | CF stretch | ν_3 | 1197 | 1212 |
| | CC stretch | ν_4 | 932 | 935 |
| | CCl stretch | ν_5 | 713 | 721 |
| | CCO scissors | ν_6 | 570 | 571 |
| | CCO scissors | ν_7 | 491 | 485 |
| | CCO rock | ν_8 | 287 | - |
| | CCO rock | ν_9 | - ⁺⁺ | 228 |
| a'' | out-of-plane wag | ν_{10} | 409 | 380 |
| | out-of-plane wag | ν_{11} | 360 | 357 |
| | torsion | ν_{12} | 129 ⁺ | - |

⁺ calculated from combination frequencies.

⁺⁺ not observed above 250 cm⁻¹.

TABLE 4.4

RAMAN FREQUENCIES FOR
OXALYL BROMIDE¹⁸

| <u>a_g</u> Fundamentals | | <u>cm⁻¹</u> |
|-----------------------------------|---------|------------------------|
| CO stretch | ν_1 | 1784 ⁺ |
| CC stretch | ν_2 | 1032 |
| CBr stretch | ν_3 | 600 |
| CCO scissors | ν_4 | 415 |
| CCO rock | ν_5 | 191 |

⁺ The strong infrared band at 1817 cm⁻¹ is most likely the antisymmetric (b_u) CO stretch and the b_u C-Br stretch is either 766 or 734 cm⁻¹.

requires a consideration of the transition moment

$$\vec{R}_{ev} = \int \psi'_{ev}{}^* \vec{\mu} \psi''_{ev} d\tau_{ev} \quad (4.22)$$

If we assume that

$$\vec{\mu} = \vec{\mu}_e + \vec{\mu}_v \quad (4.23)$$

and

$$\psi_{ev} = \psi_e \psi_v \quad (4.24)$$

then

$$\begin{aligned} \vec{R}_{ev} &= \int \psi'_v{}^* \psi''_v d\tau_v \int \psi'_e{}^* \vec{\mu}_e \psi''_e d\tau_e \\ &+ \int \psi'_v{}^* \vec{\mu}_v \psi''_v d\tau_v \int \psi'_e{}^* \psi''_e d\tau_e \end{aligned} \quad (4.25)$$

$$\vec{R}_{ev} = \vec{R}_e \int \psi'_v{}^* \psi''_v d\tau_v \quad (4.26)$$

since the electronic wave functions are orthogonal.

\vec{R}_e is a mean electronic transition moment. Thus, a transition is allowed from a vibrational level of the lower state ($\psi''_e \psi''_v$) to a vibrational level of the upper state ($\psi'_e \psi'_v$) only if the two vibrational levels are of the same symmetry species. While there is no restriction on the change of vibrational quantum number for a totally symmetric vibration, quantum numbers for non-totally symmetric vibrations can only change by an even number

$$\Delta v = 0, \pm 2, \pm 4, \dots$$

A series of bands, formed by transitions which

originate on a common vibrational level in one electronic state and terminate on successive levels in the other state, is called a progression. If the particular level in common is a ground state level, then the bands form a progression in the excited state frequency. Such a progression is illustrated in Figure 4.1a where all transitions arise from the vibrationless ground state. The progression, $v' = 0 \leftarrow v'' = 0$, $v' = 1 \leftarrow v'' = 0$, ..., $v' = n \leftarrow v'' = 0$ is termed an (n-0) progression.

The various transitions which form a sequence have $v' - v'' = \text{constant}$. The most common type of sequence is one where $v' - v'' = 0$. An example of such an n-n sequence is shown in Figure 4.1b. Sequences may be found in vibrations of any one symmetry species in the ground and excited states.

4.3 The Franck-Condon Effect.

According to equation (4.26), the intensity of a vibronic (vibrational-electronic) transition in a molecule depends on the magnitude of the integral

$$\int \psi_v'^* \psi_v'' d\tau_v.$$

The Principle of Franck⁷² and Condon⁷³ assumes that an electronic transition in a molecule takes place in a negligibly short time compared to the period of nuclear vibration. That is, it is assumed there is no

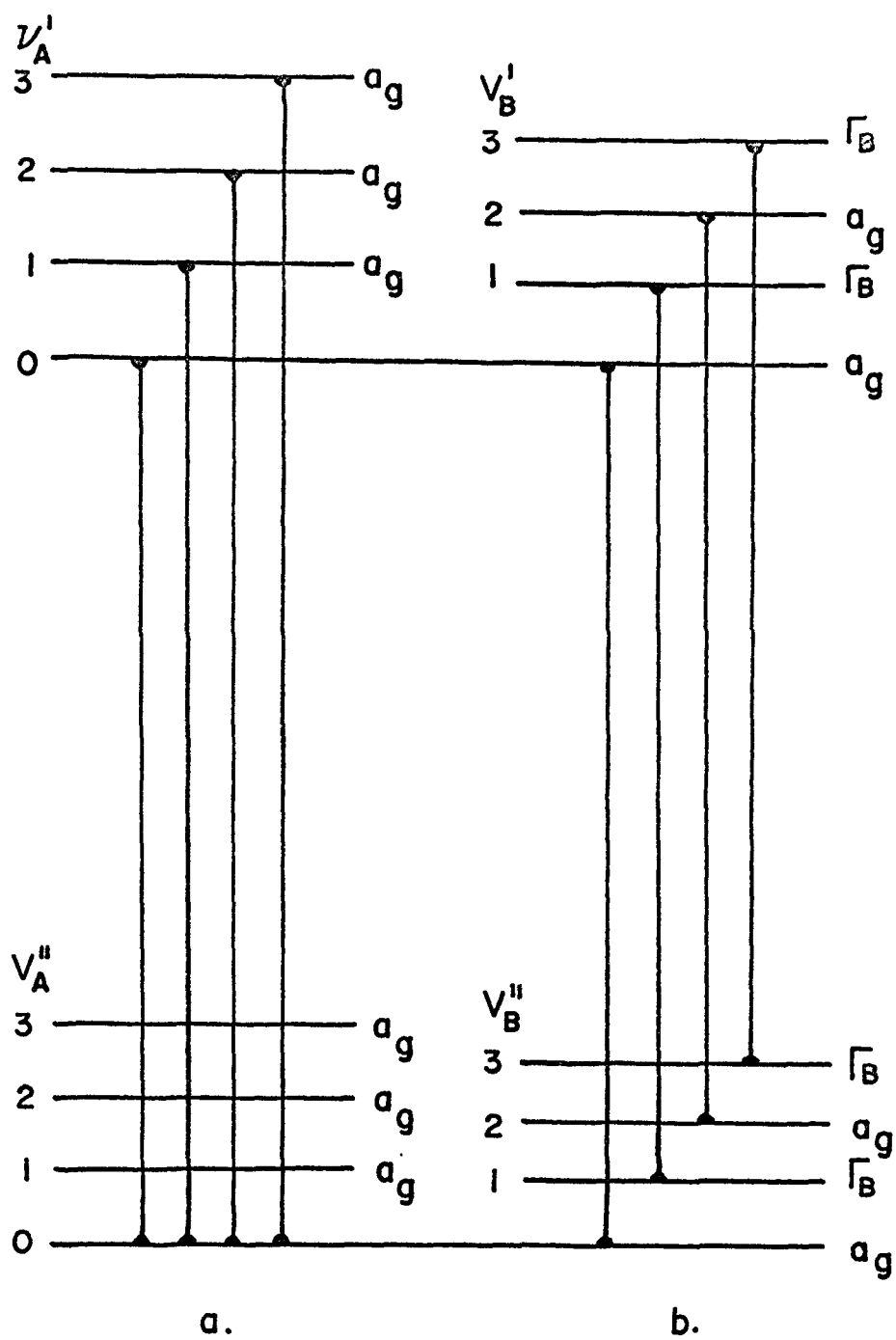


FIGURE 4-1

a. n - o progression

b. n - n sequence

change of position or velocity of the nuclei in a molecule during electronic excitation.

We consider the example of a diatomic molecule with a ground state equilibrium nuclear separation of r_e'' and excited state separation of r_e' . (Figure 4.2.)

The classical picture of Franck states that the vertical transition, $0 \rightarrow n$, will be the most probable one and thus, the most intense. Quantum mechanically, the same conclusion may be arrived at by considering the overlap of the various excited state wave functions, ψ_{v_n}' , with that of the vibrationless ground state, ψ_{v_0}'' . Apart from a small dependence on the change in elastic constants, the intensity distribution is governed by the change q in molecular dimensions in the two electronic states.

$$q = |r_e' - r_e''| \quad (4.27)$$

The relative intensity distribution is given by

$$I_n = k' \frac{\nu_{on}}{\nu_{oo}} \left[\int \psi_{v_n}'^* \psi_{v_0}'' d\tau_v \right]^2 \quad (4.28)$$

I_n is the intensity (relative to the (0,0) band) of the transition from $v'' = 0$ to $v' = n$ and ν_{on} is the frequency for this transition. ν_{oo} is the corresponding frequency for the (0,0) transition, while k' is a constant.

Craig⁷⁴ has shown that, using harmonic oscillator

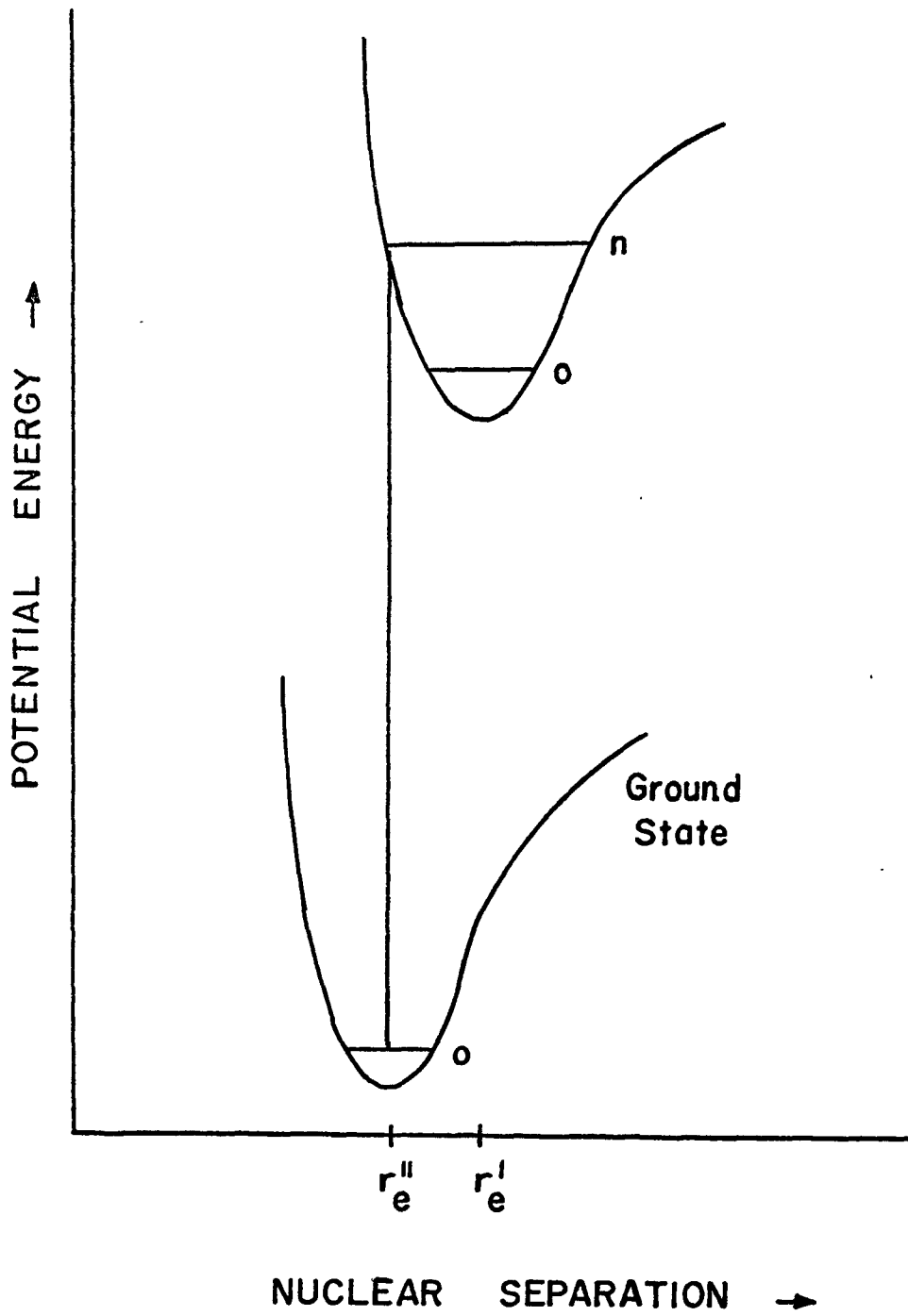


FIGURE 4.2 THE FRANCK-CONDON EFFECT

wave functions, the overlap integral in equation (4.28) may be written in closed form.

$$\int \psi_{v_n}'^* \psi_{v_0}'' d\tau_v = \exp \left\{ -\beta_1 q^2 / 2(1+\rho) \right\} \\ \times \sum_{r=1}^n \left(\frac{\sqrt{\beta_2} q \rho}{1+\rho} \right)^{n-r} \left(\frac{n!}{r!(n-r)!} \right)^{1/2} \left(\frac{2^{n-r}}{(n-r)!} \right)^{1/2} S_{or} \quad (4.29)$$

where, for r even,

$$S_{or} = \frac{1}{(r/2)!} \sqrt{\frac{r!}{2^r}} \left(\frac{2\sqrt{\rho}}{1+\rho} \right)^{1/2} \left(\frac{1-\rho}{1+\rho} \right)^{r/2} \quad (4.3)$$

and for r odd,

$$S_{or} = 0.$$

ρ is the ratio of the vibrational frequencies in the ground and excited states.

$$\rho = \frac{\nu''}{\nu'}; \quad \beta = (2\pi/h) \sqrt{\mu k}$$

where μ is the reduced mass and k , the force constant,
 $= 4\pi^2 \nu^2 \mu$. β_1 refers to the ground state, β_2 to the upper state.

Craig's formulae have been applied successfully to progressions in benzene⁷⁴, acetylene⁷⁵, and propynal⁷⁶. Howe and Goldstein used the derived expressions to calculate the approximate increase in the carbonyl bond length for propynal using a pseudo-diatomic model with the oxygen being one point mass and the rest of the

molecule being the other. Their agreement with the values predicted from Clark's rule⁷⁷, Badger's rule⁷⁸ and the empirical curve of Layton and collaborators⁷⁹ was good.

In the I ${}^1A_u \leftarrow {}^1A_g$ spectral system of oxalyl chloride, a prominent progression is observed in a vibrational frequency of 1460 to 1420 cm^{-1} . This excited state frequency is assigned to the symmetric carbonyl stretching mode (ν_1') which has a ground state value of 1778 cm^{-1} (Raman, liquid). The vapour pressure, 139 mm Hg at 23° C, is sufficiently high to enable intensity measurements to be made on the carbonyl progression with a Cary 14 spectrophotometer. The observed and calculated intensity distributions are listed in Table 4.5.

A value of $\sim 0.08 \text{ \AA}$ for the change in carbonyl bond length agrees well with the observed intensity data. In Table 4.6 a comparison is given for the estimates of Δr_{CO} from the various semi-empirical methods.

Although the Franck-Condon calculation does not determine the sign of the bond length change, Clark's and Badger's rules indicate that the carbonyl bond lengthens in the excited state as simple molecular orbital theory predicts.

No Franck-Condon calculations were carried out for either oxalyl bromide or oxalyl fluoride since the

TABLE 4.5

RELATIVE INTENSITIES OF CARBONYL PROGRESSION
IN OXALYL CHLORIDE

| Band $v'' \rightarrow v'$ | $\overset{q}{=}0.076 \text{ \AA}$ | $\overset{q}{=}0.077 \text{ \AA}$ | $\overset{q}{=}0.078 \text{ \AA}$ | $\overset{q}{=}0.079 \text{ \AA}$ | Obsd. |
|------------------------------|-----------------------------------|-----------------------------------|-----------------------------------|-----------------------------------|-------|
| 0 \rightarrow 0 | 1.00 | 1.00 | 1.00 | 1.00 | 1.00 |
| 0 \rightarrow 1 | 2.24 | 2.30 | 2.36 | 2.42 | 2.14 |
| 0 \rightarrow 2 | 2.27 | 2.40 | 2.53 | 2.67 | 2.52 |
| 0 \rightarrow 3 | 1.38 | 1.50 | 1.64 | 1.78 | 1.64 |
| 0 \rightarrow 4 | 0.55 | 0.62 | 0.70 | 0.79 | 0.73 |

$$\begin{aligned}
 \nu''_{\text{CO}} &= 1778 \text{ cm}^{-1}, & \nu'_{\text{CO}} &= 1462 \text{ cm}^{-1} \\
 \nu_{00} &= 27192 \text{ cm}^{-1}; & \nu_{01} &= 28651 \text{ cm}^{-1}; \\
 \nu_{02} &= 30075 \text{ cm}^{-1}; & \nu_{03} &= 31495 \text{ cm}^{-1}; \\
 & & \nu_{04} &= 32960 \text{ cm}^{-1}.
 \end{aligned}$$

TABLE 4.6

CARBONYL BOND LENGTH CHANGES IN

$$I \ ^1A_u \leftarrow \ ^1A_g \text{ SYSTEM}$$

OF $(COCl)_2$

| <u>Method</u> | <u>r'_e/r''_e</u> | <u>$q(\text{\AA})^+$</u> |
|----------------------|--------------------------------|-------------------------------------|
| Clark's Rule | 1.07 | +0.08 |
| Badger's Rule | 1.06 | +0.07 |
| Layton <u>et al.</u> | 1.07 | +0.08 |
| Franck-Condon | 1.07 | ± 0.08 |

⁺ assumed $r''_{CO} = 1.195 \text{ \AA}$.

vapour pressure of the former is very low (19 mm Hg at 23° C), while the I ${}^1A_u \leftarrow {}^1A_g$ spectrum of the latter is strongly predissociated in the region of the higher members of the carbonyl progression. The results for some empirical calculations are compared in Table 4.7.

TABLE 4.7

CHANGES IN CARBONYL BOND LENGTHS IN THE
 $I \ ^1A_u \leftarrow \ ^1A_g$ SYSTEMS OF SOME OXALYL COMPOUNDS

| | $\Delta r_{co}(\text{\AA})$ | | | |
|---------------------------|-----------------------------|------------|------------|-----------|
| | $(COF)_2$ | $(COCl)_2$ | $(COBr)_2$ | $(CHO)_2$ |
| Clark's Rule | +0.11 | +0.08 | +0.06 | +0.10 |
| Badger's Rule | +0.10 | +0.07 | +0.05 | +0.09 |
| Layton <u>et al.</u> | +0.11 | +0.08 | +0.06 | +0.10 |
| assumed $r''(\text{\AA})$ | 1.18 | 1.195 | 1.17 | 1.22 |
| average r'/r'' | 1.09 | 1.07 | 1.03 | 1.08 |

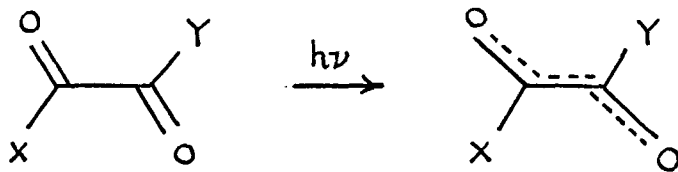
CHAPTER 5

VIBRATIONAL ANALYSES OF THE FIRST ${}^1A_u \leftarrow {}^1A_g$ $n \rightarrow \pi^*$ SYSTEMS OF THE OXALYL HALIDES.

5.1 Introduction.

In general appearance, the first singlet-singlet $n \rightarrow \pi^*$ absorption systems of the oxalyl halides show resemblances to the corresponding spectra of other, similar, conjugated carbonyl compounds. Vibrational analyses have been reported for glyoxal⁶⁰, biacetyl⁶², propenal^{80,81} and propynal⁵⁸, and it is found that small geometry changes on excitation occur in these molecules.

The simple valence-bond picture predicts that $n \rightarrow \pi^*$ promotion in the oxalyl halides should lead to a redistribution of π -electron density.



The geometry changes accompanying such a rearrangement can be predicted as

- a) an extension of the C=O bond; and
- b) a shortening of the C-C bond.

A change of hybridization at the carbon atom may result in a change of $\hat{C}CO$.

We therefore expect from the Franck-Condon Principle, that the totally symmetric CO and CC stretching and also the two in-plane symmetric bending vibrations will be active in forming progressions. The extent to which the carbon-halogen symmetric stretching frequency is active in the spectrum will depend on how much of the internal coordinate for CO bond stretching contributes to the normal coordinate which describes the carbon-halogen stretch. However, we must not overlook the fact that, when setting up crude molecular orbitals, we ignored any contribution that the p and d electrons of the halogen atoms may make to these.

Detailed analyses of the vibrational structure of the singlet-singlet electronic transitions of the oxalyl halides are presented in the following sections. For these, as well as for the singlet-triplet transitions analyzed in the subsequent chapter, all of the more intense band features are accounted for. Some additional, very weak or diffuse headlike features observed under high resolution, whose identity is less certain, have also been observed but are not listed in the tables.

In the assignment of vibrational quantum numbers we adopt the convention of Brand and Watson⁸² where transitions are labelled $A_q^p B_s^r \dots$. The labels A, B, ... etc. refer to the number of the vibration in the ground state (see Tables 4.1 to 4.4); while the superscripts and subscripts refer to the number of quanta excited in the upper and lower states, respectively. The origin band is denoted by O_0^0 .

5.2 Oxalyl chloride.

a) Introduction.

The bands of the I ${}^1A_u \leftarrow {}^1A_g$ system of oxalyl chloride appear sharp under high resolution and, in many cases, the absorption bands of the naturally-occurring isotopic species $(CO^{35}Cl)_2$, $CO^{35}ClCO^{37}Cl$, and $(CO^{37}Cl)_2$ are sufficiently well resolved to aid in the analysis. The bands in the spectrum of each isotopic species are double-headed and degraded to the violet; all measurements in Table 5.1 refer to the more intense lower frequency head. The separation between the two heads is $\sim 3.5 \text{ cm}^{-1}$.

The origin band is located at 27188.9 cm^{-1} and going from this to higher frequencies we find a long progression in the totally symmetric carbonyl stretching vibration at $\sim 1450 \text{ cm}^{-1}$ in the upper state. The

intervals between successive members of this progression are not regular which suggests that a vibrational perturbation, possibly Fermi resonance, is present. Each member of the carbonyl progression acts as a pseudo-band origin so that, effectively, the spectrum repeats itself about every 1450 cm^{-1} .

b) Ground state intervals.

The strong bands[†] on the low frequency side of the origin, found at $\nu_{00} - 498.5 \text{ cm}^{-1}$ and $\nu_{00} - 1217.1 \text{ cm}^{-1}$ are assigned as 4_1^0 and 2_1^0 , respectively. In oxalyl chloride ν_4 is the symmetric scissors motion and ν_2 is the CC stretching motion. The Raman displacements observed¹⁶ for these modes are 465 cm^{-1} (very broad) and 1078 cm^{-1} .

Weak bands, 5_1^0 , 3_1^0 and 1_1^0 are found at $\nu_{00} - 283.0$, $\nu_{00} - 612.1$ and $\nu_{00} - 1783.3 \text{ cm}^{-1}$, respectively. The frequencies for ν_5'' (COCl rocking mode), ν_3'' (C-Cl stretch) and ν_1'' (C=O stretch) have been observed¹⁶ at 276, 619 and 1778 cm^{-1} , respectively, by Raman spectroscopy on the liquid.

[†] For simplicity, only the frequencies of the most abundant isotopic species (CO^{13}Cl)₂, are referred to here.

c) Excited state fundamentals.

The gross structure of the spectrum to higher frequencies is readily explained in terms of the five totally symmetric excited state fundamentals, 281.8, 398.5, 619.2, 970, and 1460 cm^{-1} which are $\nu'_5 - \nu'_1$, respectively. (Here, and throughout the thesis, the numbering of the excited state vibrations is the same as in the ground state.). The intensity distribution of the bands is very similar to that found in the oxalyl bromide spectrum (see Section 5.3), where 4^1_0 and 1^1_0 are very strong, while 5^1_0 , 3^1_0 and 2^1_0 are of medium intensity. Four members of the ν'_5 progression and two members of the ν'_4 progression have been identified.

Brand and coworkers⁸³ have found that the chlorine vibrational isotope shifts in the 5340 Å band system of thiocarbonyl chloride are linear in the quantum numbers. This is also found in the spectrum of oxalyl chloride. Figure 5.1 shows the experimental isotope effect (in the excited state) for the two in-plane symmetric bending vibrations ν'_5 and ν'_4 . For the vibrational modes ν_5 , ν_4 and ν_3 (C-Cl stretch), where considerable motion of the chlorine atoms is involved, the excited state isotopic splittings are fairly large. $\nu(\text{CO}^{35}\text{Cl})_2 - \nu(\text{CO}^{35}\text{ClCO}^{37}\text{Cl})$ is +1.8 cm^{-1} for ν'_5 , +2.6 cm^{-1} for ν'_4 and +2.8 cm^{-1} for ν'_3 .

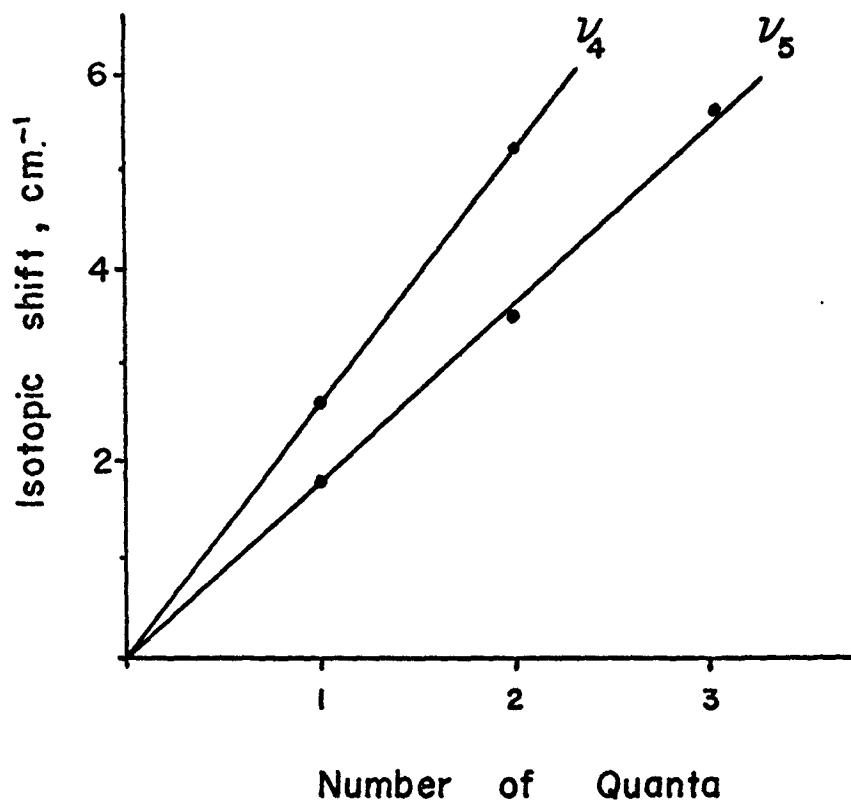


FIGURE 5.1 THE CHLORINE VIBRATIONAL ISOTOPE EFFECT IN THE $1A_u-1A_g$ SYSTEM OF OXALYL CHLORIDE.

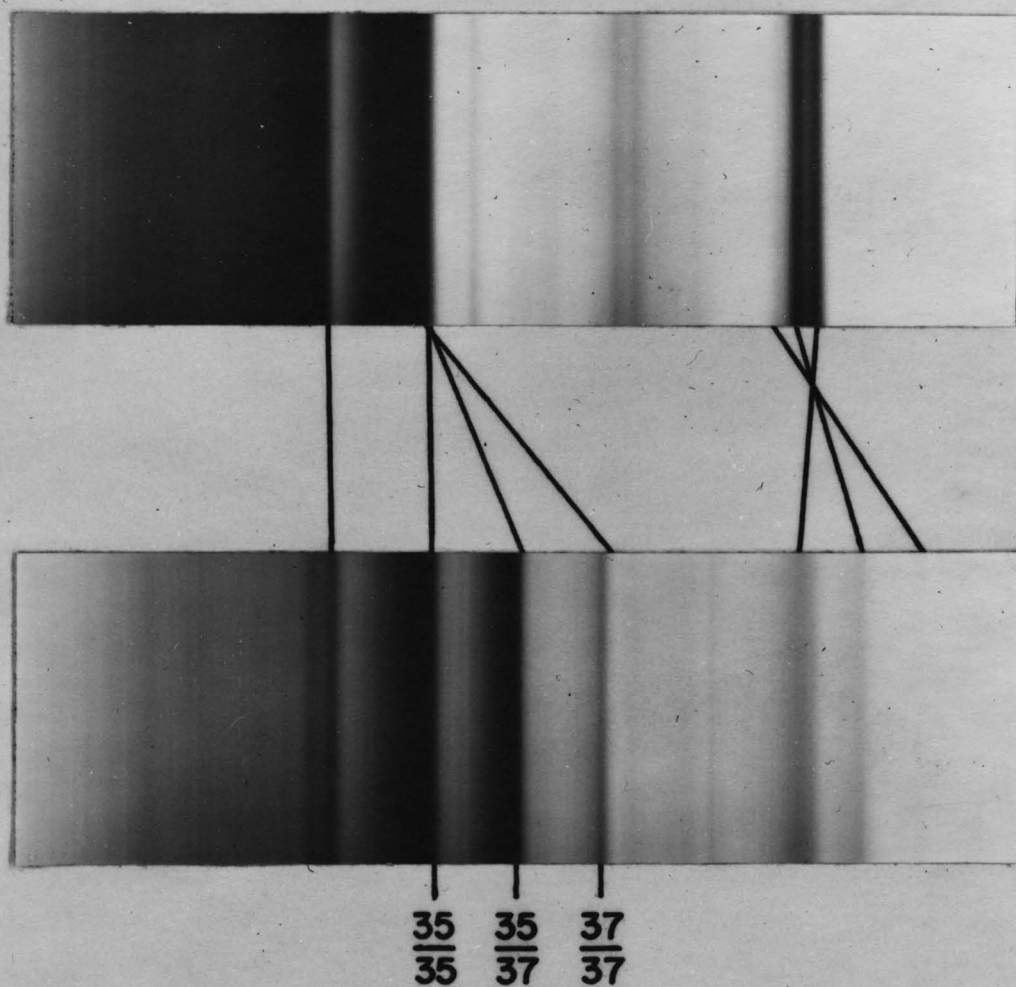


FIGURE 5.2 THE CHLORINE VIBRATIONAL ISOTOPE EFFECT IN THE $1A_u-1A_g$ SYSTEM OF OXALYL CHLORIDE.

Upper O_o^o , Lower 4_o^i

Figure 5.2 contains photographs of the 0_0^0 and 4_0^1 bands of the I ${}^1A_u \leftarrow {}^1A_g$ system of oxalyl chloride taken at a resolving power of 150,000. The relative intensities of the bands belonging to $(CO^{35}Cl)_2$, $CO^{35}ClCO^{37}Cl$, and $(CO^{37}Cl)_2$ follow the 9:6:1 predicted from natural abundance ratios⁸⁴. The isotopic splitting in the (0,0) band is not resolved, indicating that

$$\left| \nu_{00}(CO^{35}Cl)_2 - \nu_{00}(CO^{35}ClCO^{37}Cl) \right| < 0.2 \text{ cm}^{-1}$$

This agrees well with the observation in Figure 5.1 that the lines of ν_5' and ν_4' both extrapolate to the graphic origin, within experimental error.

In addition to being useful in assigning fundamentals and overtones in the spectrum, the vibrational isotope effect has proved of great value in confirming the assignment of combination bands. The combination band $4_0^1 5_0^1$ is particularly strong in the spectra of the oxalyl halides. In the spectrum of oxalyl chloride, the isotopic splitting in this band is exactly the sum of the individual splittings in $4_0^1 5_0^1$.

d) Sequences.

Three sequence intervals have been identified in the singlet-singlet spectrum; + 78.2, + 31.5 and - 11.8 cm^{-1} . The + 78 cm^{-1} and - 12 cm^{-1} sequences are strong but the + 32 cm^{-1} sequence is relatively weak.

The intensity of the + 78 cm^{-1} sequence suggests that a low-lying ($\nu'' < 200 \text{ cm}^{-1}$) non-totally symmetric vibration is involved, most probably the torsion ν_7 . The isotopic splitting in the first sequence member is $\sim 1.0 \text{ cm}^{-1}$.

Similar prominent sequences are found in oxalyl fluoride, oxalyl chloride fluoride and oxalyl bromide where the respective intervals are + 97.0, + 84 and + 65 cm^{-1} .

Three members of the - 12 cm^{-1} sequence are observed at room temperature indicating that the frequency responsible has a low ground state value. This sequence is assigned to the lowest-lying b_u vibration, ν_{12} . ($\nu_{12}'' = 198 \text{ cm}^{-1}$). The + 32 cm^{-1} sequence is thought to involve $\nu_6(a_u)$, the out-of-plane oxygen wagging motion.

e) Discussion.

The band at $\nu_{oo} - 1217.1 \text{ cm}^{-1}$ is assigned as 2_1^0 despite the large difference between the ultraviolet and Raman values. The polarization of the band is perpendicular like the origin and progressions and sequence intervals built upon it indicate that the band belongs to the singlet-singlet system. We expect the CC "hot" band to be present with appreciable intensity since

$\nu_{oo} - \nu_{cc}''$ appears as the most strong band at low frequencies in the $I \ ^1A_u \leftarrow \ ^1A_g$ spectrum of oxalyl fluoride. (Section 5.4) There is no band near $\nu_{oo} - 1078 \text{ cm}^{-1}$ which can reasonably be assigned to 2_1^0 and $\nu_{oo} - 1217.1 \text{ cm}^{-1}$

cannot be explained in terms of any known ground state frequencies.

The difference between ultraviolet and Raman frequencies is also anomalously large for ν''_{CC} in oxalyl bromide and glyoxal, although liquid and gas phase values of ν''_{CC} in oxalyl fluoride and oxalyl chloride fluoride are almost equal. In glyoxal, the ultraviolet spectrum gives $\nu''_{CC} = 1207 \text{ cm}^{-1}$ in contrast to the value of 1060 cm^{-1} deduced from the infrared spectrum⁸⁵.

No reason for the large ν''_{CC} frequency shift between phases is apparent; intermolecular interactions, for example hydrogen-bonding in glyoxal and $\text{C-X} \cdots \text{O}=\text{C}$ charge transfer bonding in oxalyl chloride and bromide, would be expected to influence the symmetric CO stretching vibration also and this is not found.

The $+ 78 \text{ cm}^{-1}$ sequence is assigned to the torsional mode by analogy with the spectra of glyoxal and propenal. Prominent positively-running sequences have been observed for these molecules, ($+ 106$ and $+ 92 \text{ cm}^{-1}$, respectively). Brand was able to verify his assignments in glyoxal by identifying both ground and excited state overtone bands. However, in spite of a thorough search, no bands which could be assigned with certainty to 7_0^2 and 7_2^0 could be identified in the spectrum of oxalyl chloride.

The Boltzmann factors for ν''_9 (1790 cm^{-1}) and

ν''_{10} (778 cm^{-1}) will be low and it is unlikely that the $+ 32 \text{ cm}^{-1}$ sequence involves either of these modes. In addition, the assignment of the a_g fundamentals shows that no vibration of this symmetry species is responsible for the $+ 32 \text{ cm}^{-1}$ sequence. This leaves three possible modes ν'_{11} (b_u scissors motion) and the two out-of-plane C=O bending vibrations, $\nu'_6(a_u)$ and $\nu'_8(b_g)$. Since the symmetric analogue of ν'_{11} , namely ν'_4 , drops from 498.5 to 398.5 cm^{-1} on excitation, it is unlikely that ν'_{11} will show an increase of 32 cm^{-1} . The $+ 32 \text{ cm}^{-1}$ sequence is tentatively assigned to ν'_6 . This is reasonable in view of the fact that the same vibrational motion ($\nu'_{30}; b_{3u}$ under D_{2h}) gives prominent sequences of $+ 34 \text{ cm}^{-1}$ in the $n \rightarrow \pi^*$ electronic spectrum of p-benzoquinone^{86,87}.

A small section of the spectrum is shown in Figure 5.3. The assigned spectral bands may be found in Table 5.1 and a complete list of observed frequencies is given in the Appendix, Table A.1.

5.3 Oxalyl bromide.

a) Introduction.

All bands of the I ${}^1A_u \leftarrow {}^1A_g$ system of oxalyl bromide appear diffuse under high resolution. Vacuum wavenumbers for the observed spectral heads are given in the Appendix, Table A.2.

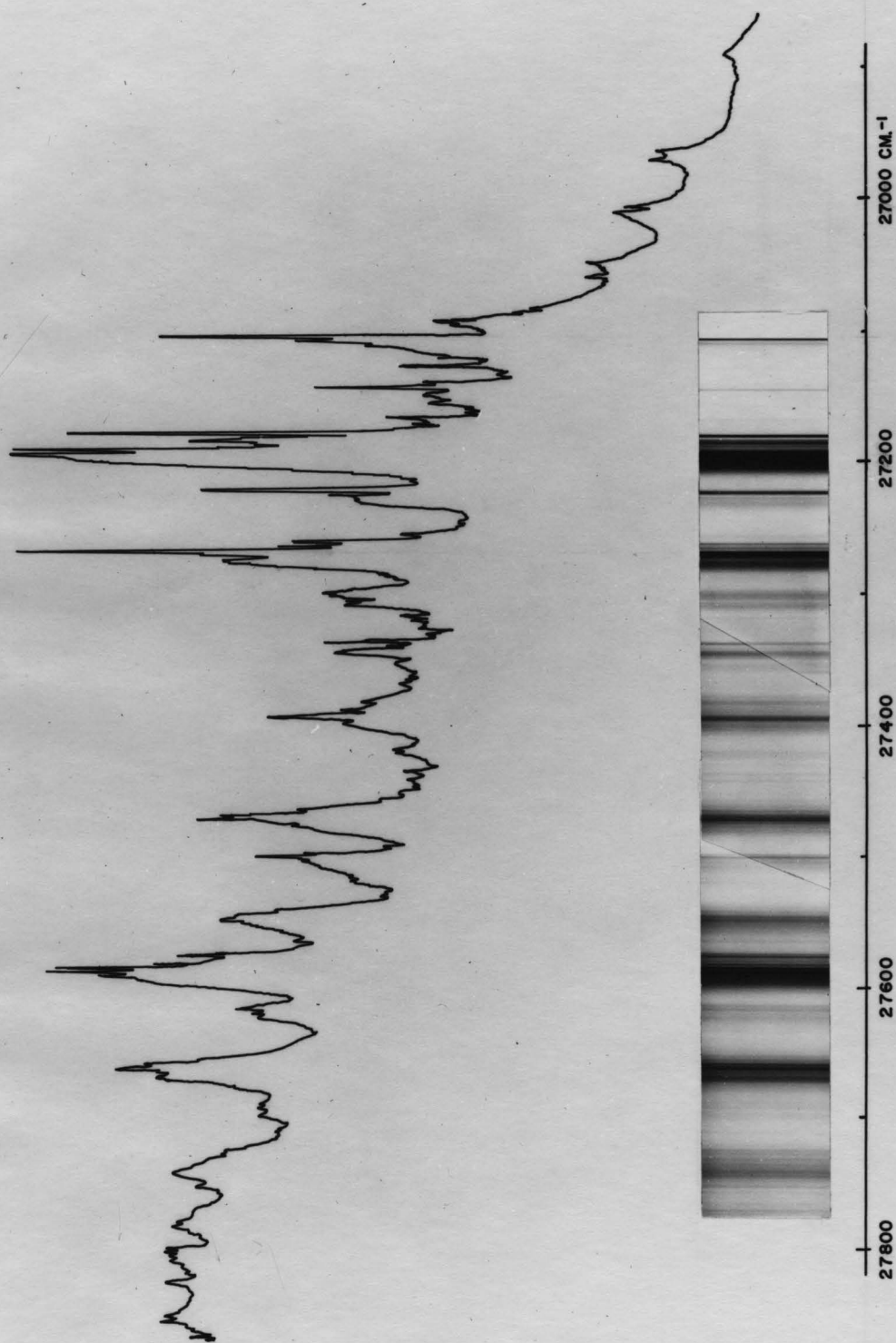


FIGURE 5.3 THE ${}^1A_u \leftarrow {}^1A_g$ ABSORPTION SPECTRUM OF $(\text{COCl})_2$ IN THE REGION 3710 - 3590 \AA

TABLE 5.1

THE I ${}^1A_u \leftarrow {}^1A_g$ ABSORPTION SPECTRUM OF
 $(CO^{35}Cl)_2$

| cm^{-1}^+ | Int. | Notation | Assignment |
|-------------|------|--------------------------|--------------------------|
| 25890.2 | vvvw | $2_1^{\circ} 11_1'$ | $\nu_{oo} - 1217.1-81.6$ |
| 940.5 | vvvw | $2_1^{\circ} 12_3^3$ | - 1217.1-10.8-10.4-10.1 |
| 950.6 | vw | $2_1^{\circ} 12_2^2$ | - 1217.1-10.8-10.4 |
| 961.0 | w | $2_1^{\circ} 12_1'$ | - 1217.1-10.8 |
| 971.8 | mw | 2_1° | - 1217.1 |
| 26007.2 | vw | $2_1^{\circ} 6_1'$ | - 1217.1+35.4 |
| 052.3 | w | $2_1^{\circ} 7_1'$ | - 1217.1+80.5 |
| 087.5 | vvw | $2_1^{\circ} 6_1' 7_1'$ | - 1217.1+80.5+35.2 |
| 136.7 | vw | $2_1^{\circ} 7_2^2$ | - 1217.1+80.5+84.4 |
| 178.6 | vw | $2_1^{\circ} 8_0'$ | - 1217.1+206.8 |
| 256.0 | vvw | $2_1^{\circ} 7_1' 8_0'$ | - 1217.1+206.8+77.4 |
| 257.3 | vw | $2_1^{\circ} 5_0'$ | - 1217.1+285.5 |
| 287.0 | vvw | $2_1^{\circ} 4_0' 11_1'$ | - 1217.1+398.6-83.4 |
| 331.9 | vvw | $2_1^{\circ} 5_0' 7_1'$ | - 1217.1+285.5+74.3 |
| 370.4 | mw | $2_1^{\circ} 4_0'$ | - 1217.1+398.6 |
| 406.8 | vvvw | $2_1^{\circ} 4_0' 6_1'$ | - 1217.1+398.6+36.4 |
| 447.6 | vvw | $2_1^{\circ} 4_0' 7_1'$ | - 1217.1+398.6+77.2 |
| 477.4 | vvw | 6_2° | - 2(355.8) |
| 543.8 | vvw | $2_1^{\circ} 5_0^2$ | - 1217.1+285.5+286.5 |
| 576.8 | vw | 3_1° | - 612.1 |

| cm^{-1} | Int. | Notation | Assignment |
|------------------|------|----------------------|---------------------------|
| 26590.2 | mw | $2_1^0 3_0^1$ | $\nu_{00} - 1217.1+618.4$ |
| 605.3 | vvw | $4_1^0 11_1^1$ | - 498.5-85.1 |
| 628.7 | vvw | 5_2^0 | - 283.0-277.2 |
| 643.0 | mw | $2_1^0 4_0^1 5_0^1$ | - 1217.1+398.6+272.6 |
| 652.7 | vvw | $3_1^0 7_1^1$ | - 612.1+75.9 |
| 666.1 | vw | $4_1^0 12_2^2$ | - 498.5-12.1-12.2 |
| 678.3 | mw | $4_1^0 12_1^1$ | - 498.5-12.1 |
| 690.4 | m | 4_1^0 | - 498.5 |
| 722.7 | mw | $4_1^0 6_1^1$ | - 498.5+32.3 |
| 757.4 | vvw | $4_1^0 7_1^1 12_1^1$ | - 498.5+78.8-11.8 |
| 769.2 | mw | $4_1^0 7_1^1$ | - 498.5+78.8 |
| 802.5 | w | $4_1^0 6_1^1 7_1^1$ | - 498.5+78.8+33.3 |
| 848.2 | vw | $4_1^0 7_2^2$ | - 498.5+78.8+79.0 |
| 883.1 | vw | $4_1^0 6_1^1 7_2^2$ | - 498.5+78.8+79.0+34.9 |
| 896.5 | vw | $4_1^0 8_0^1$ | - 498.5+206.1 |
| 905.9 | vw | 5_1^0 | - 283.0 |
| 924 | vvvw | $4_1^0 7_3^3$ | - 498.5+78.8+79.0+76 |
| 973.8 | vw | $4_1^0 5_0^1$ | - 498.5+283.4 |
| 27012.1 | vvw | 11_2^2 | - 84.6-92.4 |
| 088.6 | vvvw | 4_1^1 | - 498.5+398.2 |
| 091.8 | vvvw | $11_1^1 12_1^1$ | - 84.6-12.5 |
| 104.3 | ms | 11_1^1 | - 84.6 |
| 137.8 | vvw | $6_1^1 11_1^1$ | - 84.6+33.5 |
| 153.4 | vvvw | 12_3^3 | - 11.8-11.8-11.9 |

| cm^{-1} | Int. | Notation | Assignment |
|------------------|------|-------------------------|------------------------|
| 27165.3 | vw | 12_2^2 | $\nu_{00} - 11.8-11.8$ |
| 170.0 | mw | $7_1^1, 11_1^1, 12_1^1$ | + 78.4-84.5-12.8 |
| 177.1 | ms | 12_1^1 | - 11.8 |
| 182.8 | vw | $7_1^1, 11_1^1$ | + 78.4-84.5 |
| 188.9 | s | 0_0^0 | origin |
| 220.5 | m | 6_1^1 | + 31.6 |
| 255.4 | vw | $7_1^1, 12_1^1$ | + 78.4-11.9 |
| 267.3 | ms | 7_1^1 | + 78.4 |
| 299.6 | w | $6_1^1, 7_1^1$ | + 78.4+32.3 |
| 345.7 | w | 7_2^2 | + 78.4+78.4 |
| 387.6 | w | $5_0^1, 11_1^1$ | + 281.8-83.1 |
| 392.5 | mw | 8_0^1 | + 203.6 |
| 423.2 | vvvw | 7_3^3 | + 78.4+78.4+77.5 |
| 468.4 | w | $7_1^1, 8_0^1$ | + 203.6+75.9 |
| 470.7 | mw | 5_0^1 | + 281.8 |
| 499.3 | w | $4_0^1, 11_1^1$ | + 398.5-88.1 |
| 503.2 | vvw | $5_0^1, 6_1^1$ | + 281.8+32.5 |
| 547.6 | w | $5_0^1, 7_1^1$ | + 281.8+76.9 |
| 564.4 | vvw | $4_0^1, 12_2^2$ | + 398.5-11.5-11.5 |
| 575.9 | mw | $4_0^1, 12_1^1$ | + 398.5-11.5 |
| 587.4 | ms | 4_0^1 | + 398.5 |
| 617.6 | vw | $4_0^1, 6_1^1$ | + 398.5+30.2 |
| 663.9 | mw | $4_0^1, 7_1^1$ | + 398.5+76.5 |
| 724.5 | mw | $3_0^1, 11_1^1$ | + 619.2-83.6 |

| cm ⁻¹ | Int. | Notation | Assignment |
|------------------|------|---|------------------------------|
| 27739.9 | w | 4 ₀ ¹ 7 ₂ ² | $\nu_{00} + 398.5+76.5+76.0$ |
| 750.1 | w | 5 ₀ ² | + 281.8+279.4 |
| 808.1 | w | 3 ₀ ¹ | + 619.2 |
| 815.3 | vvw | 4 ₀ ¹ 7 ₃ ³ | + 398.5+76.5+76.0+75.4 |
| 864.3 | w | 4 ₀ ¹ 5 ₀ ¹ | + 398.5+276.9 |
| 942.1 | vw | 4 ₀ ¹ 5 ₀ ¹ 7 ₁ ¹ | + 398.5+276.9+77.8 |
| 985.3 | vvw | 4 ₀ ² | + 398.5+397.9 |
| 28024.9 | vw | 5 ₀ ³ | + 281.8+279.4+274.8 |
| 061.9 | vvw | 4 ₀ ² 7 ₁ ¹ | + 398.5+397.9+76.6 |
| 144 | w | 1 ₀ ¹ 4 ₁ ⁰ | + 1460-505 |
| 159 | s | 2 ₀ ¹ | + 970 |
| 172 | w | 1 ₀ ¹ 4 ₁ ⁰ 6 ₁ ¹ | + 1460-505+34 |
| 212 | w | 1 ₀ ¹ 4 ₁ ⁰ 7 ₁ ¹ | + 1460-505+74 |
| 239 | s | 2 ₀ ¹ 7 ₁ ¹ | + 970+80 |
| 358 | mw | 2 ₀ ¹ 8 ₀ ¹ | + 970+201 |
| 438 | m | 2 ₀ ¹ 5 ₀ ¹ | + 970+279 |
| 563 | s | 1 ₀ ¹ 11 ₁ ¹ | + 1460-86 |
| 649 | } vs | 1 ₀ ¹ | + 1460 |
| 662 | | | |
| 728 | } s | 1 ₀ ¹ 7 ₁ ¹ | + 1460+79 |
| 736 | | | |
| 802 | vw | 1 ₀ ¹ 7 ₂ ² | + 1460+79+74 |
| 845 | w | 1 ₀ ¹ 8 ₀ ¹ | + 1460+196 |
| 924 | } m | 1 ₀ ¹ 5 ₀ ¹ | + 1460+275 |
| 929 | | | |

| cm ⁻¹ | Int. | Notation | Assignment |
|--------------------|------|--|------------------------------------|
| 28999 } 29009 } | m | 1 ₀ ¹ 5 ₀ ¹ 7 ₁ ¹ | $\nu_{00} + 1460+275+75$ |
| 041 } 060 } | s | 1 ₀ ¹ 4 ₀ ¹ | + 1460+393 |
| 125 | m | 1 ₀ ¹ 4 ₀ ¹ 7 ₁ ¹ | + 1460+393+84 |
| 203 | mw | { 1 ₀ ¹ 5 ₀ ² 1 ₀ ¹ 4 ₀ ¹ 7 ₂ ² | + 1460+275+279 + 1460+393+84+78 |
| 271 } 280 } | m | 1 ₀ ¹ 3 ₀ ¹ | + 1460+622 |
| 410 | vvw | 1 ₀ ¹ 4 ₀ ² | + 1460+393+369 |
| 602 | m | 1 ₀ ¹ 2 ₀ ¹ | + 1460+953 |
| 675 | mw | 1 ₀ ¹ 2 ₀ ¹ 7 ₁ ¹ | + 1460+953+73 |
| 810 | vvw | { 1 ₀ ¹ 2 ₀ ¹ 8 ₀ ¹ 1 ₀ ² 5 ₁ ⁰ | + 1460+953+208 + 1460+1435-274 |
| 891 | w | 1 ₀ ¹ 2 ₀ ¹ 5 ₀ ¹ ? | + 1460+953+289 |
| 30084 | vvs | 1 ₀ ² | + 1460+1435 |
| 162 | s | 1 ₀ ² 7 ₁ ¹ | + 1460+1435+78 |
| 237 | mw | 1 ₀ ² 7 ₂ ² | + 1460+1435+78+75 |
| 274 | w | 1 ₀ ² 8 ₀ ¹ | + 1460+1435+190 |
| 356 | m | 1 ₀ ² 5 ₀ ¹ | + 1460+1435+272 |
| 432 | mw | 1 ₀ ² 5 ₀ ¹ 7 ₁ ¹ | + 1460+1435+272+76 |
| 482 | s | 1 ₀ ² 4 ₀ ¹ | + 1460+1435+398 |
| 543 | mw | 1 ₀ ¹ 2 ₀ ² ? | + 1460+953+961 |
| 706 | m | 1 ₀ ² 3 ₀ ¹ | + 1460+1435+622 |

| cm ⁻¹ | Int. | Notation | Assignment |
|------------------|------|---------------------|-----------------------------|
| 30793 | vw | $1_0^2 3_0^1 7_1^1$ | $2_{00} + 1460+1435+622+87$ |
| 874 | vw | $1_0^2 4_0^2$ | $+ 1460+1435+398+392$ |
| 31011 | m | $1_0^2 2_0^1 ?$ | $+ 1460+1435+927$ |
| 088 | w | $1_0^2 2_0^1 7_1^1$ | $+ 1460+1435+927+77$ |
| 213 | vw | $1_0^3 5_1^0$ | $+ 1460+1435+1404-275$ |
| 488 | vvs | 1_0^3 | $+ 1460+1435+1404$ |
| 561 | s | $1_0^3 7_1^1$ | $+ 1460+1435+1404+73$ |
| 633 | mw | $1_0^3 7_2^2$ | $+ 1460+1435+1404+73+72$ |
| 765 | mw | $1_0^3 5_0^1$ | $+ 1460+1435+1404+277$ |
| 32910 | s | 1_0^4 | $+ 1460+1435+1404+1422$ |

+ approximate errors: 26000 - 27500, ± 0.3 cm⁻¹;
 27500-28000, ± 0.5 cm⁻¹; 28000-28500, ± 2 cm⁻¹;
 28500-30000, ± 5 cm⁻¹; 30000-31000, ± 10 cm⁻¹;
 31000-33000, ± 20 cm⁻¹.

TABLE 5.1a

THE I ${}^1A_u \leftarrow {}^1A_g$ ABSORPTION SPECTRUM OF
 $CO^{35}ClCO^{37}Cl$

| cm ⁻¹ | Notation | Assignment |
|------------------|---------------------|------------------------------|
| 25952.3 | $2_1^0 12_2^2$ | $\nu_{00} - 1216.7-10.2-9.7$ |
| 962.0 | $2_1^0 12_1^1$ | - 1216.7-10.2 |
| 972.2* | 2_1^0 | - 1216.7 |
| 26051.3 | $2_1^0 7_1^1$ | - 1216.7+79.1 |
| 256.0 | $2_1^0 5_0^1$ | - 1216.7+283.8 |
| 368.0 | $2_1^0 4_0^1$ | - 1216.7+395.8 |
| 444.7 | $2_1^0 4_0^1 7_1^1$ | - 1216.7+395.8+76.7 |
| 540.6 | $2_1^0 5_0^2$ | - 1216.7+283.8+284.6 |
| 579.5 | 3_1^0 | - 609.4 |
| 27104.7 | 11_1^1 | - 84.2 |
| 155.5 | 12_3^3 | - 11.2-11.2-11.0 |
| 166.5 | 12_2^2 | - 11.2-11.2 |
| 177.7 | 12_1^1 | - 11.2 |
| 183.3 | $7_1^1 11_1^1$ | + 77.3-82.6 |
| 188.9* | 0_0^0 | origin |
| 220.3 | 6_1^1 | + 31.4 |
| 266.2 | 7_1^1 | + 77.3 |
| 298.3 | $6_1^1 7_1^1$ | + 77.3+32.1 |
| 344.2 | 7_2^2 | + 77.3+78.0 |
| 386.4 | $5_0^1 11_1^1$ | + 280.0-82.5 |

| cm ⁻¹ | Notation | Assignment |
|------------------|--|---------------------|
| 27391.1 | 8 ₀ ¹ | $\nu_{00} + 202.2$ |
| 466.1 | 7 ₁ ¹ 8 ₀ ¹ | + 202.2+75.0 |
| 468.9 | 5 ₀ ¹ | + 280.0 |
| 497.2 | 4 ₀ ¹ 11 ₁ ¹ | + 395.9-87.6 |
| 500.9 | 5 ₀ ¹ 6 ₁ ¹ | + 280.0+32.0 |
| 545.1 | 5 ₀ ¹ 7 ₁ ¹ | + 280.0+76.2 |
| 574.2 | 4 ₀ ¹ 12 ₁ ¹ | + 395.9-10.6 |
| 584.8 | 4 ₀ ¹ | + 395.9 |
| 614.3 | 4 ₀ ¹ 6 ₁ ¹ | + 395.9+29.5 |
| 660.6 | 4 ₀ ¹ 7 ₁ ¹ | + 395.9+75.8 |
| 746.7 | 5 ₀ ² | + 280.0+277.8 |
| 805.4 | 3 ₀ ¹ | + 616.5 |
| 860.1 | 4 ₀ ¹ 5 ₀ ¹ | + 395.9+275.3 |
| 980.1 | 4 ₀ ² | + 395.9+395.3 |
| 28019.3 | 5 ₀ ³ | + 280.0+277.8+272.6 |
| 055.9 | 4 ₀ ² 7 ₁ ¹ | + 395.9+395.3+75.8 |
| 154 | 2 ₀ ¹ | + 965 |
| 233 | 2 ₀ ¹ 7 ₁ ¹ | + 965+79 |

* by extrapolation

TABLE 5.1b

THE I ${}^1A_u \leftarrow {}^1A_g$ ABSORPTION SPECTRUM OF
 $CO^{37}ClCO^{37}Cl$

| cm ⁻¹ | Notation | Assignment |
|------------------|----------------------|-------------------------|
| 25962.9 | $2_1^{\circ} 12_1^!$ | $\nu_{00} - 1216.4-9.6$ |
| 972.5* | 2_1° | - 1216.4 |
| 26365.7 | $2_1^{\circ} 4_0^!$ | - 1216.4+393.2 |
| 27178.4 | $12_1^!$ | - 10.5 |
| 188.9* | 0_0° | origin |
| 265.6 | $7_1^!$ | + 76.7 |
| 384.8 | $5_0^! 11_1^!$ | + 278.1-82.2 |
| 390.0 | $8_0^!$ | + 201.1 |
| 467.0 | $5_0^!$ | + 278.1 |
| 495.6 | $4_0^! 11_1^!$ | + 393.4-86.7 |
| 498.5 | $5_0^! 6_1^!$ | + 278.1+31.5 |
| 572.2 | $4_0^! 12_1^!$ | + 393.4-10.1 |
| 582.3 | $4_0^!$ | + 393.4 |
| 657.3 | $4_0^! 7_1^!$ | + 393.4+75.0 |
| 856.0 | $4_0^! 5_0^!$ | + 393.4+273.7 |

* by extrapolation

The dominant feature of the spectrum is an excited state progression with a spacing progressively decreasing from 1538 cm^{-1} to 1456 cm^{-1} . Five members of this progression are observed before the spectrum is swamped by the continuous absorption of the II $A_u \leftarrow A_g$ system. The frequency involved is certainly that of the totally symmetric C=O stretching vibration ν_1' which is 1784 cm^{-1} (Raman) in the ground state.

The band at 25371 cm^{-1} , which is the most prominent band in the low frequency end of the spectrum and which is the starting point for the carbonyl progression, is assigned as the electronic origin.

b) Ground state intervals.

Two of the strongest bands to the red of the (0,0) band appear at $\nu_{00} - 186 \text{ cm}^{-1}$ and $\nu_{00} - 441 \text{ cm}^{-1}$ and can be assigned as 5_1^0 and 4_1^0 , respectively. The corresponding Raman displacements in the liquid for these two in-plane symmetric bending vibrations are 191 cm^{-1} and 415 cm^{-1} .

If the Raman assignments are correct, then the transitions 3_1^0 , 2_1^0 and 1_1^0 ought to lie close to $\nu_{00} - 600$, $\nu_{00} - 1032$, and $\nu_{00} - 1784 \text{ cm}^{-1}$, respectively. A weak band is present at $\nu_{00} - 608 \text{ cm}^{-1}$, which is taken to be 3_1^0 and a band, very weak at $\nu_{00} - 1801 \text{ cm}^{-1}$, is possibly 1_1^0 . However, this latter assignment is not definite

since a strong singlet-triplet band occurs at approximately the same frequency. The band at $\nu_{00} = 1116 \text{ cm}^{-1}$ is assigned as 2_1^0 .

c) Excited state fundamentals.

A large number of intense bands in the spectrum can be explained satisfactorily in terms of progressions and combinations involving five excited state fundamentals, 180, 296, 621, 953 and 1538 cm^{-1} . Most of the remaining vibrational structure is the result of positively-running sequences which accompany nearly every strong band.

The five excited state frequencies can be assigned unambiguously to the five a_g fundamentals. The magnitudes and signs of the observed frequency changes on excitation are as expected. As in the spectrum of oxalyl chloride, the vibrational pattern accompanying each member of the strong, excited state carbonyl progression is very similar to that found in association with the origin band. The combination band $4_0^1 5_0^1$ is quite strong in the spectrum.

As anticipated, the two most intense excited state progressions involve the Franck-Condon active vibrations ν_1' , CO bond stretching, and ν_4' , the COBr scissors motion. Both of these frequencies, like their counterparts in the oxalyl chloride spectrum, are much

lower than their corresponding values in the ground state. The frequencies associated with C-Br stretching and COBr rocking do not change significantly on $n \rightarrow \pi^*$ promotion and the corresponding bands 3_0^1 and 5_0^1 appear in the spectrum with only medium intensity.

d) Sequences.

Two positively-running sequences of $+65 \text{ cm}^{-1}$ and $+32 \text{ cm}^{-1}$ appear throughout the spectrum. The $+65 \text{ cm}^{-1}$ sequence is the more intense of the two and is assigned to the torsional mode, ν_7 , while, as in the spectrum of oxalyl chloride, the $+32 \text{ cm}^{-1}$ interval is thought to be due to a sequence in ν_6 , the a_u C=O out-of-plane bending vibration.

e) Discussion.

The assignment of the excited state fundamentals differs from that of Kanda *et al.*¹⁸ with respect to the value of the CC stretch, ν_2' . Two equally strong bands are observed in the spectrum, one at 26324 cm^{-1} ($\nu_{00} + 953 \text{ cm}^{-1}$), the other at 26468 cm^{-1} ($\nu_{00} + 1097 \text{ cm}^{-1}$). In the present analysis the former band is chosen as 2_0^1 ($\nu_{00} + \nu_{cc}'$) in preference to the latter since, with 26468 cm^{-1} assigned as 2_0^1 the band at 26324 cm^{-1} is difficult to explain, whereas if 2_0^1 lies at 26324 cm^{-1} the 26468 cm^{-1} band can be assigned to the expected transition $1_0^1 4_1^0$.

The behaviour of the C-C stretching frequency ν_2' resembles that observed in the I ${}^1A_u \leftarrow {}^1A_g$ systems of glyoxal and oxalyl chloride. The 2_0^1 band, which ought to be prominent is actually quite weak and, in addition, despite a predicted shortening of the CC bond on electronic excitation, the excited state frequency is considerably lower than that of the ground state. It is believed that both these unexpected observations are the result of large contributions to the normal coordinate of the 953 cm^{-1} vibration from C=O bond extension and CCO angle bending motions. This is discussed in more detail in Section 5.6.

Part of the observed spectrum is shown in Figure 5.4. Table 5.2 contains a list of assigned frequencies for the I ${}^1A_u \leftarrow {}^1A_g$ system.

5.4 Oxalyl fluoride.

a) Introduction.

A small portion of the I ${}^1A_u \leftarrow {}^1A_g$ spectrum of oxalyl fluoride is shown in Figure 5.5. The relative intensities of the bands in the spectrum are considerably different from those of oxalyl chloride and oxalyl bromide although the three systems do have some common features.

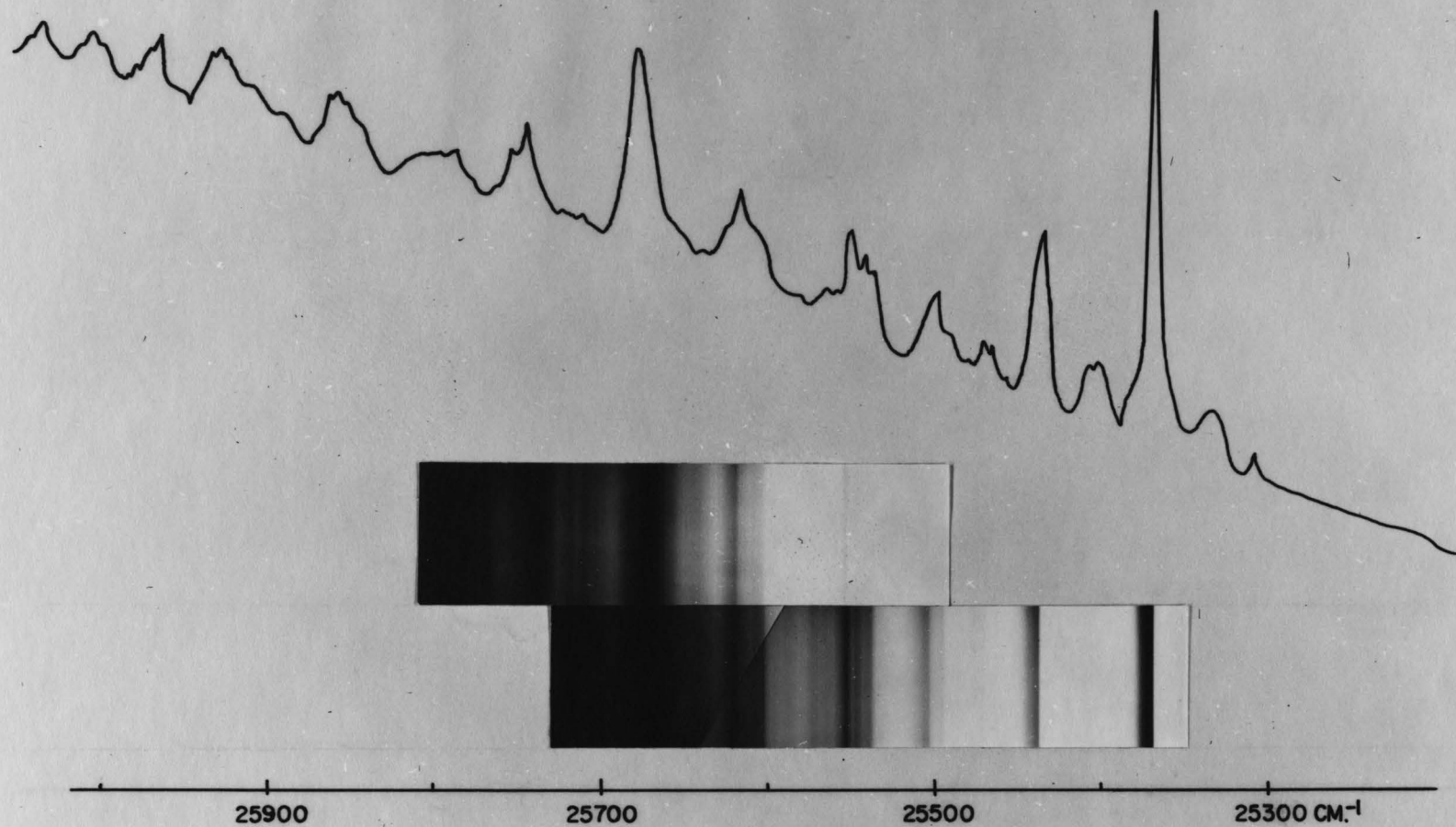


FIGURE 5.4 THE ${}^1A_u \leftarrow {}^1A_g$ ABSORPTION SPECTRUM OF $(\text{COBr})_2$
IN THE REGION $3960 - 3840 \text{ \AA}$.

TABLE 5.2

THE I ${}^1A_u \leftarrow {}^1A_g$ ABSORPTION SPECTRUM OF
OXALYL BROMIDE

| cm^{-1} ⁺ | Int. ⁺⁺ | Notation | Assignment |
|-------------------------------|--------------------|---------------------|-----------------------|
| 23570 | vvw | 1_1^0 | ν_{00} - 1801 (?) |
| 602 | vvw | $1_1^0 6_1^1$ | - 1801+32 |
| 641 | vvw | $1_1^0 7_1^1$ | - 1801+71 |
| 750 | vvw | $1_1^0 5_0^1$ | - 1801+180 |
| 865 | vvw | $1_1^0 4_0^1$ | - 1801+295 |
| 24255 | w | 2_1^0 | - 1116 |
| 286 | vw | $2_1^0 6_1^1$ | - 1116+31 |
| 316 | vw | $2_1^0 7_1^1$ | - 1116+61 |
| 436 | vw | $2_1^0 5_0^1$ | - 1116+181 |
| 552 | vvw | $2_1^0 4_0^1$ | - 1116+297 |
| 763 | vvw | 3_1^0 | - 608 |
| 858 | vvw | $6_2^0 ?$ | - 2 (256.5) |
| 930 | mw | 4_1^0 | - 441 |
| 961 | vw | $4_1^0 6_1^1$ | - 441+31 |
| 998 | w | $4_1^0 7_1^1$ | - 441+68 |
| 25020 | vvw | $12_2^0 ?$ | - 2 (175.5) |
| 028 | vw | $4_1^0 6_1^1 7_1^1$ | - 441+68+30 |
| 067 | vw | $4_1^0 7_2^1$ | - 441+68+69 |
| 185 | mw | 5_1^0 | - 186 |
| 227 | mw | 4_1^1 | - 441+297 |

| cm ⁻¹ | Int. | Notation | Assignment |
|------------------|------|---|--------------|
| 25371 | vs | 0 ₀ ⁰ | ν_{00} |
| 403 | m | 6 ₁ ¹ | + 32 |
| 436 | ms | 7 ₁ ¹ | + 65 |
| 470 | m | 6 ₁ ¹ 7 ₁ ¹ | + 65+34 |
| 502 | m | 7 ₂ ² | + 65+66 |
| 536 | m | 8 ₀ ¹ ? | + 165 |
| 551 | ms | 5 ₀ ¹ | + 180 |
| 568 | vvw | 7 ₃ ³ | + 65+66+66 |
| 600 | m | 7 ₁ ¹ 8 ₀ ¹ ? | + 165+64 |
| 616 | m | 5 ₀ ¹ 7 ₁ ¹ | + 180+65 |
| 636 | vw | 7 ₀ ² ? | + 2 (132.5) |
| 667 | vs | 4 ₀ ¹ | + 296 |
| 700 | w | 4 ₀ ¹ 6 ₁ ¹ | + 296+33 |
| 735 | s | 4 ₀ ¹ 7 ₁ ¹ | + 296+68 |
| 780 | mw | 12 ₀ ² ? | + 2 (204.5) |
| 847 | s | 4 ₀ ¹ 5 ₀ ¹ | + 296+180 |
| 914 | w | 4 ₀ ¹ 5 ₀ ¹ 7 ₁ ¹ | + 296+180+67 |
| 960 | s | 4 ₀ ² | + 296+293 |
| 992 | m | 3 ₀ ¹ | + 621 |
| 26024 | w | 3 ₀ ¹ 6 ₁ ¹ | + 621+32 |
| 061 | m | 3 ₀ ¹ 7 ₁ ¹ | + 621+69 |
| 168 | m | 3 ₀ ¹ 5 ₀ ¹ | + 621+176 |
| 285 | ms | 3 ₀ ¹ 4 ₀ ¹ | + 621+293 |
| 324 | m | 2 ₀ ¹ | + 953 |

| cm ⁻¹ | Int. | Notation | Assignment |
|------------------|------|---|--------------------------|
| 26398 | m | 2 ₀ ¹ 7 ₁ ¹ | 2 ₀₀ + 953+74 |
| 432 | m | 2 ₀ ¹ 6 ₁ ¹ 7 ₁ ¹ | + 953+74+34 |
| 468 | s | 1 ₀ ¹ 4 ₁ ⁰ | + 1538-441 |
| 501 | vw | 2 ₀ ¹ 5 ₀ ¹ | + 953+177 |
| 532 | m | 1 ₀ ¹ 4 ₁ ⁰ 7 ₁ ¹ | + 1538-441+64 |
| 566 | w | 1 ₀ ¹ 4 ₁ ⁰ 6 ₁ ¹ 7 ₁ ¹ | + 1538-441+64+34 |
| 657 | mw | 1 ₀ ¹ 4 ₁ ⁰ 5 ₀ ¹ | + 1538-441+189 |
| 724 | mw | 1 ₀ ¹ 5 ₁ ⁰ | + 1538-185 |
| 777 | ms | 1 ₀ ¹ 4 ₁ ¹ | + 1538-441+309 |
| 909 | vvs | 1 ₀ ¹ | + 1538 |
| 944 | m | 1 ₀ ¹ 6 ₁ ¹ | + 1538+35 |
| 979 | vs | 1 ₀ ¹ 7 ₁ ¹ | + 1538+70 |
| 27087 | vs | 1 ₀ ¹ 5 ₀ ¹ | + 1538+178 |
| 158 | ms | 1 ₀ ¹ 5 ₀ ¹ 7 ₁ ¹ | + 1538+178+71 |
| 216 | vvs | 1 ₀ ¹ 4 ₀ ¹ | + 1538+307 |
| 255 | m | 1 ₀ ¹ 4 ₀ ¹ 6 ₁ ¹ | + 1538+307+39 |
| 282 | vs | 1 ₀ ¹ 4 ₀ ¹ 7 ₁ ¹ | + 1538+307+66 |
| 314 | w | 1 ₀ ¹ 4 ₀ ¹ 6 ₁ ¹ 7 ₁ ¹ | + 1538+307+66+32 |
| 347 | m | 1 ₀ ¹ 4 ₀ ¹ 7 ₂ ² | + 1538+307+66+65 |
| 389 | w | 1 ₀ ¹ 4 ₀ ¹ 5 ₀ ¹ | + 1538+307+173 |
| 462 | vw | 1 ₀ ¹ 4 ₀ ¹ 5 ₀ ¹ 7 ₁ ¹ | + 1538+307+173+73 |
| 519 | vww | 1 ₀ ¹ 3 ₀ ¹ | + 1538+610 |
| | | 1 ₀ ¹ 4 ₀ ² | + 1538+307+303 |
| 795 | vww | 1 ₀ ² 3 ₁ ⁰ | + 1538+1503-617 |

| cm ⁻¹ | Int. | Notation | Assignment |
|------------------|------|---------------------------|------------------------|
| 27861 | ms | $1_0^1 2_0^1$ | $\nu_{00} + 1538+952$ |
| 927 | m | $1_0^1 2_0^1 7_1^1$ | + 1538+952+68 |
| 983 | s | $1_0^2 4_1^0$ | + 1538+1503-429 |
| 28048 | vw | $1_0^2 4_1^0 7_1^1$ | + 1538+1503-429+65 |
| 160 | ms | $1_0^2 4_1^0 5_0^1$ | + 1538+1503-429+177 |
| 230 | m | $1_0^2 4_1^0 5_0^1 7_1^1$ | + 1538+1503-429+177+70 |
| | | $1_0^2 5_1^0$ | + 1538+1503-182 |
| 289 | m | $1_0^2 4_1^1$ | + 1538+1503-429+306 |
| 353 | ms | $1_0^2 4_1^1 7_1^1$ | + 1538+1503-429+306+64 |
| 412 | vvs | 1_0^2 | + 1538+1503 |
| 451 | ms | $1_0^2 6_1^1$ | + 1538+1503+39 |
| 478 | vs | $1_0^2 7_1^1$ | + 1538+1503+66 |
| 519 | w | $1_0^2 6_1^1 7_1^1$ | + 1538+1503+66+41 |
| 545 | mw | $1_0^2 7_2^2$ | + 1538+1503+66+67 |
| 592 | ms | $1_0^2 5_0^1$ | + 1538+1503+180 |
| 655 | ms | $1_0^2 5_0^1 7_1^1$ | + 1538+1503+180+63 |
| 707 | vs | $1_0^2 4_0^1$ | + 1538+1503+295 |
| 757 | mw | $1_0^2 4_0^1 6_1^1$ | + 1538+1503+295+50 |
| 777 | m | $1_0^2 4_0^1 7_1^1$ | + 1538+1503+295+70 |
| 821 | vw | $1_0^2 4_0^1 6_1^1 7_1^1$ | + 1538+1503+295+70+44 |
| 883 | ms | $1_0^2 4_0^1 5_0^1$ | + 1538+1503+295+176 |
| 960 | mw | $1_0^2 4_0^1 5_0^1 7_1^1$ | + 1538+1503+295+176+77 |
| 29026 | vw | $1_0^2 3_0^1$ | + 1538+1503+614 |
| | | $1_0^2 4_0^2$ | + 1538+1503+295+319 |

| cm ⁻¹ | Int. | Notation | Assignment |
|------------------|------|---------------------|----------------------------|
| 29364 | m | $1_0^2 2_0^1$ | $\nu_{00} + 1538+1503+952$ |
| 460 | m | $1_0^3 4_0^0$ | + 1538+1503+1483-435 |
| 784 | mw | $1_0^3 4_0^1$ | + 1538+1503+1483-435+324 |
| 895 | vs | 1_0^3 | + 1538+1503+1483 |
| 930 | w | $1_0^3 6_0^1$ | + 1538+1503+1483+35 |
| 959 | s | $1_0^3 7_0^1$ | + 1538+1503+1483+66 |
| 30020 | m | $1_0^3 7_2^2$ | + 1538+1503+1483+66+61 |
| 067 | ms | $1_0^3 5_0^1$ | + 1538+1503+1483+172 |
| 140 | m | $1_0^3 5_0^1 7_1^1$ | + 1538+1503+1483+172+63 |
| 196 | ms | $1_0^3 4_0^1$ | + 1538+1503+1483+301 |
| 259 | mw | $1_0^3 4_0^1 7_1^1$ | + 1538+1503+1483+301+63 |
| 31351 | s | 1_0^4 | + 1538+1503+1483+1456 |
| 419 | ms | $1_0^4 7_1^1$ | + 1538+1503+1483+1456+68 |

+ approximate errors: 23500-25500, ± 1 cm⁻¹; 25500-26500, ± 5 cm⁻¹; 26500-31500, ± 10 cm⁻¹

++ The intensities are visual estimates relative to the background continuum.

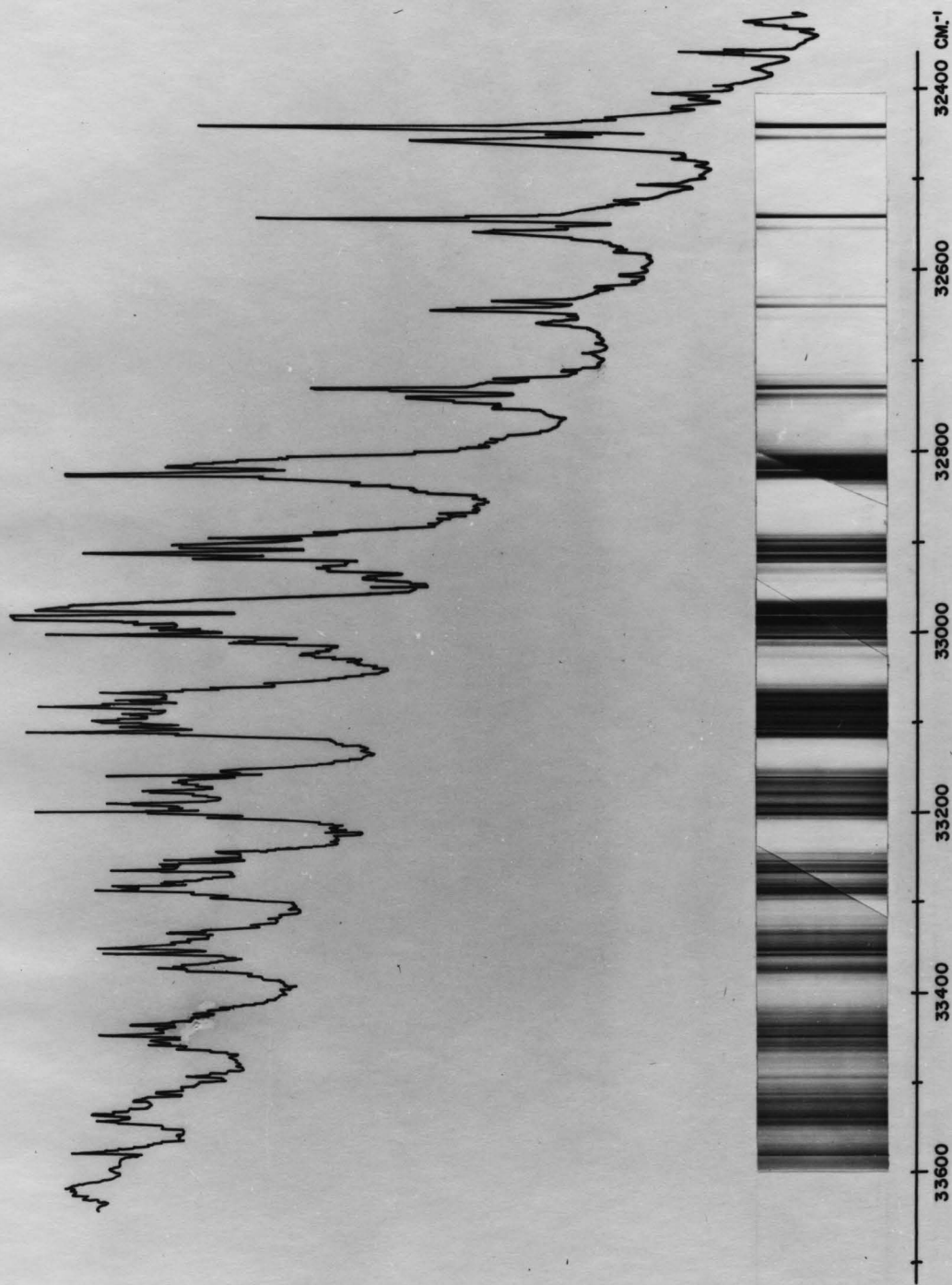


FIGURE 5.5 THE ${}^1\text{A}_u \leftarrow {}^1\text{A}_g$ ABSORPTION SPECTRUM OF $(\text{COF})_2$ IN THE REGION 3100-2970 \AA

Many bands near the origin show complex rotational structure at a resolving power of 300,000 but all bands to the violet of $\nu_{00} + 1000 \text{ cm}^{-1}$ are rotationally diffuse. Oxalyl fluoride is a very asymmetric top (Ray's asymmetry parameter⁸⁸, $\kappa'' = -0.26$) and consequently the band contours are sensitive to small changes in excited state rotational constants. (See Chapter 7.)

Several regions of the spectrum are extremely complex owing to many closely overlapping bands and, even at a resolving power of 300,000, it was not always possible to decide which features were rotational heads of the same band and which were due to other bands. The analysis in Table 5.3 is not complete but does account for a major portion of the more intense bands.

The most obvious similarities with the spectra of oxalyl chloride and oxalyl bromide are

- (i) Prominent sequences in the torsional motion ν_7 and weak sequences in the lowest-lying in-plane b_u bending frequency, ν_{12} .
- (ii) Progressions and combinations involving the symmetric scissors and rocking vibrations, ν_4' and ν_5' .
- (iii) The presence of $\nu_{00} - \nu_{cc}''$ as a band of appreciable intensity. This band is relatively stronger in $(\text{COF})_2$ than in the spectra of the other oxalyl halides because of a more favorable Boltzmann factor.

The spectrum differs from those of oxalyl chloride and oxalyl bromide in that the symmetric carbonyl stretching vibration in the excited state does not form a prominent progression. The reason is that although the 0_0^0 band of oxalyl fluoride is extremely sharp, the spectrum rapidly becomes diffuse near the first carbonyl 1_0^1 .

b) Ground state intervals.

The origin of the spectral system lies at 32445.0 cm^{-1} . There is a moderately strong band 801.7 cm^{-1} to the red of this which is assigned as the CC stretch 3_1^0 ⁺. The gas phase (ultraviolet) value of ν_{CC}'' (ν_3) is not shifted appreciably from the liquid frequency 809 cm^{-1} found in the Raman spectrum (c.f. oxalyl chloride and oxalyl bromide).

The only other ground state intervals which have been found are 318.1 cm^{-1} and 231.9 cm^{-1} . The bands $\nu_{\text{OO}} - 318.1 \text{ cm}^{-1}$ and $\nu_{\text{OO}} - 231.9 \text{ cm}^{-1}$ are also present in the singlet-triplet system. These are assigned as 5_1^0 and 7_2^0 , respectively. Unlike the singlet-singlet

⁺ In oxalyl fluoride there is a difference in the numbering of the a_g modes, ν_{CC} and ν_{CX} , from that of oxalyl chloride and oxalyl bromide. For, $(\text{COF})_2$, $\nu_{\text{CC}} = \nu_3$ and $\nu_{\text{CF}} = \nu_2$ whereas, for $(\text{COCl})_2$ and $(\text{COBr})_2$, $\nu_{\text{CC}} = \nu_2$ and $\nu_{\text{CX}} = \nu_3$.

spectra of oxalyl chloride and bromide, 5_1^0 is very weak and there is no band which may be assigned unambiguously to 4_1^0 .

c) Excited state fundamentals.

Three very strong bands are observed at displacements of +280.5, +370.3 and +531.4 cm^{-1} from both 3_1^0 and 0_0^0 . These frequencies are active in progressions and combinations and it is thought that all three correspond to excited state fundamentals. It is reasonable to assume that 280.5 and 531.4 cm^{-1} are the excited state values of the a_g bending vibrations ν_5 and ν_4 , respectively. 4_0^1 and 5_0^1 are observed as strong bands in the spectra of oxalyl chloride and oxalyl bromide. $\nu_4'' = 565 \text{ cm}^{-1}$ and $\nu_5'' = 292 \text{ cm}^{-1}$ in the Raman spectrum of liquid $(\text{COF})_2$. The assignment of the 370.3 cm^{-1} frequency is not as straightforward since no a_g fundamental is expected at this frequency. Other intervals of 710.3, 1145.9 and 1440.2 cm^{-1} to higher frequencies are assigned to ν_3^1 (CC stretch), ν_2^1 (CF stretch) and ν_1^1 (CO stretch), respectively.

d) Sequences.

The three sequences identified in the $I \ ^1A_u \leftarrow \ ^1A_g$ system of oxalyl fluoride are +97.0, -41.5 and -86.9 cm^{-1} . The +97 cm^{-1} interval is the analogue

of the $+78 \text{ cm}^{-1}$ sequence in oxalyl chloride and the $+65 \text{ cm}^{-1}$ sequence in oxalyl bromide, both of which are thought to involve the torsional frequency. At room temperature the torsional sequence can be followed to the fourth member so that the ground state frequency is probably less than 150 cm^{-1} . Hencher and King¹⁷ suggest a value of $\sim 127 \text{ cm}^{-1}$ from combination bands in the infrared spectrum. The band at 231.9 cm^{-1} to the red of the (0,0) band is tentatively assigned as the torsional overtone, 7_2^0 . A similar band, $\nu_{00}(\text{ST}) - 228.6 \text{ cm}^{-1}$, is found in the singlet-triplet spectrum.

The sequence of -41 cm^{-1} is attributed to the next lowest-lying ground state fundamental ν_{12} . Since $\nu_{12}'' = 255 \text{ cm}^{-1}$, the weak band at $\nu_{00} + 422 \text{ cm}^{-1}$ can be assigned as 12_0^2 . The -87 cm^{-1} sequence, by analogy with the spectrum of oxalyl chloride, may involve ν_{11} .

e) Discussion.

The band at $\nu_{00} + 370.3 \text{ cm}^{-1}$ is one of the stronger bands of the spectrum. It acts as a false origin so that much of the vibrational structure built upon it resembles closely that found accompanying the (0,0) band of the system. Two possible explanations of the 370.3 cm^{-1} frequency have been considered.

(i) that 370 cm^{-1} corresponds to the overtone of an excited state frequency of $\sim 185 \text{ cm}^{-1}$;

(ii) that 370 cm^{-1} is $\nu_8'(b_g)$ and the band appears in the spectrum through intensity borrowing. The ground state value of ν_8 is 420 cm^{-1} (Raman).

The lowest ground state vibrational frequency in oxalyl fluoride is that for torsion about the CC bond (ν_7). A comparison with the corresponding singlet-triplet absorption spectrum shows that 370 cm^{-1} is not the excited state torsional overtone, $2\nu_7'$. The torsional sequences in the $I \ ^1A_u \leftarrow \ ^1A_g$ and $I \ ^3A_u \leftarrow \ ^1A_g$ systems are $+97.0$ and $+100.5 \text{ cm}^{-1}$, respectively, which means that if $\nu_{00} + 370 \text{ cm}^{-1}$ is ν_0^2 then ν_0^2 should be found in the singlet-triplet spectrum at $\nu_{00}(\text{ST}) + 377 \text{ cm}^{-1}$. There is no band at this position: the band is actually observed at $\nu_{00}(\text{ST}) + 387 \text{ cm}^{-1}$. The only other low frequency, ν_{12} , which is 255 cm^{-1} in the ground state is not expected to drop to 185 cm^{-1} on electronic excitation. Thus it seems that the assignment of 370 cm^{-1} to an overtone is unsatisfactory, unless the band in question is displaced from its true position by Fermi resonance. This is unlikely as combination bands involving the 370 cm^{-1} interval are normal.

The general theory of vibronic transitions in polyatomic molecules has been treated by Herzberg and Teller⁸⁹. During a non-totally symmetric vibration, the molecule assumes a conformation which is of lower

symmetry than the equilibrium conformation. States which are of different symmetry in the equilibrium position may belong to the same symmetry species in the point group of lower symmetry of the displaced position, and may interact.

The strength of the interaction depends upon

$$\frac{\int \psi_k \mathcal{H}' \psi_l d\tau}{E_k - E_l}$$

where the excited state "borrowing" the intensity is described by ψ_l and the excited state in close proximity which is "lending" the intensity is described by ψ_k .

The perturbing potential is given by

$$\mathcal{H}' = \sum_i \left(\frac{\partial \mathcal{H}}{\partial Q_i} \right)_0 Q_i$$

\mathcal{H} is the electronic Hamiltonian and Q is the normal coordinate.

Group theory shows that, in an $A_u \leftarrow A_g$ electronic transition, the forbidden vibrational component of b_g symmetry is made allowed through interaction with an excited state of B_u symmetry. ($B_u \leftarrow A_g$ is symmetry allowed and $A_u \otimes b_g = B_u$). In glyoxal and the oxalyl halides, where there is only one normal vibration of b_g symmetry, suitable low-lying B_u excited states are present.

The ν'_8 fundamental is found as a very strong hybrid band in the I ${}^1A_u \leftarrow {}^1A_g$ spectrum of glyoxal. Glyoxal is a near-prolate symmetric top with $\kappa'' = -0.985$, and the hybrid bands which are predominantly type A, have distinctly different contours from the allowed C-type (perpendicular) bands. Away from prolate and oblate limits type A and type C bands tend to resemble one another so that perpendicular and hybrid bands in oxalyl fluoride need not have radically different contours. However, the profiles of bands $\nu_{00} + 370.3 \text{ cm}^{-1}$ and 4_0^1 ($\nu_{00} + 531.4 \text{ cm}^{-1}$) are remarkably similar so that an explanation of the 370 cm^{-1} interval as ν'_8 must remain, at present, tentative.

In the absence of a detailed knowledge of the b'_g normal coordinates and of the exact form of the excited state wave functions and their energies, it is not possible to predict the strength of the forbidden component in the spectra of the oxalyl halides relative to that in glyoxal. Empirically, the intensity of the forbidden component decreases in the order $(\text{CHO})_2 \rightarrow (\text{COF})_2 \rightarrow (\text{COCl})_2 \rightarrow (\text{COBr})_2$ ⁺.

⁺ The bands at $\nu_{00}(\text{ss}) + 203.6 \text{ cm}^{-1}$ in oxalyl chloride and $\nu_{00}(\text{ss}) + 160.6 \text{ cm}^{-1}$ are probably the analogues of the $\nu_{00}(\text{ss}) + 370.3 \text{ cm}^{-1}$ band in oxalyl fluoride.

A complete list of band heads is given in the Appendix, Table A.3. The vibrational assignment is drawn up in Table 5.3.

f) The II $A_u \leftarrow A_g$ system.

The diffuse $n \rightarrow \pi^*$ system of oxalyl fluoride shows some gross vibrational structure at high frequencies. The bands are broad with a width at half-height of $\sim 40 \text{ cm}^{-1}$. The observed vibrational features are given in Table 5.4. Two vibrational intervals can be picked out which may be ν'_4 and ν'_1 . The average values of the frequencies are 358 and 1540 cm^{-1} , respectively.

5.5 Oxalyl chloride fluoride.

A small amount of oxalyl chloride fluoride was obtained as a by-product during the preparation of oxalyl fluoride. The sample ($\sim 0.5 \text{ ml}$) was sufficient for the observation of the strong bands of the spectrum under low resolution. Mr. K. G. Kidd of this research group is presently synthesizing larger quantities of oxalyl chloride fluoride in order to investigate the spectrum at greater pressure path lengths and under high resolution. The observed spectrum will therefore be commented upon only briefly. Part of the low resolution spectrum of oxalyl chloride fluoride is shown in Figure 5.6.

TABLE 5.3

THE I ${}^1A_u \leftarrow {}^1A_g$ ABSORPTION SPECTRUM OF
OXALYL FLUORIDE.

| cm ⁻¹ | Int. | Notation | Assignment |
|------------------|------|----------------------|-------------------------|
| 31556.5 | vvw | $3_1^0 11_1^1$ | $\nu_{00} - 801.7-86.8$ |
| 601.1 | vw | $3_1^0 12_1^1$ | - 801.7-42.2 |
| 643.3 | mw | 3_1^0 | - 801.7 |
| 655.0 | vvw | $3_1^0 7_1^1 11_1^1$ | - 801.7+97.0-85.3 |
| 698.0 | vvvw | $3_1^0 7_1^1 12_1^1$ | - 801.7+97.0-42.2 |
| 740.3 | w | $3_1^0 7_1^1$ | - 801.7+97.0 |
| 753.6 | vvvw | $3_1^0 7_2^2 11_1^1$ | - 801.7+97.0+96.9-83.6 |
| 797.6 | vvvw | $3_1^0 7_2^2 12_1^1$ | - 801.7+97.0+96.9-39.6 |
| 837.2 | vw | $3_1^0 7_2^2$ | - 801.7+97.0+96.9 |
| 841.6 | vvw | $3_1^0 5_0^1 11_1^1$ | - 801.7+280.4-82.1 |
| 923.7 | vw | $3_1^0 5_0^1$ | - 801.7+280.4 |
| 934.4 | vvvw | $3_1^0 7_3^3$ | - 801.7+97.0+96.9+97.2 |
| 32012.3 | mw | $3_1^0 8_0^1 ?$ | - 801.7+369.0 |
| 019.8 | vw | $3_1^0 5_0^1 7_1^1$ | - 801.7+280.4+97.1 |
| 091.4 | vvw | $3_1^0 4_0^1 11_1^1$ | - 801.7+530.8-82.4 |
| 126.9 | w | 5_1^0 | - 318.1 |
| 173.8 | vw | $3_1^0 4_0^1$ | - 801.7+530.8 |
| 202.3 | vvw | $3_1^0 5_0^2$ | - 801.7+280.4+278.6 |
| 213.1 | mw | 7_2^0 | - 2 (116.0) |

| cm ⁻¹ | Int. | Notation | Assignment |
|------------------|------|--|------------------------|
| 32272.1 | vvw | 11 ₂ ² | $\nu_{00} - 86.9-86.0$ |
| 358.1 | w | 11 ₁ ¹ | - 86.9 |
| 403.5 | mw | 12 ₁ ¹ | - 41.5 |
| 445.0 | vs | 0 ₀ ⁰ | origin |
| 456.5 | m | 7 ₁ ¹ 11 ₁ ¹ | + 97.0-85.8 |
| 500.4 | w | 7 ₁ ¹ 12 ₁ ¹ | + 97.0-41.6 |
| 542.0 | s | 7 ₁ ¹ | + 97.0 |
| 553.8 | mw | 7 ₂ ² 11 ₁ ¹ | + 97.0+96.6-84.8 |
| 598.0 | vvw | 7 ₂ ² 12 ₁ ¹ | + 97.0+96.6-40.6 |
| 638.6 | m | 7 ₂ ² | + 97.0+96.6 |
| 683.1 | vw | 5 ₀ ¹ 12 ₁ ¹ | + 280.5-42.4 |
| 725.5 | ms | 5 ₀ ¹ | + 280.5 |
| 728.3 | m | 8 ₀ ¹ 11 ₁ ¹ | + 370.3-87.0 |
| 735.2 | w | 7 ₃ ³ | + 97.0+96.6+96.6 |
| 744.9 | vw | 4 ₀ ¹ 7 ₂ ⁰ | + 531.4-231.5 |
| 773.0 | vvw | 8 ₀ ¹ 12 ₁ ¹ | + 370.3-42.3 |
| 815.3 | vs | 8 ₀ ¹ ? | + 370.3 |
| 822.9 | m | 5 ₀ ¹ 7 ₁ ¹ | + 280.5+97.4 |
| 831.5 | vvw | 7 ₄ ⁴ | + 97.0+96.6+96.6+96.3 |
| 866.0 | vvvw | 7 ₁ ¹ 8 ₀ ¹ 12 ₁ ¹ | + 370.3+92.5-41.8 |
| 867.1 | vvvw | 12 ₀ ² ? | + 2 (211.1) |
| 874.3 | vvvw | 7 ₀ ² ? | + 2 (214.7) |
| 888.9 | mw | 4 ₀ ¹ 11 ₁ ¹ | + 531.4-88.3 |
| 907.8 | s | 7 ₁ ¹ 8 ₀ ¹ | + 370.3+92.5 |

| cm ⁻¹ | Int. | Notation | Assignment |
|------------------|------|--|--------------------------------|
| 32931.4 | vvw | 4 ₀ ¹ 12 ₁ ¹ | $\nu_{00} + 531.4 - 45.0$ |
| 976.4 | vvs | 4 ₀ ¹ | + 531.4 |
| 996.9 | w | 7 ₂ ² 8 ₀ ¹ | + 370.3 + 92.5 + 89.1 |
| 33003.8 | s | 5 ₀ ² | + 280.5 + 278.3 |
| 030.7 | vvw | 4 ₀ ¹ 7 ₁ ¹ 12 ₁ ¹ | + 531.4 + 95.4 - 41.1 |
| 071.8 | m | 4 ₀ ¹ 7 ₁ ¹ | + 531.4 + 95.4 |
| 096.6 | ms | 5 ₀ ¹ 8 ₀ ¹ | + 370.3 + 281.4 |
| 100.7 | ms | 5 ₀ ² 7 ₁ ¹ | + 280.4 + 278.3 + 96.9 |
| 155.3 | m | 3 ₀ ¹ | + 710.3 |
| 167.5 | w | 4 ₀ ¹ 7 ₂ ² | + 531.4 + 95.4 + 95.7 |
| 177.9 | mw | 8 ₀ ² | + 370.3 + 362.6 |
| 249.0 | mw | 3 ₀ ¹ 7 ₁ ¹ | + 710.3 + 93.7 |
| 257.7 | w | 4 ₀ ¹ 5 ₀ ¹ | + 531.4 + 281.3 |
| 280.0 | w | 5 ₀ ³ | + 280.5 + 278.3 + 276.2 |
| 345.4 | w | 4 ₀ ¹ 8 ₀ ¹ | + 531.4 + 369.0 |
| 355.2 | m | 4 ₀ ¹ 5 ₀ ¹ 7 ₁ ¹ | + 531.4 + 281.6 + 97.5 |
| 373.4 | vvw | 5 ₀ ³ 7 ₁ ¹ | + 280.5 + 278.3 + 276.2 + 93.4 |
| 433.1 | vvw | 3 ₀ ¹ 5 ₀ ¹ | + 710.3 + 277.8 |
| 491.7 | vvvw | 4 ₀ ² | + 531.4 + 515.3 |
| 521.4 | mw | 3 ₀ ¹ 8 ₀ ¹ | + 710.3 + 366.1 |
| 590.9 | ms | 2 ₀ ¹ | + 1145.9 |
| 681.7 | m | 3 ₀ ¹ 4 ₀ ¹ | + 710.3 + 526.4 |
| 687.8 | w | 2 ₀ ¹ 7 ₁ ¹ | + 1145.9 + 96.9 |
| 782.9 | w | 2 ₀ ¹ 7 ₂ ² | + 1145.9 + 96.9 + 95.1 |

| cm^{-1} | Int. | Notation | Assignment |
|------------------|------|---------------|-----------------------------|
| 53866.2 | vw | $2_0^1 5_0^1$ | $\nu_{00} + 1145.9 + 275.3$ |
| 885.2 | ms | 1_0^1 | + 1440.2 |
| 982.2 | ms | $1_0^1 7_1^1$ | + 1440.2 + 97.0 |

TABLE 5.4

OBSERVED BANDS IN II $A_u \leftarrow A_g$ SYSTEM
OF OXALYL FLUORIDE.

| cm^{-1} | Intensity | | |
|------------------|-----------|------|------|
| 43554 | s | 383 | 1532 |
| 937 | ms | | |
| 45086 | ms | 348 | 1556 |
| 434 | m | | |
| 46642 | s | 350 | 1574 |
| 992 | m | | |
| 48216 | s | 351 | 1412 |
| 567 | ms | | |
| 49628 | s | 1628 | |
| 51256 | s | | |

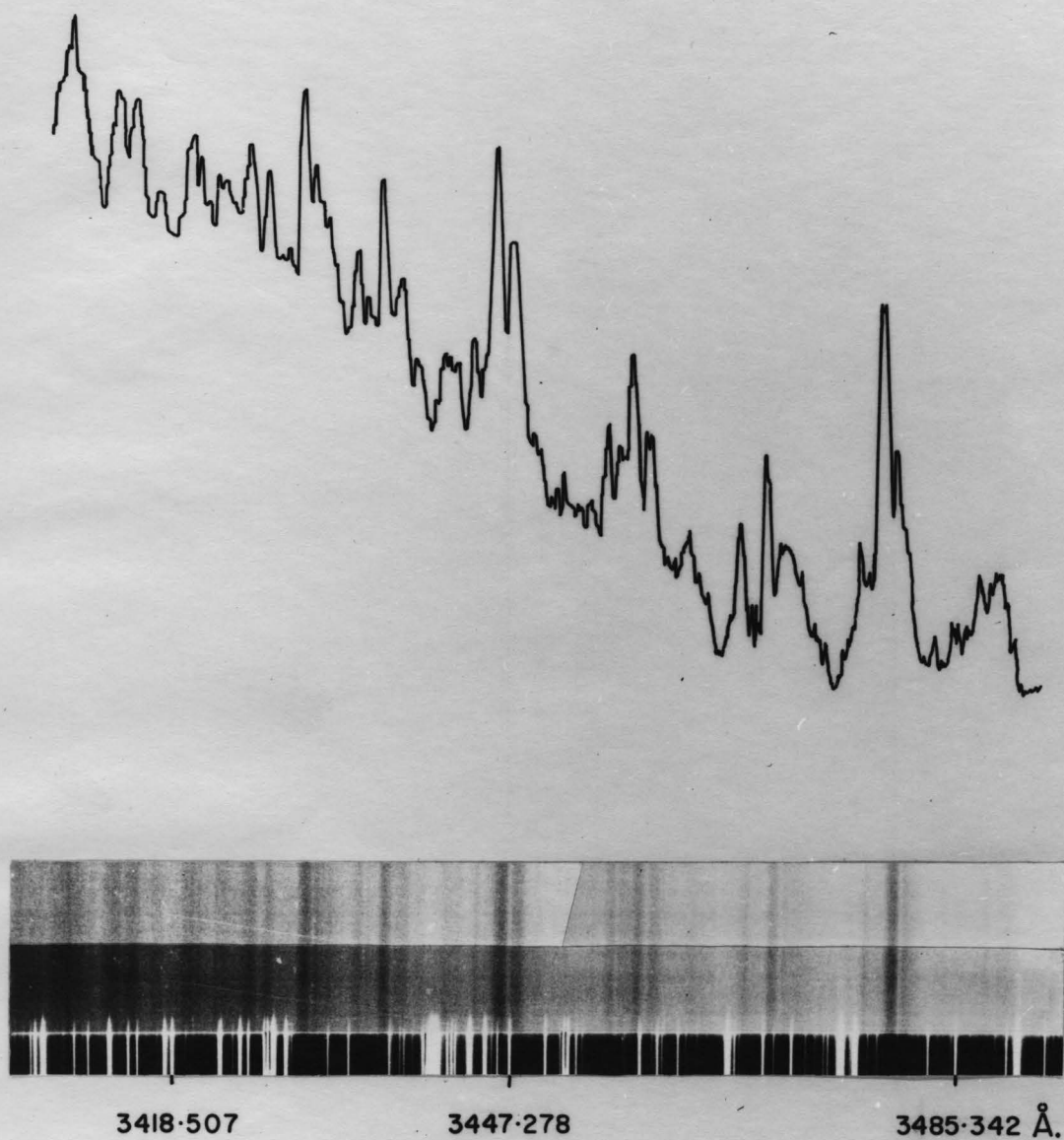


FIGURE 5.6. A SECTION OF THE $1A'' \leftarrow 1A'$ SPECTRUM
OF COFCOCl UNDER LOW RESOLUTION.

The strong band at 28724 cm^{-1} is probably the electronic origin. Progressions and combination bands are found in six excited state fundamentals; 180, 277, 419, 912, 1111, and 1280 cm^{-1} . The frequencies 277 and 419 are assigned to ν_8' and ν_7' the a' CCO rocking and scissors motions, respectively. ($\nu_8'' = 287 \text{ cm}^{-1}$ and $\nu_7'' = 491 \text{ cm}^{-1}$ from infrared spectroscopy.) As was observed for the other oxalyl halides, the in-plane "symmetric" rocking vibration changes little on excitation while the frequency of the "symmetric" scissors motion drops considerably.

The fundamental frequency of 180 cm^{-1} must be that of the lowest-lying a' vibration, ν_9' . The remaining fundamentals, 912, 1111 and 1280 cm^{-1} , are assigned to ν_4' (CC stretch), ν_3' (CF stretch) and ν_1' (CO stretch), respectively. The most prominent sequence interval is $+84 \text{ cm}^{-1}$ (torsion). A weak positive sequence of 23 cm^{-1} is also observed.

The assigned frequencies are collected in Table 5.5. The pseudo-origins $\nu_{00} - 626 \text{ cm}^{-1}$ and $\nu_{00} - 391 \text{ cm}^{-1}$ cannot be explained in terms of any of the known fundamental vibrations of the molecule. Presumably these bands result from sequences or progressions stacked upon bands to lower frequency which have not been observed due to the lack of sample. These bands are labelled A and B in Table 5.5.

TABLE 5.5

THE I ${}^1A'' \leftarrow {}^1A'$ ABSORPTION SPECTRUM OF
OXALYL CHLORIDE FLUORIDE.

| cm ⁻¹ | Int. | Notation | Assignment |
|------------------|------|----------------|-------------------|
| 28098 | vvw | A | $\nu_{00}' - 626$ |
| 183 | vvw | A $12_1'$ | - 626+85 |
| 269 | vvw | A 12_2^2 | - 626+85+86 |
| 278 | vvw | A $9_0'$ | - 626+180 |
| 333 | vw | B | - 391 |
| 362 | vvw | A $9_0' 12_1'$ | - 626+180+84 |
| 375 | vvw | A $8_0'$ | - 626+277 |
| 414 | vvw | B $12_1'$ | - 391+81 |
| 434 | vvw | 8_1^0 | - 290 |
| 460 | vvw | A $8_0' 12_1'$ | - 626+277+85 |
| 514 | vw | B $9_0'$ | - 391+181 |
| 518 | vvw | A $7_0'$ | - 626+420 |
| 519 | vvw | $8_1^0 12_1'$ | - 290+85 |
| 556 | vvw | A $8_0' 9_0'$ | - 626+277+181 |
| 610 | vw | B $8_0'$ | - 391+277 |
| 724 | s | 0_0^0 | origin |
| 747 | w | $10_1'$ | + 23 |
| 808 | m | $12_1'$ | + 84 |
| 832 | w | $10_1' 12_1'$ | + 84+24 |
| 893 | mw | 12_2^2 | + 84+85 |

| cm ⁻¹ | Int. | Notation | Assignment |
|------------------|------|---|------------------|
| 28904 | m | 9 ₀ ¹ | $\nu_{00} + 180$ |
| 927 | w | 9 ₀ ¹ 10 ₁ ¹ | + 180+23 |
| 979 | vvw | 12 ₃ ³ | + 84+85+86 |
| 989 | mw | 9 ₀ ¹ 12 ₁ ¹ | + 180+85 |
| 29001 | s | 8 ₀ ¹ | + 277 |
| 024 | w | 8 ₀ ¹ 10 ₁ ¹ | + 277+23 |
| 073 | ms | 9 ₀ ¹ 12 ₂ ² | + 180+85+84 |
| 086 | ms | 8 ₀ ¹ 12 ₁ ¹ | + 277+85 |
| 108 | w | 8 ₀ ¹ 10 ₁ ¹ 12 ₁ ¹ | + 277+85+22 |
| 143 | s | 7 ₀ ¹ | + 419 |
| 158 | vvw | 9 ₀ ¹ 12 ₃ ³ | + 180+85+84+85 |
| 170 | mw | 8 ₀ ¹ 12 ₂ ² | + 277+85+84 |
| 183 | m | 8 ₀ ¹ 9 ₀ ¹ | + 277+182 |
| 229 | mw | 7 ₀ ¹ 12 ₁ ¹ | + 419+86 |
| 267 | m | 8 ₀ ¹ 9 ₀ ¹ 12 ₁ ¹ | + 277+182+84 |
| 281 | m | 8 ₀ ² | + 277+280 |
| 314 | w | 7 ₀ ¹ 12 ₂ ² | + 419+86+85 |
| 324 | m | 7 ₀ ¹ 9 ₀ ¹ | + 419+181 |
| 354 | w | 8 ₀ ¹ 9 ₀ ¹ 12 ₂ ² | + 277+182+84+87 |
| 366 | mw | 8 ₀ ² 12 ₁ ¹ | + 277+280+85 |
| 421 | mw | 7 ₀ ¹ 8 ₀ ¹ | + 419+278 |
| 562 | vw | 7 ₀ ² | + 419+419 |
| 599 | vvw | 7 ₀ ¹ 8 ₀ ¹ 9 ₀ ¹ | + 419+278+178 |
| 636 | ms | 4 ₀ ¹ | + 912 |

| cm ⁻¹ | Int. | Notation | Assignment |
|------------------|------|----------------------|---------------------|
| 29715 | m | $4_0^1 12_1^1$ | $\nu_{00} + 912+79$ |
| 800 | m | $4_0^1 12_2^2$ | + 912+79+85 |
| 835 | m | 3_0^1 | + 1111 |
| 30004 | vvs | 1_0^1 | + 1280 |
| 089 | s | $1_0^1 12_1^1$ | + 1280+85 |
| 174 | mw | $1_0^1 12_2^2$ | + 1280+85+85 |
| 199 | s | $1_0^1 9_0^1 ?$ | + 1280+195 |
| 282 | vvs | $1_0^1 8_0^1$ | + 1280+278 |
| 366 | mw | $1_0^1 8_0^1 12_1^1$ | + 1280+278+84 |
| 404 | vvs | $1_0^1 7_0^1$ | + 1280+400 |
| 477 | ms | $1_0^1 8_0^1 9_0^1$ | + 1280+278+195 |
| 489 | m | $1_0^1 7_1^1 12_1^1$ | + 1280+400+85 |
| 561 | w | $1_0^1 8_0^2$ | + 1280+278+279 |
| 680 | ms | $1_0^1 7_0^1 8_0^1$ | + 1280+276+400 |
| 31112 | s | $1_0^1 3_0^1$ | + 1280+1108 |
| 195 | ms | $1_0^1 3_0^1 12_1^1$ | + 1280+1108+83 |
| 275 | s | 1_0^2 | + 1280+1271 |
| 357 | mw | $1_0^2 12_1^1$ | + 1280+1271+82 |
| 32360vb | s | $1_0^2 3_0^1$ | + 1280+1271+1085 |
| 530vb | s | 1_0^3 | + 1280+1271+1255 |

5.6 General Discussion of the Singlet-Singlet Systems.

Simple molecular orbital theory predicts that the central C-C bond in glyoxal, biacetyl and the oxalyl halides should be stronger in the I $^1A_u(n, \pi^*)$ state than in the ground state. The observations that the torsional frequency ν_τ almost doubles on excitation supports the idea of increased π -character across the CC bond and rotational analysis in the case of glyoxal³⁰ indicates that the excited state CC bond is indeed shorter.

The torsional overtone bands $\nu_{00} - 2\nu_\tau''$ and $\nu_{00} + 2\nu_\tau'$ have not been located in the spectra of the oxalyl halides. The Herzberg-Teller selection rules⁹⁰ predict that, within the harmonic approximation, these overtone bands will be extremely weak.

$$\frac{\text{Intensity of } 0-0 \text{ band}}{\text{Intensity of all } v-0 \text{ bands}} = \frac{(\nu' \nu'')^{1/2}}{1/2(\nu' + \nu'')}$$

for all $v = 0, 2, 4, \dots$. Even when $\nu' = 2\nu''$ the (0,0) band accounts for 94.3% of the total intensity of the progression, while the remaining 5.7% is distributed among the (2,0), (4,0), \dots bands.

Sidman and McClure⁶² suggest that $\nu_\tau' = 35 \text{ cm}^{-1}$ in the I $^1A_u(n, \pi^*)$ state of biacetyl. There are two objections to this assignment: first, it is improbable

that ν_{τ} will drop in frequency on $n \rightarrow \pi^*$ promotion ($\nu_{\tau}'' = 48 \text{ cm}^{-1}$ ⁹¹) and secondly, $\nu_{00} + 69 \text{ cm}^{-1}$ and $\nu_{00} + 138 \text{ cm}^{-1}$ appear as very strong bands in the spectrum. Instead of assigning $\nu_{00} + 35 \text{ cm}^{-1}$ and $\nu_{00} + 69 \text{ cm}^{-1}$ as $1 \leftarrow 0$ and $2 \leftarrow 0$ transitions in the acetyl torsional frequency, it is much more probable, in the light of observations on the spectra of the oxalyl halides, that the two intervals are unrelated and are due to sequences in the a_u vibrations, C=O out-of-plane wag and acetyl torsion. Values of $\nu_{\tau}' - \nu_{\tau}''$ are given in Table 5.6 for some related molecules.

The separation is almost constant between successive members in the torsional sequences of the oxalyl halides. For example, the intervals in oxalyl fluoride are 97.0, 96.6, 96.6 and 96.3 cm^{-1} . Since $\nu_{\tau}' \gg \nu_{\tau}''$, the regular spacing must mean that the anharmonicity constants in the two states are very small, unless we accept some very improbable coincidences. The torsional frequency would not be harmonic in the upper state if the molecule were twisted into a non-planar form on electronic excitation.

In spite of the strong evidence that the CC bond is considerably shorter in the excited state, the CC stretching vibration in glyoxal and the oxalyl halides is not strongly Franck-Condon active. Contrary to

TABLE 5.6

TORSIONAL SEQUENCES IN SINGLET-SINGLET $n \rightarrow \pi^*$
SYSTEMS OF SOME CONJUGATED KETONES.

| Molecule | Sequence (cm^{-1}) | Reference |
|-------------------|-------------------------------|-----------|
| glyoxal | +106 | 60 |
| propenal | + 92 | 80, 81 |
| biacetyl | + 69 | 62 |
| $(\text{COF})_2$ | + 97 | This work |
| COFCOCl | + 85 | " " |
| $(\text{COCl})_2$ | + 78 | " " |
| $(\text{COBr})_2$ | + 65 | " " |

Badger's and Clark's rules, the frequency is lower in the excited state.

A normal coordinate analysis, using a Urey-Bradley force field, has been carried out for the in-plane ground state vibrations of oxalyl chloride, oxalyl chloride fluoride and oxalyl fluoride by Hencher⁹². The calculations indicate that the so-called "CC stretch" is by no means a pure CC valence stretching mode.

The potential energy distribution for the ground state, in terms of internal coordinates, shows that the vibration of frequency 1078 cm^{-1} in oxalyl chloride contains only 33% CC valence stretching and has a large contribution (28%) from CCO angle bending. What is important when considering the Franck-Condon effect is not the change in internal coordinate but rather the change in normal coordinate⁹³. The contribution to the change in normal coordinate from a 0.08 \AA decrease in r_{CC} is opposite in sign and almost equal in magnitude to that from an increase of 0.08 \AA in r_{CO} accompanied by an opening of the \hat{CCO} by 2° . For $(\text{COCl})_2$:

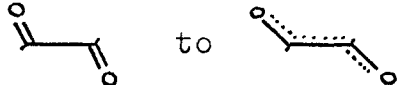
$$0.33 \times \Delta r_{CC} = -0.0264 \text{ \AA} \quad \text{and}$$

$$0.28 \times \Delta (r_{CO} \sin(\hat{CCO} - 90^\circ)) = +0.0225 \text{ \AA}$$

Hence, the change in normal coordinate is very small.

A simple calculation using the pseudo-diatomic approxima-

tion of Craig⁷⁴ shows that the normal coordinate must change by 0.04 Å for O_0^0 and 2_0^1 to be equally intense.

The rearrangement of electron density from  is expected to reinforce the planar structure. It is, therefore, reasonable for the out-of-plane oxygen wagging frequency⁺ to show a slight increase in value as a result of $n \rightarrow \pi^*$ promotion. The sequences +23, +32, +32 and +35 cm^{-1} in oxalyl chloride fluoride, oxalyl chloride, oxalyl bromide and biacetyl, respectively, are thought to involve this vibration. In oxalyl fluoride and glyoxal where $\nu_6'' > 400 \text{ cm}^{-1}$, the sequence is too weak to observe. In biacetyl +35 cm^{-1} is exactly half the torsional sequence interval which led Sidman and McClure to conclude that the two intervals were related. It would appear that this relationship is coincidental for, when we consider the spectrum of oxalyl chloride, we find the two sequences are +32 and +78 cm^{-1} .

The assignments of the a_g fundamental vibrational frequencies of the oxalyl halides in the ground electronic state and $I^1,^3A_u(n, \pi^*)$ states ($I^1,^3A''$ for COFCOCl) may be found in Tables 6.6 to 6.9 and the observed sequences are given in Tables 6.10 and 6.11.

⁺ $\nu_6(a_u)$ for $(\text{COX})_2$, $\nu_{10}(a'')$ for COFCOCl and $\nu_{11}(a_u)$ for biacetyl.

CHAPTER 6

VIBRATIONAL ANALYSES OF THE FIRST ${}^3A_u \leftarrow {}^1A_g$ $n \rightarrow \pi^*$ SYSTEMS OF THE OXALYL HALIDES.

6.1 Introduction.

Singlet-triplet $n \rightarrow \pi^*$ absorption spectra have been reported for several carbonyl compounds but relatively few vibrational analyses have been published. Analyses have appeared in the literature for formaldehyde⁹⁴, biacetyl⁶², p-benzoquinone⁸⁴ and propynal⁵⁹. In formaldehyde and propynal, where transitions are observed from the ground state to excited singlet and triplet states of the same electronic configuration, the vibrational frequencies in the two excited states are very similar. This is not surprising as the singlet and triplet (n, π^*) states should have very similar electronic charge distributions. Small differences that are found should be due to weak Pauli repulsion forces between the two unpaired electrons in the triplet state.

The x, y and z components of the spin-orbit Hamiltonian $\mathcal{H}'_{s.o.}$ have the symmetry properties of the corresponding rotation operators under the molecular point group. It has been shown⁹⁵ that if a triplet

state T is perturbed by a singlet state S, then the matrix element for the transition $T \leftarrow X$, where X is the singlet ground state, is given by

$$\frac{\int \psi(T) \mathcal{H}'_{so} \psi(S) d\tau}{E(S) - E(T)} \int \psi(S) \vec{\mu} \psi(X) d\tau$$

The perturbation does not occur unless

$$\overline{\psi(T)} \otimes \overline{\psi(S)} = \overline{R_x}, \overline{R_y} \text{ or } \overline{R_z}.$$

Table 6.1 summarizes spin-orbit coupling in C_{2h} . The 3A_u state must be perturbed by either a 1A_u or a 1B_u state, and the bands will show a corresponding polarization.

Which of these states is responsible for making the I ${}^3A_u \leftarrow {}^1A_g$ transition allowed in the oxalyl halides is not known. A partial rotational analysis of the (0,0) band of the I ${}^3A_u \leftarrow {}^1A_g$ system of glyoxal⁹⁶ suggests that the perturbing state is 1B_u in that molecule.

The spin wave functions of the triplet state have the symmetry properties of the rotations R_x , R_y and R_z . Under C_{2h} ,

$$\overline{R} = a_g \oplus 2b_g$$

Spin interactions, for example spin-spin, spin-orbit and

TABLE 6.1
 SPIN-ORBIT COUPLING BETWEEN
 TRIPLET AND SINGLET STATES
 IN C_{2h} .

| C_{2h} | x | y | z |
|----------|--------|--------|--------|
| $3A_g$ | $1B_g$ | $1B_g$ | $1A_g$ |
| $3A_u$ | $1B_u$ | $1B_u$ | $1A_u$ |
| $3B_g$ | $1A_g$ | $1A_g$ | $1B_g$ |
| $3B_u$ | $1A_u$ | $1A_u$ | $1B_u$ |

spin-other orbit coupling, will be different for the $\psi_s(a_g)$ level than for the $\psi_s(b_g)$ levels. However, in asymmetric top molecules there can be no electronic angular momentum and the spin-splittings caused by the above effects⁺ are very small. In formaldehyde⁵⁷, (the only carbonyl compound for which transitions to the different triplet state components have been resolved), the spin-splitting is of the order of 0.2 cm^{-1} . The spin-splittings in the 3A_u states of the oxalyl halides are expected to be of approximately the same magnitude as the rotational constants.

The energy separation between singlet-singlet and singlet-triplet systems is $\sim 2500 \text{ cm}^{-1}$ for each of the oxalyl halides and, consequently, the higher frequency bands of the singlet-triplet systems overlap those of the corresponding singlet-singlet systems. In general, the singlet-triplet bands have a sufficiently different profile from the singlet-singlet bands to enable the two systems to be sorted out where they overlap.

Predissociation is more common in the singlet-singlet spectra than in the singlet-triplet spectra

⁺ There is no strong spin-orbit coupling since the transition probability for the singlet-triplet transition is very small in the oxalyl halides.

(especially in the case of oxalyl bromide) so that the degree of diffuseness towards higher frequencies has also proved useful in distinguishing between the bands of the two systems.

6.2 Oxalyl chloride.

a) Excited state fundamentals.

A satisfactory analysis of the vibrational structure of the I ${}^3A_u \leftarrow {}^1A_g$ absorption spectrum of oxalyl chloride may be made assuming the band at 24370.2 cm^{-1} is the electronic origin.

The values proposed for the excited state a_g fundamentals differ in two respects from those previously reported¹⁸. Kanda *et al.* assigned the frequencies 278, 479, 1026 and 1436 cm^{-1} to ν'_5 (COCl rock), ν'_4 (CCO scissors), ν'_2 (CC stretch) and ν'_1 (CO stretch), respectively, while ν'_3 (CCl stretch) was not located. The present analysis favours the excited state fundamental values 281.1, 401.1, 634.6, 1028.2 and 1508.4 cm^{-1} .

b) Sequences.

The sequences in ν'_6 ($+31.6 \text{ cm}^{-1}$) and ν'_7 ($+78 \text{ cm}^{-1}$), the two a_u vibrations, are almost identical to those in the I ${}^1A_u \leftarrow {}^1A_g$ system. Intervals of -71.1 and -11.1 cm^{-1} are less prominent than the other sequences and are tentatively assigned to

$X_0^1 \leftarrow X_1^0$ transitions in the b_u bending modes ν_{11} and ν_{12} , respectively.

c) Discussion.

A careful examination of the spectrum with pressure path lengths of up to 3.4 m. atm. failed to show any significant absorption at or near 25810 cm^{-1} ($\nu_{00} + 1436 \text{ cm}^{-1}$) where Kanda and coworkers¹⁸ report 1_0^1 . We assume the band they observed was due to an impurity. On the other hand, a moderately strong band at 25877.7 cm^{-1} ($\nu_{00} + 1508.4 \text{ cm}^{-1}$) appears in the spectrum and it is more reasonable to assign this as 1_0^1 .

Of the two bands $\nu_{00} + 401 \text{ cm}^{-1}$ and $\nu_{00} + 479 \text{ cm}^{-1}$, the latter appears the stronger under low resolution. High resolution photographs reveal that this higher intensity arises from two overlapping bands both at $\sim \nu_{00} + 479 \text{ cm}^{-1}$. The $\nu_{00} + 401.1 \text{ cm}^{-1}$ band is assigned as 4_0^1 and the band at $\nu_{00} + 478.6 \text{ cm}^{-1}$ as $4_0^1 7_1^1$. The isotopic shifts confirm this assignment which makes $\nu_4' ({}^3A_u) \simeq \nu_4' ({}^1A_u)$.

The long progression in ν_5' shows a linear isotopic splitting with quantum number (Figure 6.1) and extrapolation indicates, as is the case in the I ${}^1A_u \leftarrow {}^1A_g$ system, that

$$|\nu_{00}(\text{CO}^{35}\text{Cl})_2 - \nu_{00}(\text{CO}^{35}\text{ClCO}^{37}\text{Cl})| < 0.2 \text{ cm}^{-1}.$$

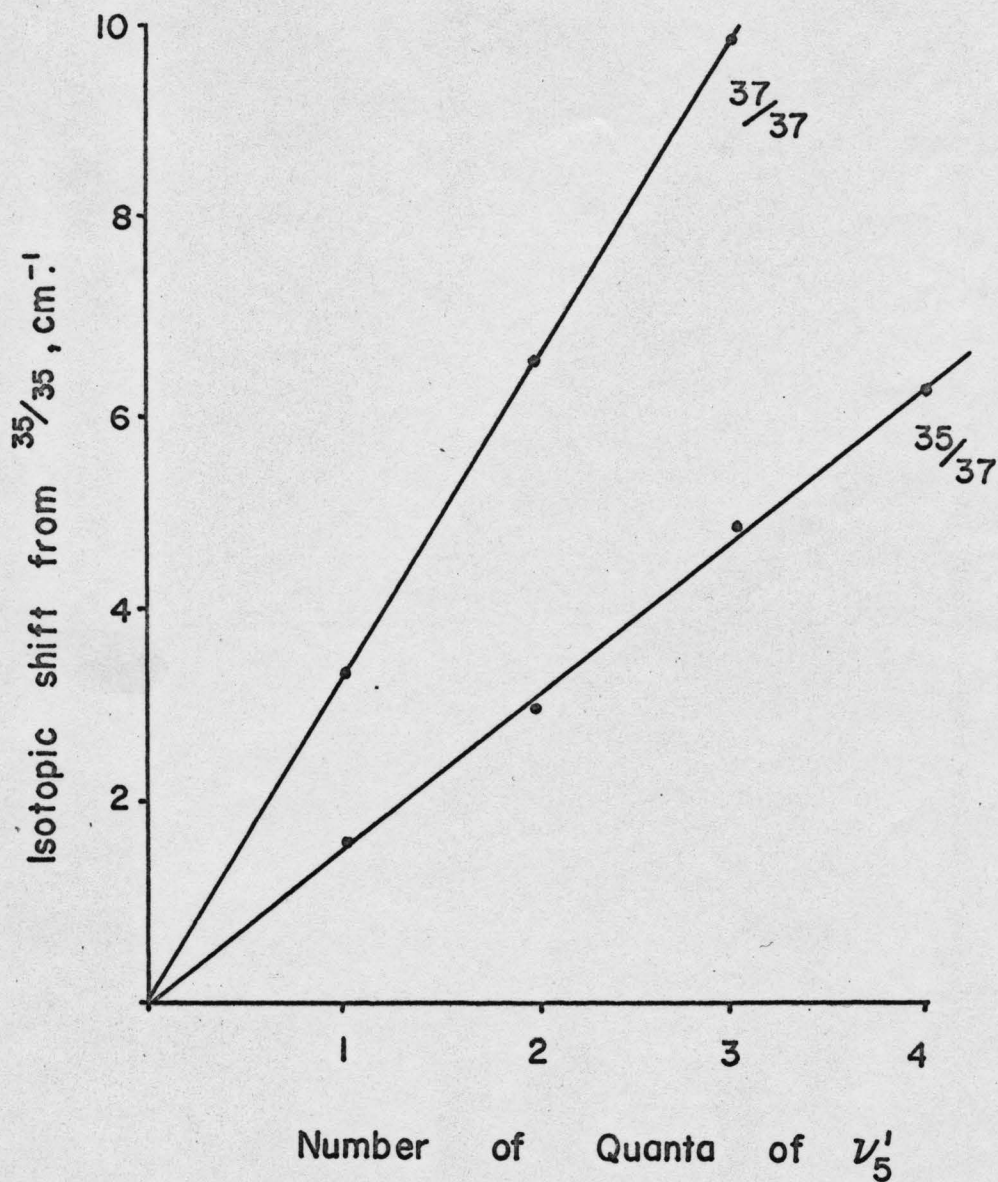


FIGURE 6.1 THE CHLORINE VIBRATIONAL ISOTOPE EFFECT IN THE ${}^3A_u - {}^1A_g$ SYSTEM OF OXALYL CHLORIDE.

The isotopic splittings in 5_0^1 and 4_0^1 are +1.6 and 2.7 cm^{-1} , respectively. The splitting in 3_0^1 (C-Cl stretch) is somewhat larger; +3.6 cm^{-1} .

A complete list of observed frequencies is given in the Appendix, Table A.5. The assigned bands are contained in Table 6.2 and a microdensitometer trace of part of the spectrum is shown in Figure 6.2.

6.3 Oxalyl bromide.

a) Introduction.

The bands of the I $^3A_u \leftarrow ^1A_g$ system of oxalyl bromide are much sharper under high resolution than the bands of the I $^1A_u \leftarrow ^1A_g$ spectrum and, in a few bands, the absorptions of the different isotopic species are resolved. Because the natural abundances of ^{79}Br and ^{81}Br are almost equal, the relative intensities of the absorption bands of the species $(\text{CO}^{79}\text{Br})_2$, $\text{CO}^{79}\text{BrCO}^{81}\text{Br}$ and $(\text{CO}^{81}\text{Br})_2$ are 1:2:1.

b) Fundamentals.

The strong band at 22938.0 cm^{-1} is identified as the electronic origin. 5_1^0 and 4_1^0 are observed, (as expected from observations in the singlet-singlet system), at $\nu_{00} - 185$ and $\nu_{00} - 441$ cm^{-1} , respectively. All five excited state a_g fundamentals are active in the spectrum, the values being 185.9, 312.3, 641.9, 1002.9 and 1537.2 cm^{-1} .

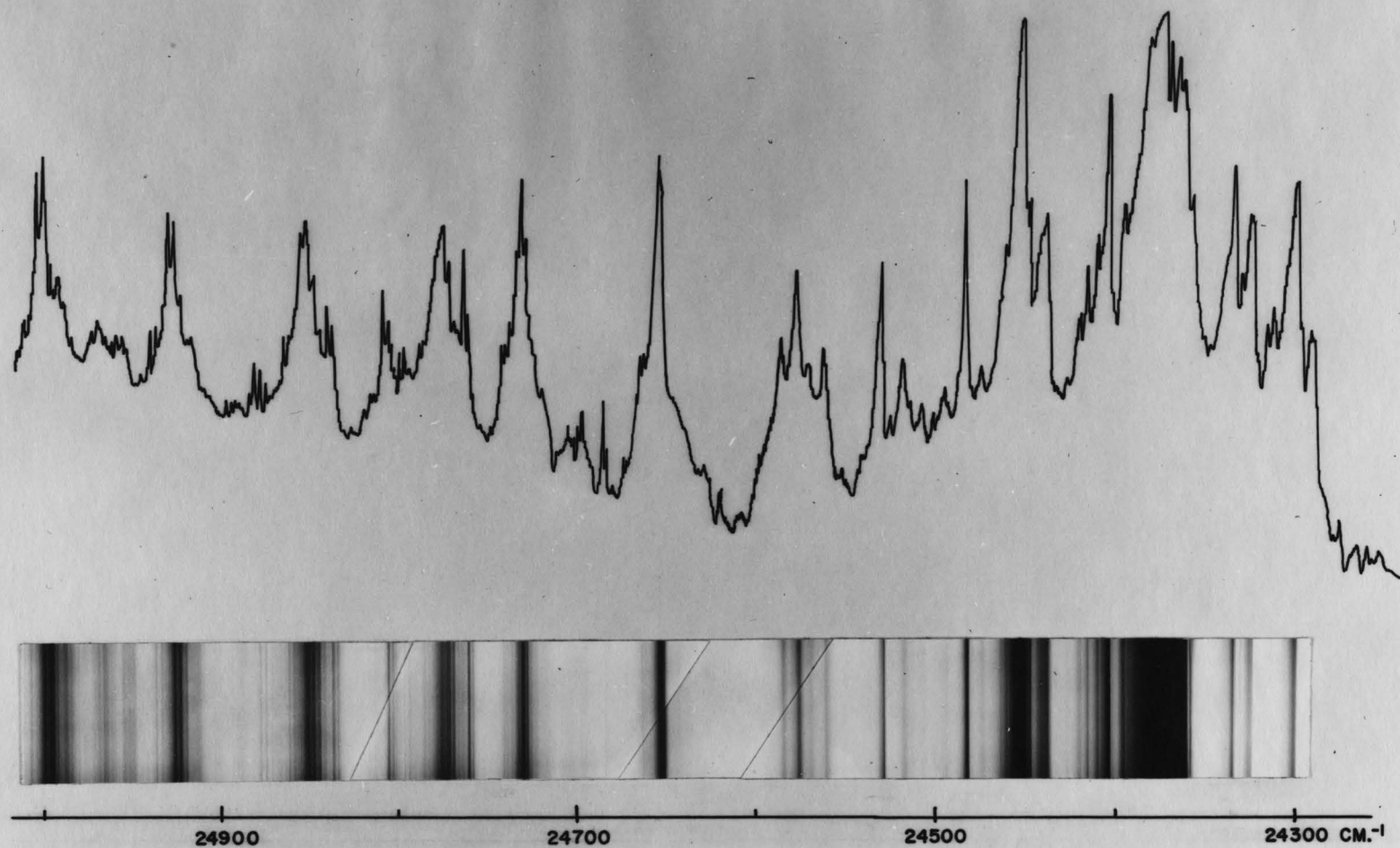


FIGURE 6.2 THE ${}^3A_u \leftarrow {}^1A_g$ ABSORPTION SPECTRUM OF $(\text{COCl})_2$
IN THE REGION $4120-4000\text{\AA}$.

TABLE 6.2

THE I ${}^3A_u \leftarrow {}^1A_g$ ABSORPTION SPECTRUM OF
 $(CO^{35}Cl)_2$

| cm ⁻¹ | Int. | Notation | Assignment |
|------------------|------|-----------------------|------------------------|
| 24232.2 | vw | 11_2^2 | ν_{00} - 71.1-66.9 |
| 266.8 | vw | $6_1^1 11_2^2$ | - 71.1-66.9+34.6 |
| 290.1 | w | $11_1^1 12_1^1$ | - 71.1-9.0 |
| 299.1 | m | 11_1^1 | - 71.1 |
| 312.0 | w | $7_1^1 11_2^2$ | - 71.1-66.9+79.4 |
| 333.8 | mw | $6_1^1 11_1^1$ | - 71.1+34.7 |
| 359.1 | ms | 12_1^1 | - 11.1 |
| 367.5 | ms | $7_1^1 11_1^1 12_1^1$ | - 71.1-9.0+77.4 |
| 370.2 | vs | 0_0^0 | origin |
| 378.9 | w | $7_1^1 11_1^1$ | + 78.3-69.6 |
| 401.6 | m | 6_1^1 | + 31.4 |
| 435.6 | vw | 6_2^2 | + 31.4+34.0 |
| 436.8 | w | $7_1^1 12_1^1$ | + 78.3-11.7 |
| 448.5 | s | 7_1^1 | + 78.3 |
| 458.4 | vw | $7_2^2 11_1^1$ | + 78.3+78.1-68.2 |
| 480.5 | m | $6_1^1 7_1^1$ | + 78.3+32.0 |
| 514.1 | vw | $7_2^2 12_1^1$ | + 78.3+78.1-12.5 |
| 526.6 | m | 7_2^2 | + 78.3+78.1 |
| 559.4 | w | $6_1^1 7_2^2$ | + 78.3+78.1+32.8 |
| 574.7 | m | $8_0^1 ?$ | + 204.5 |

| cm ⁻¹ | Int. | Notation | Assignment |
|------------------|------|--|-------------------------|
| 24583.0 | mw | 5 ₀ ¹ 11 ₁ ¹ | $\nu_{00} + 281.1-68.3$ |
| 616.9 | w | 5 ₀ ¹ 6 ₁ ¹ 11 ₁ ¹ | + 281.1-68.3+33.9 |
| 651.3 | ms | 5 ₀ ¹ | + 281.1 |
| 661.5 | vw | 5 ₀ ¹ 7 ₁ ¹ 11 ₁ ¹ | + 281.1+77.2-67.0 |
| 682.2 | w | 5 ₀ ¹ 6 ₁ ¹ | + 281.1+30.9 |
| 693.9 | vw | 5 ₀ ¹ 6 ₁ ¹ 7 ₁ ¹ 11 ₁ ¹ | + 281.1+77.2+32.4-67.0 |
| 698.7 | vvw | 4 ₀ ¹ 11 ₁ ¹ | + 401.1-72.6 |
| 728.5 | m | 5 ₀ ¹ 7 ₁ ¹ | + 281.1+77.2 |
| 735.5 | vw | 5 ₀ ¹ 7 ₂ ² 11 ₁ ¹ | + 281.1+77.2+77.5-70.5 |
| 760.9 | m | 5 ₀ ¹ 6 ₁ ¹ 7 ₁ ¹ | + 281.1+77.2+32.4 |
| 771.3 | ms | 4 ₀ ¹ | + 401.1 |
| 777.0 | vw | 4 ₀ ¹ 7 ₁ ¹ 11 ₁ ¹ | + 401.1+77.5-71.8 |
| 794.6 | w | 5 ₀ ¹ 7 ₂ ² 12 ₁ ¹ | + 281.1+77.2+77.5-11.4 |
| 801.9 | w | 4 ₀ ¹ 6 ₁ ¹ | + 401.1+30.6 |
| 806.0 | mw | 5 ₀ ¹ 7 ₂ ² | + 281.1+77.2+77.5 |
| 838.9 | w | 5 ₀ ¹ 6 ₁ ¹ 7 ₂ ² | + 281.1+77.2+77.5+32.9 |
| 848.8 | m | 4 ₀ ¹ 7 ₁ ¹ | + 401.1+77.5 |
| 852.5 | w | 4 ₀ ¹ 7 ₁ ¹ 11 ₁ ¹ | + 401.1+77.5+77.0-73.3 |
| 863.3 | vw | 5 ₀ ² 11 ₁ ¹ | + 281.1+277.4-65.4 |
| 880.0 | w | 4 ₀ ¹ 6 ₁ ¹ 7 ₁ ¹ | + 401.1+77.5+31.2 |
| 883.0 | vvw | 5 ₀ ¹ 7 ₃ ³ | + 281.1+77.2+77.5+77.0 |
| 925.8 | m | 4 ₀ ¹ 7 ₂ ² | + 401.1+77.5+77.0 |
| 928.7 | ms | 5 ₀ ² | + 281.1+277.4 |
| 932.5 | vvw | 3 ₀ ¹ 11 ₁ ¹ | + 634.6-72.3 |

| cm ⁻¹ | Int. | Notation | Assignment |
|------------------|------|----------------------|-----------------------------------|
| 24956.1 | vw | $4_0^1 6_1^1 7_2^2$ | $\nu_{00} + 401.1+77.5+77.0+30.3$ |
| 959.5 | vw | $5_0^2 6_1^1$ | + 281.1+277.4+30.8 |
| 991.8 | vw | $3_0^1 12_1^1$ | + 634.6-13.0 |
| 25000.2 | w | $4_0^1 7_3^3$ | + 401.1+77.5+77.0+74.4 |
| 004.8 | ms | 3_0^1 | + 634.6 |
| 010.3 | vw | $3_0^1 7_1^1 11_1^1$ | + 634.6+75.8-71.8 |
| 036.6 | w | $3_0^1 6_1^1$ | + 634.6+31.8 |
| 051.6 | w | $4_0^1 5_0^1$ | + 401.1+280.3 |
| 080.6 | m | $3_0^1 7_1^1$ | + 634.6+75.8 |
| 113.3 | vvvw | $3_0^1 6_1^1 7_1^1$ | + 634.6+75.8+32.7 |
| 126.7 | mw | $6_0^2 ?$ | + 2(378.3) |
| 156.2 | vw | $3_0^1 7_2^2$ | + 634.6+75.8+75.6 |
| 156.8 | vw | 6_1^3 | + 2(378.3)+30.1 |
| 171.3 | vw | 4_0^2 | + 401.1+400.0 |
| 201.5 | mw | $6_0^2 7_1^1$ | + 2(378.3) + 74.8 |
| 202.0 | m | 5_0^3 | + 281.1+277.4+273.3 |
| 233.8 | vw | $6_1^3 7_1^1$ | + 2(378.3)+74.8+31.8 |
| 276.4 | m | $5_0^3 7_1^1$ | + 281.1+277.4+273.3+74.4 |
| 277.9 | w | $6_0^2 7_2^2$ | + 2(378.3)+74.8+76.4 |
| 290.1 | vw | $3_0^1 5_0^1$ | + 634.6+285.3 |
| 323.4 | mw | $2_0^1 11_1^1 ?$ | + 1028.2-75.0 |
| 350.6 | w | $5_0^3 7_2^2$ | + 281.1+277.4+273.3+ 74.4+74.2 |
| 366.2 | vw | $3_0^1 5_0^1 7_1^1$ | + 634.6+285.3+76.1 |
| 398.4 | m | 2_0^1 | + 1028.2 |

| cm ⁻¹ | Int. | Notation | Assignment |
|------------------|------|---------------|------------------------------------|
| 25430.8 | vvw | $2_0^1 6_1^1$ | $\nu_{00} + 1028.2+32.4$ |
| 469.5 | ms | 5_0^4 | + 281.1+277.4+273.3+267.5 |
| 473.1 | m | $2_0^1 7_1^1$ | + 1028.2+74.7 |
| 543.7 | mw | $5_0^4 7_1^1$ | + 281.1+277.4+273.3+267.5+ 74.2 |
| 548.1 | vw | $2_0^1 7_2^2$ | + 1028.2+74.7+75.0 |
| 677.0 | mw | $2_0^1 5_0^1$ | + 1028.2+278.6 |
| 795.7 | vw | $2_0^1 4_0^1$ | + 1028.2+397.3 |
| 877.7 | s | 1_0^1 | + 1508.4 |
| 26158.8 | mw | $1_0^1 5_0^1$ | + 1508.4+280.2 |
| 275.0 | vw | $1_0^1 4_0^1$ | + 1508.4+396.4 |

TABLE 6.2a

THE I ${}^3A_u \leftarrow {}^1A_g$ ABSORPTION SPECTRUM OF
 $CO^{35}ClCO^{37}Cl$

| cm ⁻¹ | Notation | Assignment |
|------------------|--|------------------------|
| 24370.2* | 0 ₀ ⁰ | origin |
| 448.0 | 7 ₁ ¹ | $\nu_{00} + 77.8$ |
| 479.8 | 6 ₁ ¹ 7 ₁ ¹ | + 77.8+31.8 |
| 525.7 | 7 ₂ ² | + 77.8+77.7 |
| 558.2 | 6 ₁ ¹ 7 ₂ ² | + 77.8+77.7+32.5 |
| 573.9 | 8 ₀ ¹ ? | + 203.7 |
| 581.7 | 5 ₀ ¹ 11 ₁ ¹ | + 279.5-68.0 |
| 615.6 | 5 ₀ ¹ 6 ₁ ¹ 11 ₁ ¹ | + 279.5-68.0+33.9 |
| 649.7 | 5 ₀ ¹ | + 279.5 |
| 659.9 | 5 ₀ ¹ 7 ₁ ¹ 11 ₁ ¹ | + 279.5+76.9-66.7 |
| 680.4 | 5 ₀ ¹ 6 ₁ ¹ | + 279.5+76.9 |
| 692.3 | 5 ₀ ¹ 6 ₁ ¹ 7 ₁ ¹ 11 ₁ ¹ | + 279.5+76.9+32.1-66.4 |
| 726.6 | 5 ₀ ¹ 7 ₁ ¹ | + 279.5+76.9 |
| 758.7 | 5 ₀ ¹ 6 ₁ ¹ 7 ₁ ¹ | + 279.5+76.9+32.1 |
| 768.6 | 4 ₀ ¹ | + 398.4 |
| 799.2 | 4 ₀ ¹ 6 ₁ ¹ | + 398.4+30.6 |
| 803.5 | 5 ₀ ¹ 7 ₂ ² | + 279.5+76.9+76.9 |
| 836.0 | 5 ₀ ¹ 6 ₁ ¹ 7 ₂ ² | + 279.5+76.9+76.9+32.5 |
| 845.4 | 4 ₀ ¹ 7 ₁ ¹ | + 398.4+76.8 |
| 850.3 | 4 ₀ ¹ 7 ₂ ² 11 ₁ ¹ | + 398.4+76.8+76.8-71.9 |

| cm ⁻¹ | Notation | Assignment |
|------------------|---------------------|-------------------------------|
| 24860.6 | $5_0^2 11_1^1$ | $\nu_{00} + 279.5+276.1-65.2$ |
| 876.7 | $4_0^1 6_1^1 7_1^1$ | + 398.4+76.8+31.3 |
| 922.2 | $4_0^1 7_2^2$ | + 398.4+76.8+76.8 |
| 925.8 | 5_0^2 | + 279.5+276.1 |
| 952.7 | $4_0^1 6_1^1 7_2^2$ | + 398.4+76.8+76.8+30.5 |
| 956.1 | $5_0^2 6_1^1$ | + 279.5+276.1+30.4 |
| 25001.2 | 3_0^1 | + 631.0 |
| 032.5 | $3_0^1 6_1^1$ | + 631.0+31.3 |
| 048.0 | $4_0^1 5_0^1$ | + 398.4+279.4 |
| 076.6 | $3_0^1 7_1^1$ | + 631.0+75.4 |
| 122.3 | $6_0^2 ?$ | + 2(376.1) |
| 151.5 | 6_1^3 | + 2(376.1)+29.2 |
| 165.6 | 4_0^2 | + 398.4+397.0 |
| 196.7 | $6_0^2 7_1^1$ | + 2(376.1)+74.4 |
| 197.2 | 5_0^3 | + 279.5+276.1+271.4 |
| 228.6 | $6_1^3 7_1^1$ | + 2(376.1)+74.4+31.9 |
| 271.4 | $5_0^3 7_1^1$ | + 279.5+276.1+271.4+ 74.2 |
| 272.7 | $6_0^2 7_2^2$ | + 2(376.1)+74.4+76.0 |
| 286.2 | $3_0^1 5_0^1$ | + 631.0+285.0 |
| 317.9 | $2_0^1 11_1^1 ?$ | + 1022.5-74.8 |
| 361.0 | $3_0^1 5_0^1 7_1^1$ | + 631.0+285.0+74.8 |
| 392.7 | 2_0^1 | + 1022.5 |
| 463.3 | 5_0^4 | + 279.5+276.1+271.4+ 266.1 |
| 466.9 | $2_0^1 7_1^1$ | + 1022.5+74.2 |
| 541.9 | $2_0^1 7_2^2$ | + 1022.5+74.2+75.0 |

TABLE 6.2b

THE I ${}^3A_u \leftarrow {}^1A_g$ ABSORPTION SPECTRUM OF
 $(CO^{37}Cl)_2$

| cm ⁻¹ | Notation | Assignment |
|------------------|---------------------|------------------------------|
| 24370.2 * | 0_0^0 | origin |
| 572.8 | $8_0^1 ?$ | $\nu_{00} + 202.6$ |
| 648.0 | 5_0^1 | + 277.8 |
| 678.7 | $5_0^1 6_1^1$ | + 277.8+30.7 |
| 724.2 | $5_0^1 7_1^1$ | + 277.8+76.2 |
| 766.2 | 4_0^1 | + 396.0 |
| 842.0 | $4_0^1 7_1^1$ | + 396.0+75.8 |
| 873.4 | $4_0^1 6_1^1 7_1^1$ | + 396.0+75.8+31.4 |
| 922.9 | 5_0^2 | + 277.8+274.9 |
| 997.7 | 3_0^1 | + 627.5 |
| 25118.1 | $6_0^2 ?$ | + 2(374.0) |
| 192.2 | 5_0^3 | + 277.8+274.9+269.3 |
| 266.0 | $5_0^3 7_1^1$ | + 277.8+274.9+269.3+ 73.8 |
| 267.3 | $6_0^2 7_2^2$ | + 2(374.0)+74.6+74.6 |

* by extrapolation

Several sequence intervals and excited state fundamentals are found in association with two bands of medium intensity in the spectrum, one at $\nu_{00} + 917.4 \text{ cm}^{-1}$, the other at $\nu_{00} + 1169.9 \text{ cm}^{-1}$. It is probable that these bands are $2 \leftarrow 0$ transitions in non-totally symmetric vibrations with excited state frequencies of ~ 459 and $\sim 585 \text{ cm}^{-1}$. As the infrared spectrum of oxalyl bromide has not been fully analyzed these vibrations cannot be positively identified. They may be the b_u bending modes ν'_{11} and ν'_{10} .

c) Sequences.

Three sequences are found in association with the stronger bands of the spectrum. These are $+64.6$, $+31.5$ and -74.5 cm^{-1} . There is also the possibility of a very weak, negative sequence of $\sim 27 \text{ cm}^{-1}$. The sequences of $+64.6$ and $+31.5 \text{ cm}^{-1}$ are assigned to the two a_u -type out-of-plane bending vibrations, ν_7 and ν_6 , respectively. The negative sequence of 74.5 cm^{-1} may involve ν_{11} .

d) Discussion.

The bromine vibrational isotope effect is clearly resolved in the bands 5_0^1 and 5_1^0 . $\nu_5 \{(\text{CO}^{79}\text{Br})_2\} - \nu_5 \{\text{CO}^{79}\text{BrCO}^{81}\text{Br}\}$ is $+1.1 \text{ cm}^{-1}$ in the ground state and $+0.8 \text{ cm}^{-1}$ in the excited state. The isotope

effect in oxalyl bromide is not as useful analytically as that in oxalyl chloride since the splittings are much smaller for the bromide.

The assigned spectral bands of $\text{CO}^{79}\text{BrCO}^{81}\text{Br}$ are given in Table 6.3. Part of the observed spectrum is shown in Figure 6.3 and vacuum wavenumbers for all spectral features are to be found in the Appendix, Table A.6.

6.4 Oxalyl fluoride.

a) Introduction.

The singlet-triplet spectrum of oxalyl fluoride is extremely sharp and several bands close to the system-origin show extensive rotational structure under high resolution. Since the bands degrade towards the red, frequency measurements refer to the violet edge of the bands. Vacuum wavenumbers of the band heads may be found in the Appendix, Table A.7.

The (0,0) band is found as the most intense band of the system, at 29941.9 cm^{-1} . The three bands to longer wavelengths, $\nu_{00} - 802.9$, $\nu_{00} - 319$ and $\nu_{00} - 228.6 \text{ cm}^{-1}$, which are also found in the singlet-singlet system are assigned to the transitions 3_1^0 , 5_1^0 and 7_2^0 , respectively.

b) Excited state fundamentals.

The spectrum has been analyzed in terms of five excited state fundamentals; 287.9, 387.4, 508.7,

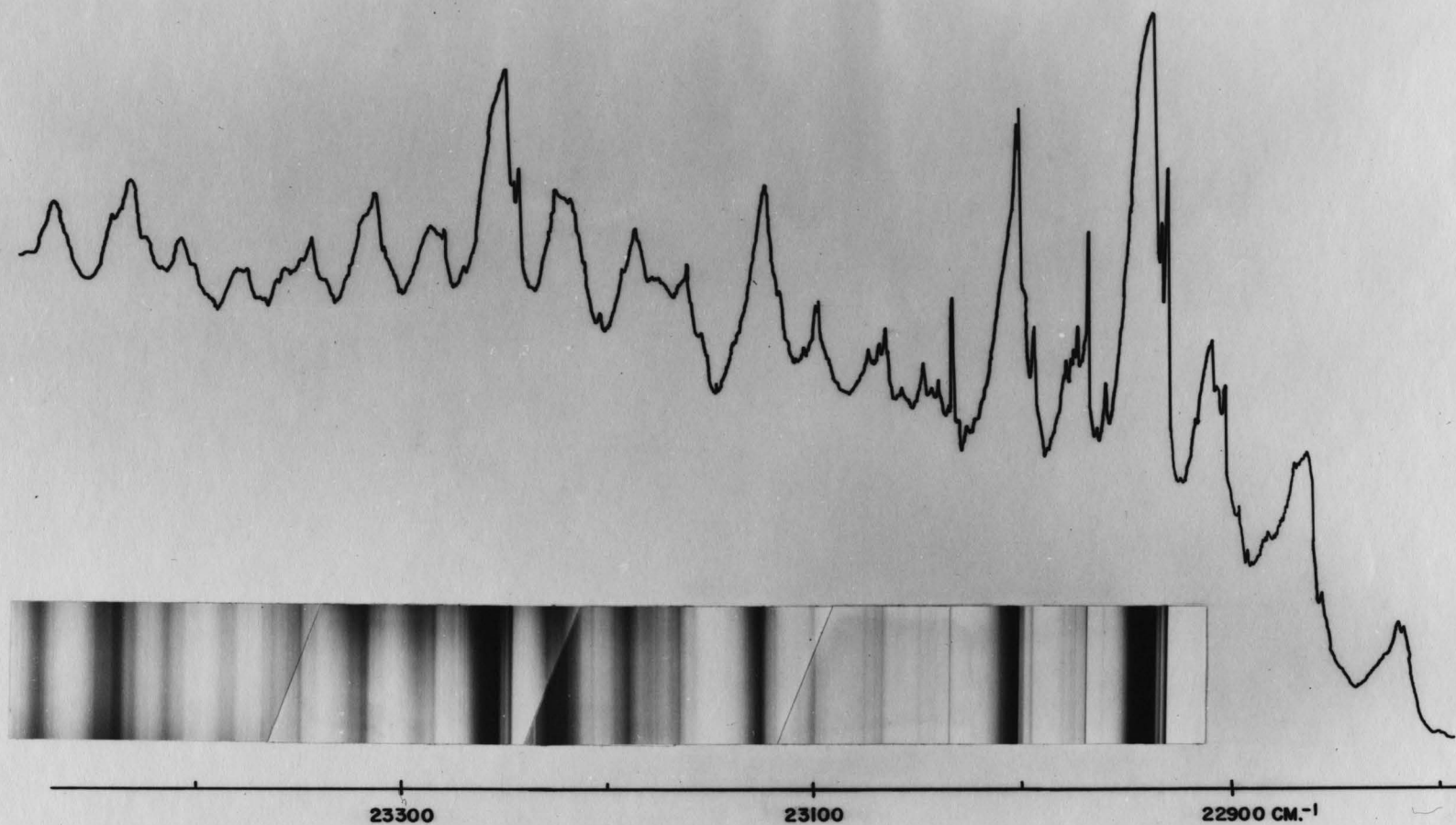


FIGURE 6.3 THE ${}^3A_u \leftarrow {}^1A_g$ ABSORPTION SPECTRUM OF $(\text{COBr})_2$
IN THE REGION 4380–4250 Å.

TABLE 6.3

THE I ${}^3A_u \leftarrow {}^1A_g$ ABSORPTION SPECTRUM OF
OXALYL BROMIDE

| cm^{-1} | Int. | Notation | Assignment |
|------------------|------|----------------------|-------------------|
| 22497 | vvvw | 4_1^0 | $\nu_{00} - 441$ |
| 587.0 | vw | $12_2^0 ?$ | - 2(175.5) |
| 652 | vw | $7_1^1 12_2^0$ | - 2(175.5)+65 |
| 677.7 | vw | $5_1^0 11_1^1$ | - 185.3-75.0 |
| 706.3 | vw | $5_1^0 6_1^1 11_1^1$ | - 185.3-75.0+28.6 |
| 752.7 | mw | 5_1^0 | - 185.3 |
| 782.2 | vw | $5_1^0 6_1^1$ | - 185.3+29.5 |
| 819.8 | mw | $5_1^0 7_1^1$ | - 185.3+67.1 |
| 855.3 | vw | $5_1^0 6_1^1 7_1^1$ | - 185.3+67.1+35.5 |
| 863.5 | m | 11_1^1 | - 74.5 |
| 885.2 | vvvw | $5_1^0 7_2^2$ | - 185.3+67.1+65.4 |
| 898.1 | vw | $4_0^1 12_2^0$ | - 2(175.5)+311.1 |
| 938.0 | vs | 0_0^0 | origin |
| 969.5 | m | 6_1^1 | + 31.5 |
| 23002.6 | s | 7_1^1 | + 64.6 |
| 034.3 | mw | $6_1^1 7_1^1$ | + 64.6+31.7 |
| 049.1 | vvvw | $5_0^1 11_1^1$ | + 185.9-74.8 |
| 065.2 | vw | $4_0^1 5_1^0$ | + 312.3-185.1 |
| 066.6 | mw | 7_2^2 | + 64.6+64.0 |
| 098.6 | w | $8_0^1 ?$ | + 160.6 |

| cm ⁻¹ | Int. | Notation | Assignment |
|------------------|------|---------------------|-----------------------------|
| 23100.1 | w | $6_1^1 7_2^2$ | $\nu_{00} + 64.6+64.0+33.5$ |
| 123.9 | s | 5_0^1 | + 185.9 |
| 156.9 | w | $5_0^1 6_1^1$ | + 185.9+33.0 |
| 163.6 | w | $7_1^1 8_0^1$ | + 160.6+65.0 |
| 187.7 | m | $5_0^1 7_1^1$ | + 185.9+63.8 |
| 220.2 | mw | $5_0^1 6_1^1 7_1^1$ | + 185.9+63.8+32.5 |
| 226.9 | mw | $7_2^2 8_0^1$ | + 160.6+65.0+63.3 |
| 250.3 | vs | 4_0^1 | + 312.3 |
| 281.5 | m | $4_0^1 6_1^1$ | + 312.3+31.2 |
| 313.3 | ms | $4_0^1 7_1^1$ | + 312.3+63.0 |
| 347.0 | mw | $4_0^1 6_1^1 7_1^1$ | + 312.3+63.0+33.7 |
| 379.3 | mw | $4_0^1 7_2^2$ | + 312.3+63.0+66.0 |
| 412 | mw | $4_0^1 8_0^1$ | + 312.3+162 |
| 436 | ms | $4_0^1 5_0^1$ | + 312.3+186 |
| 512.2 | w | $6_0^2 ?$ | + 2(287.6) |
| 563.7 | w | 4_0^2 | + 312.3+313.4 |
| 579.9 | ms | 3_0^1 | + 641.9 |
| 611.8 | w | $3_0^1 6_1^1$ | + 641.9+31.9 |
| 651.5 | mw | $3_0^1 7_1^1$ | + 641.9+71.6 |
| 684.3 | w | $3_0^1 6_1^1 7_1^1$ | + 641.9+71.6+32.8 |
| 722.8 | vw | $3_0^1 7_2^2$ | + 641.9+71.6+71.3 |
| 756.3 | vw | $3_0^1 6_1^1 7_2^2$ | + 641.9+71.6+71.3+33.5 |
| 763.1 | w | $3_0^1 5_0^1$ | + 641.9+183.2 |
| 791.0 | vw | $3_0^1 5_0^1 6_1^1$ | + 641.9+183.2+27.9 |

| cm ⁻¹ | Int. | Notation | Assignment |
|------------------|------|----------------------|-----------------------------------|
| 23792.0 | mw | $3_0^1 7_3^3$ | $\nu_{00} + 641.9+71.6+71.3+69.2$ |
| 834.1 | w | $3_0^1 5_0^1 7_1^1$ | + 641.9+183.2+71.0 |
| 855.4 | m | $11_0^2 ?$ | + 2(458.7) |
| 887.6 | vw | $6_1^1 11_0^2$ | + 2(458.7)+32.2 |
| | | $3_0^1 4_0^1$ | + 641.9+307.7 |
| 903.9 | vw | $3_0^1 5_0^1 7_2^2$ | + 641.9+183.2+71.0+ 69.8 |
| 927.0 | mw | $7_1^1 11_0^2$ | + 2(458.7)+71.6 |
| 940.9 | s | 2_0^1 | + 1002.9 |
| 959.5 | vw | $6_1^1 7_1^1 11_0^2$ | + 2(458.7)+71.6+32.5 |
| 971.3 | mw | $2_0^1 6_1^1$ | + 1002.9+30.4 |
| 997.3 | mw | $7_2^2 11_0^2$ | + 2(458.7)+71.6+70.3 |
| 24004.2 | ms | $2_0^1 7_1^1$ | + 1002.9+63.3 |
| 030.7 | vvw | $6_0^1 7_2^2 11_0^2$ | + 2(458.7)+71.6+70.3+ 33.4 |
| 035.0 | vw | $1_0^1 4_1^0$ | + 1537.2-440.2 |
| 037.7 | vvw | $2_0^1 6_1^1 7_1^1$ | + 1002.9+63.3+33.7 |
| 042.0 | vw | $5_0^1 11_0^2$ | + 2(458.7)+186.6 |
| 067 | vvvw | $2_0^1 7_2^2$ | + 1002.9+63.3+63 |
| 083.9 | vw | $6_0^4 ?$ | + 2(287.1)+2(285.9) |
| 107.9 | w | $10_0^2 ?$ | + 2(585.0) |
| 118.4 | vvvw | 6_1^5 | + 2(287.1)+2(285.9)+ 34.5 |
| 128.0 | w | $2_0^1 5_0^1$ | + 1002.9+187.1 |
| 140.4 | vvvw | $6_1^1 10_0^2$ | + 2(585.0)+32.5 |

| cm ⁻¹ | Int. | Notation | Assignment |
|------------------|------|---------------------|-------------------------------------|
| 24153.2 | vw | $6_0^4 7_1^1$ | $\nu_{00} + 2(287.1)+2(285.9)+69.3$ |
| 162.0 | vvw | $2_0^1 5_0^1 6_1^1$ | + 1002.9+187.1+34.0 |
| 163.9 | vvw | $4_0^1 11_0^2$ | + 2(458.7)+308.5 |
| 178.3 | vw | $7_1^1 10_0^2$ | + 2(585.0)+70.4 |
| 199.6 | vw | $2_0^1 5_0^1 7_1^1$ | + 1002.9+187.1+71.6 |
| 222.0 | vvw | $6_0^4 7_2^2$ | + 2(287.1)+2(285.9)+69.3+68.8 |
| 246.3 | vvw | $2_0^1 4_0^1$ | + 1002.9+305.4 |
| 248.6 | vvw | $7_2^2 10_0^2$ | + 2(585.0)+70.4+70.3 |
| 270.5 | vvvw | $5_0^1 6_0^4$ | + 2(287.1)+2(285.9)+186.6 |
| 289.4 | vw | $1_0^1 5_1^0$ | + 1537.2-185.8 |
| 359.1 | vw | $1_0^1 5_1^0 7_1^1$ | + 1537.2-185.8+69.7 |
| 397.8 | vvw | $4_0^1 6_0^4$ | + 2(287.1)+2(285.9)+313.9 |
| 428.3 | vvw | $1_0^1 5_1^0 7_2^2$ | + 1537.2-185.8+69.7+69.2 |
| 475.2 | vs | 1_0^1 | + 1537.2 |
| 506.7 | m | $1_0^1 6_1^1$ | + 1537.2+31.5 |
| 539.6 | s | $1_0^1 7_1^1$ | + 1537.2+64.4 |
| 571.3 | mw | $1_0^1 6_1^1 7_1^1$ | + 1537.2+64.4+31.7 |
| 581 | vvvw | $2_0^1 3_0^1$ | + 1002.9+640 |
| 603.4 | ms | $1_0^1 7_2^2$ | + 1537.2+64.4+63.8 |
| 637.2 | m | $1_0^1 6_1^1 7_2^2$ | + 1537.2+64.4+63.8+33.8 |
| 660 | s | $1_0^1 5_0^1$ | + 1537.2+185 |
| 670 | vvw | $1_0^1 7_3^3$ | + 1537.2+64.4+63.8+67 |

| cm^{-1} | Int. | Notation | Assignment |
|------------------|------|---------------------|----------------------------|
| 24700 | m | $1_0^1 5_0^1 6_1^1$ | $\nu_{00} + 1537.2+185+40$ |
| 731 | m | $1_0^1 5_0^1 7_1^1$ | $+ 1537.2+185+61$ |
| 783 | ms | $1_0^1 4_0^1$ | $+ 1537.2+308$ |

1241.6 and 1495.3 cm^{-1} . The frequencies 287.9 and 508.7 cm^{-1} are assigned to the two in-plane symmetric bending frequencies whose values are 280.5 and 531.4 cm^{-1} in the I 1A_u state. The symmetric carbonyl stretching frequency (1495.3 cm^{-1}) is higher in the triplet state than in the corresponding singlet state where it is 1440.2 cm^{-1} . The frequency 1241.6 cm^{-1} is assigned to the symmetric CF stretch, ν_2' , and the band at 30329 cm^{-1} ($\nu_{00} + 387.4 \text{ cm}^{-1}$), like its analogue $\nu_{00}(\text{SS}) + 370.3 \text{ cm}^{-1}$, is assigned tentatively to the formally symmetry-forbidden transition 8_0^1 .

c) Sequences.

There are three common sequence intervals in the spectrum; +100.5, -30.4 and -78.2 cm^{-1} . The +100.5 cm^{-1} sequence is most definitely that due to torsion about the C-C bond. The sequence of -30.4 cm^{-1} is thought to involve the lowest-lying in-plane bending vibration $\nu_{12}(b_u)$, while the -78.2 cm^{-1} sequence may be due to ν_{11} . Weak satellites appearing at $\sim 15 \text{ cm}^{-1}$ to the higher energy side of some of the strong bands may be part of the rotational structure, or alternatively, could possibly be due to sequences in ν_6 .

d) Discussion.

The band at 30329.3 cm^{-1} is assigned as $\nu_{00} + 387.4 \text{ cm}^{-1}$ (8_0^1) in preference to the alternative

assignment $\nu_{00} + 287.9 + 99.5 \text{ cm}^{-1}$ (i.e., $5_0^1 7_1^1$) for several reasons:

(i) It is thought that $\nu_{00}(\text{SS}) + 370.3 \text{ cm}^{-1}$ corresponds to $\nu_{00} + \nu_8'(b_g)$.

(ii) The 30329.3 cm^{-1} band is considerably more intense than that at 30229.8 cm^{-1} (5_0^1).

(iii) The band at 30613.3 cm^{-1} may be assigned as $\nu_{00} + 387.4 + 284.0 \text{ cm}^{-1}$.

(iv) A very weak band at 30330.7 cm^{-1} can be assigned to the transition $5_0^1 7_1^1$.

The argument might be raised against point (iii) that 30613.3 cm^{-1} can be assigned as $5_0^2 7_1^1$, i.e., $\nu_{00} + 287.9 + 285.4 + 98.1 \text{ cm}^{-1}$. However, the 30613.3 cm^{-1} band is more intense than 5_0^2 at 30515.2 cm^{-1} .

The torsional sequence ($+100.5 \text{ cm}^{-1}$) is strong throughout the spectrum and successive members of this sequence are equally spaced, which suggests that the torsional frequency is close to harmonic in the combining states. Hencher and King¹⁷ proposed a value of $\sim 127 \text{ cm}^{-1}$ for the ground state torsional frequency from combination bands in the infrared spectrum. If the bands found in the ultraviolet systems at $\sim \nu_{00} - 230 \text{ cm}^{-1}$ are 7_2^0 , then $\nu_7'' \approx 115 \text{ cm}^{-1}$.

Miller and coworkers⁹⁷ at the Mellon Institute have studied torsional motion around C-C single bonds in conjugated molecules and have used far infrared torsional

frequencies to obtain an estimate of the barrier height V^* resisting trans \rightarrow cis interconversion. They have shown that, when ν_t' is harmonic

$$V^* = \frac{\nu_t'^2}{F} \quad (6.1)$$

where F is related to Pitzer's⁹⁸ reduced moment of inertia for torsion, I_r , by the equation

$$F \text{ (in cm}^{-1}\text{)} = \frac{h}{8\pi^2 c I_r} = \frac{16.852}{I_r \text{ (a.m.u.-\AA}^2\text{)}} \quad (6.2)$$

When the molecular parameters for oxalyl fluoride (Table 1.2a) are substituted into Pitzer's expressions, we find $I_r(\text{COF})_2 = 21.608 \text{ a.m.u.-\AA}^2$, (i.e., $F = 0.780 \text{ cm}^{-1}$), so that if $\nu_t'' = 115 \text{ cm}^{-1}$, the barrier V^* is 17000 cm^{-1} in the ground state

Table 6.4 contains assigned frequencies and Figure 6.4 shows part of the spectrum.

6.5 Oxalyl chloride fluoride.

The small sample of oxalyl chloride fluoride gave a vapour pressure of $\sim 5 \text{ mm Hg}$ in the 185 m multiple reflection cell used. 48 traversals of the cell were required to observe the stronger bands of the singlet-triplet spectrum. A vibrational analysis similar to that of the singlet-singlet system is given in Table 6.5.

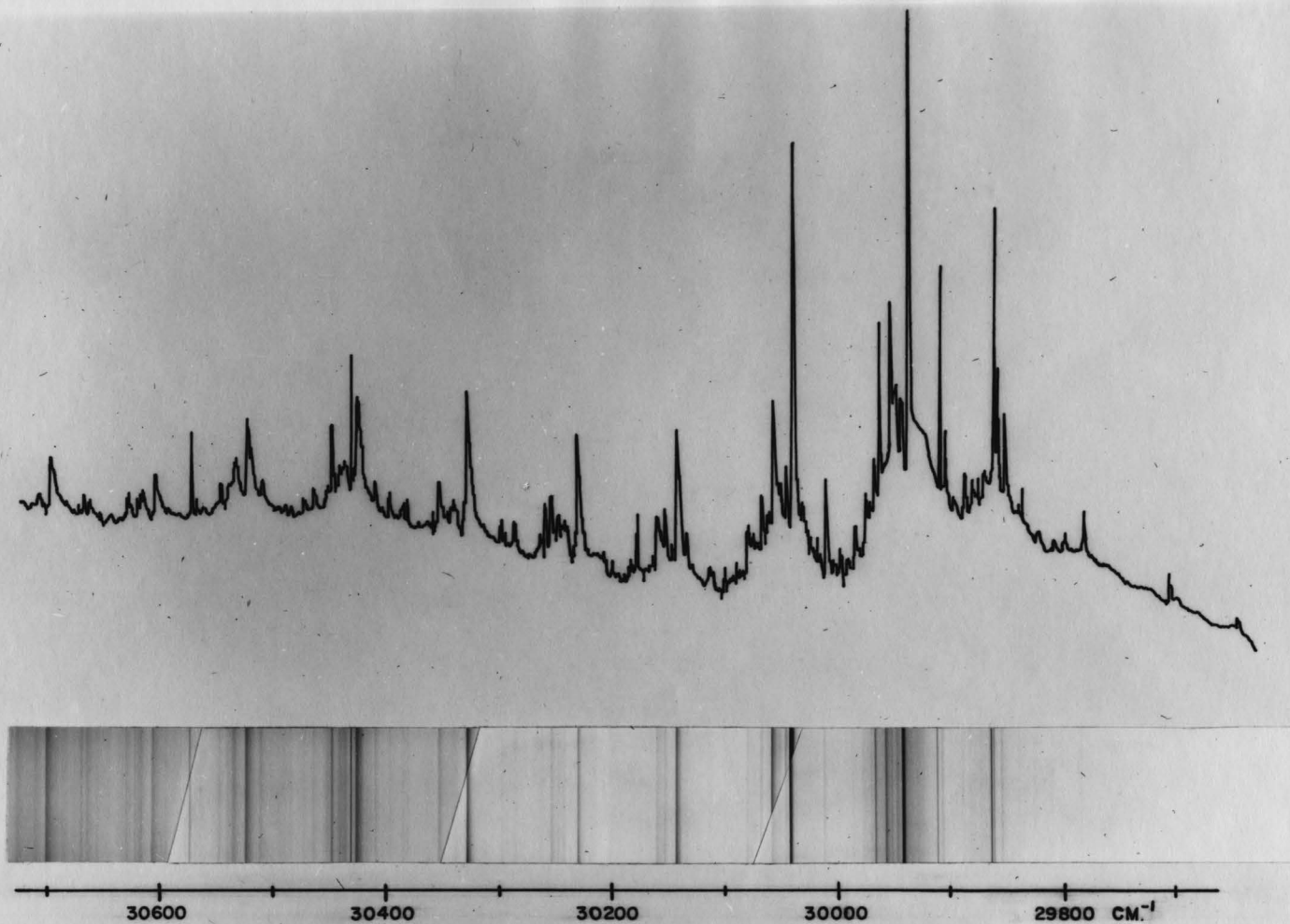


FIGURE 6.4 THE ${}^3A_u \leftarrow {}^1A_g$ ABSORPTION SPECTRUM OF $(COF)_2$
IN THE REGION 3370-3250 Å.

TABLE 6.4

THE I ${}^3A_u \leftarrow {}^1A_g$ ABSORPTION SPECTRUM OF
OXALYL FLUORIDE.

| cm ⁻¹ | Int. | Notation | Assignment |
|------------------|------|---|-----------------------|
| 29081.3 | vvw | 6 ⁰ ₂ | ν_{00} - 2(430.3) |
| 139.0 | vw | 3 ⁰ ₁ | - 802.7 |
| 486.5 | vw | 7 ⁰ ₄ | - 228.6-224.1 |
| 527.7 | vw | 3 ⁰ ₁ 8 ¹ ₀ | - 802.7+388.7 |
| 623 | vw | 5 ⁰ ₁ | - 519 |
| 626.3 | vw | 3 ⁰ ₁ 7 ¹ ₁ 8 ¹ ₀ | - 802.7+388.7+98.6 |
| 681.1 | vvw | 7 ⁰ ₂ 12 ¹ ₁ | - 228.6-32.2 |
| 705.8 | vvw | 11 ³ ₃ | - 78.2-78.7-79.2 |
| 713.3 | w | 7 ⁰ ₂ | - 2(114.3) |
| 785.0 | w | 11 ² ₂ | - 78.2-78.7 |
| 813.9 | vvw | 7 ¹ ₃ | - 2(114.3)+100.6 |
| 863.7 | m | 11 ¹ ₁ | - 78.2 |
| 882.7 | vw | 12 ² ₂ | - 30.4-28.8 |
| 888.9 | vw | 7 ¹ ₁ 11 ² ₂ | + 100.5-76.2-77.3 |
| 911.5 | mw | 12 ¹ ₁ | - 30.4 |
| 941.9 | vs | 0 ⁰ ₀ | origin |
| 956.7 | mw | 6 ¹ ₁ ? | + 14.8 |
| 966.2 | mw | 7 ¹ ₁ 11 ¹ ₁ | + 100.5-76.2 |
| 982.3 | vw | 7 ¹ ₁ 12 ² ₂ | + 100.5-30.2-29.8 |
| 30012.1 | w | 7 ¹ ₁ 12 ¹ ₁ | + 100.5-30.2 |

| cm ⁻¹ | Int. | Notation | Assignment |
|------------------|------|--|-------------------------|
| 30042.4 | s | 7 ₁ ¹ | 2 ₀₀ + 100.5 |
| 058.6 | mw | 6 ₁ ¹ 7 ₁ ¹ | + 100.5+16.2 |
| 068.3 | vw | 7 ₂ ² 11 ₁ ¹ | + 100.5+100.7-74.8 |
| 113.7 | vvw | 7 ₂ ² 12 ₁ ¹ | + 100.5+100.7-29.4 |
| 143.1 | m | 7 ₂ ² | + 100.5+100.7 |
| 152.6 | w | 5 ₀ ¹ 11 ₁ ¹ | + 287.9-77.2 |
| 160.0 | w | 6 ₁ ¹ 7 ₂ ² | + 100.5+100.7+16.9 |
| 176.5 | vvw | 8 ₀ ¹ 11 ₂ ² | + 387.4-75.6-76.6 |
| 198.6 | vw | 5 ₀ ¹ 12 ₁ ¹ | + 287.9-31.2 |
| 229.8 | m | 5 ₀ ¹ | + 287.9 |
| 243.7 | vw | 7 ₃ ³ | + 100.5+100.7+100.6 |
| 247.9 | vw | 5 ₀ ¹ 6 ₁ ¹ | + 287.9+18.1 |
| 253.7 | w | 8 ₀ ¹ 11 ₁ ¹ | + 387.4-75.6 |
| 298.0 | vw | 8 ₀ ¹ 12 ₁ ¹ | + 387.4-31.3 |
| 306.7 | vvw | 11 ₁ ¹ 12 ₀ ² | + 2(219.8)-74.7 |
| 329.3 | ms | 8 ₀ ¹ | + 387.4 |
| 330.7 | w | 5 ₀ ¹ 7 ₁ ¹ | + 287.9+100.9 |
| 354.7 | w | 7 ₁ ¹ 8 ₀ ¹ 11 ₁ ¹ | + 387.4+99.4-74.0 |
| 381.4 | w | 12 ₀ ² | + 2(219.8) |
| 398.1 | w | 7 ₁ ¹ 8 ₀ ¹ 12 ₁ ¹ | + 387.4+99.4-30.6 |
| 428.7 | m | 7 ₁ ¹ 8 ₀ ¹ | + 387.4+99.4 |
| 450.6 | mw | 4 ₀ ¹ | + 508.7 |
| 499.7 | vvvw | 7 ₂ ² 8 ₀ ¹ 12 ₁ ¹ | + 387.4+99.4+99.7-28.7 |
| 515.2 | vvw | 5 ₀ ² | + 287.9+285.4 |

| cm ⁻¹ | Int. | Notation | Assignment |
|------------------|------|---|-------------------------------------|
| 30528.4 | mw | $7_2^2 8_0^1$ | $\nu_{00} + 387.4+99.4+99.7$ |
| 552.8 | w | $4_0^1 7_1^1$ | + 508.7+102.2 |
| 574.1 | w | | + 632.2 |
| 586.6 | vw | $5_0^1 8_0^1 12_1^1$ | + 387.4+284.0-26.7 |
| 613.3 | w | $5_0^1 8_0^1$ | + 387.4+284.0 |
| 638.3 | vw | $8_0^2 11_1^1$ | + 387.4+382.0-73.0 |
| 653.5 | vvw | $4_0^1 7_2^2$ | + 508.7+102.2+100.7 |
| 674.3 | vw | | + 632.2+100.2 |
| 678.2 | vvw | $8_0^2 12_1^1$ | + 387.4+382.0-33.1 |
| 711.3 | mw | $\left\{ \begin{array}{l} 8_0^2 \\ 5_0^1 7_1^1 8_0^1 \end{array} \right.$ | + 387.4+382.0 + 387.4+284.0+98.0 |
| 739.9 | w | $4_0^1 5_0^1$ | + 508.7+289.3 |
| 771.8 | vvw | | + 632.2+100.2+97.5 |
| 779.6 | vvw | $7_1^1 8_0^2 12_1^1$ | + 387.4+382.0+98.1-29.8 |
| 809.4 | mw | $7_1^1 8_0^2$ | + 387.4+382.0+98.1 |
| 825.5 | vw | 6_0^2 | + 2(441.8) |
| 907.9 | w | $7_2^2 8_0^2$ | + 387.9+382.0+98.1+98.5 |
| 926.3 | vvw | $6_0^2 7_1^1$ | + 2(441.8)+100.8 |
| 954.9 | vvw | $\left\{ \begin{array}{l} 4_0^2 \\ 2_0^1 7_2^0 \end{array} \right.$ | + 508.7+504.3 + 1241.6-228.6 |
| 31006.6 | vw | $7_3^3 8_0^2$ | + 387.4+382.0+98.1+98.5+ 98.7 |
| 088.3 | w | $8_0^3 ?$ | + 387.4+382.0+377.0 |
| 107.0 | vvw | $2_0^1 11_1^1$ | + 1241.6-76.5 |
| 183.5 | mw | 2_0^1 | + 1241.6 |

| cm^{-1} | Int. | Notation | Assignment |
|------------------|------|---------------|----------------------------|
| 31283.3 | mw | $2_0^1 7_1^1$ | $\nu_{00} + 1241.6 + 99.8$ |
| 437.2 | s | 1_0^1 | + 1495.3 |
| 473.0 | m | $2_0^1 5_0^1$ | + 1241.6 + 289.5 |
| 530.8 | m | $1_0^1 7_1^1$ | + 1495.3 + 93.6 |
| 685.2 | w | $2_0^1 4_0^1$ | + 1241.6 + 501.7 |
| 722.5 | mw | $1_0^1 5_0^1$ | + 1495.3 + 285.3 |
| 815.9 | mw | $1_0^1 8_0^1$ | + 1495.3 + 378.7 |

TABLE 6.5

THE I $^3A'' \leftarrow ^1A'$ ABSORPTION SPECTRUM OF
OXALYL CHLORIDE FLUORIDE

| cm ⁻¹ | Int. | Notation | Assignment |
|------------------|------|---|-----------------------|
| 25827 | s | 0 ₀ ⁰ | origin |
| 913 | s | 12 ₁ ¹ | $\nu_{00} + 86$ |
| 996 | w | 12 ₂ ² | + 86+83 |
| 26009 | s | 9 ₀ ¹ | + 182 |
| 095 | ms | 9 ₀ ¹ 12 ₁ ¹ | + 182+86 |
| 110 | s | 8 ₀ ¹ | + 283 |
| 193 | mw | { 8 ₀ ¹ 12 ₁ ¹ 9 ₀ ² | + 283+83 + 182+184 |
| 245 | m | 7 ₀ ¹ | + 418 |
| 296 | mw | 8 ₀ ¹ 9 ₀ ¹ | + 283+186 |
| 334 | mw | 7 ₀ ¹ 12 ₁ ¹ | + 418+89 |
| 430 | w | 7 ₀ ¹ 9 ₀ ¹ | + 418+185 |
| 515 | w | 7 ₀ ¹ 9 ₀ ¹ 12 ₁ ¹ | + 418+185+85 |
| 547 | w | 5 ₀ ¹ ? | + 720 |
| 27121 | s | 1 ₀ ¹ | + 1294 |
| 206 | ms | 1 ₀ ¹ 12 ₁ ¹ | + 1294+85 |
| 300 | w | 1 ₀ ¹ 9 ₀ ¹ | + 1294+179 |
| 406 | mw | 1 ₀ ¹ 8 ₀ ¹ | + 1294+285 |
| 483 | vw | 1 ₀ ¹ 9 ₀ ² | + 1294+179+183 |
| 520 | s | 1 ₀ ¹ 7 ₀ ¹ | + 1294+399 |

In each system only one of the two excited state carbonyl stretching frequencies (ν'_1 and ν'_2) is observed.

6.6 Discussion.

Qualitatively, from the pressure path lengths required to observe the spectra, the ratio of intensities, $I \{ {}^0_0(I \ ^3A_u \leftarrow ^1A_g) \} / I \{ {}^0_0(^3A_u \leftarrow ^1A_g) \}$ is largest for oxalyl bromide and smallest for oxalyl fluoride. The singlet-triplet oscillator strengths in n-hexane for $(COCl)_2$ and $(COBr)_2$ are 1.34×10^{-7} and 3.13×10^{-6} , respectively¹⁸. Oxalyl bromide should indeed have the most intense singlet-triplet spectrum since the spin-orbit interaction energy increases with atomic number.

The behaviour of the symmetric carbonyl stretching frequency in the $I \ ^3A_u \leftarrow ^1A_g$ systems of the oxalyl halides is similar to that found in the singlet-triplet $n \rightarrow \pi^*$ absorption spectra of formaldehyde and propynal. The carbonyl frequency ν'_1 drops considerably on electronic excitation and we should expect the Franck-Condon effect to produce a long progression in ν'_{CO} . However, the 1_0^1 band is not very intense and no long carbonyl progression is observed. The symmetric carbonyl stretching frequencies in the $I \ ^3A_u(n, \pi^*)$ states of oxalyl chloride, oxalyl fluoride and oxalyl chloride fluoride ($^3A''$) are higher than in the corresponding singlet states (as in

formaldehyde and propynal). The frequencies of this vibration in the singlet and triplet states of oxalyl bromide are approximately equal.

A consideration of Pauli spin repulsion for the crude molecular orbital model used in section 3.3 suggests that, in $n \rightarrow \pi^*$ promotion, more electronic charge is transferred from the oxygen atoms towards the centre of the molecule on excitation to the $I \ ^3A_u$ state than on excitation to the $I \ ^1A_u$ state because of repulsion of the excited π^* -electron by the electron remaining in the n-orbital attached to the oxygen atoms. On this basis, we expect that the C-C bond in the triplet state will be stronger than in the corresponding singlet state, while for the carbonyl group the singlet bond ought to be the stronger of the two. However, the predictions of this simple model may well be modified if participation of the halogen electrons in the molecular orbitals is included.

The CC stretching frequency is not active in the singlet-triplet spectrum of oxalyl fluoride or oxalyl chloride fluoride, but the vibrational analyses of the spectra of oxalyl chloride and oxalyl bromide show that, in both these cases, $\nu'_2(I \ ^3A_u)$ is higher than $\nu'_2(I \ ^1A_u)$ by $\sim 50 \text{ cm}^{-1}$. We may infer that the CC bond in oxalyl fluoride is also slightly stronger in the triplet state

since, for $(\text{COF})_2$,

$$\nu'_t(\text{I } ^3\text{A}_u) - \nu'_t(\text{I } ^1\text{A}_u) = + 3.5 \text{ cm}^{-1}.$$

Here we have assumed, of course, complete localization of the vibration in the bond. However, it is probable that the normal coordinates are different for the different molecules.

For oxalyl chloride fluoride (C_s), theory predicts that both the transitions $n_+ \rightarrow \pi^*$ and $n_- \rightarrow \pi^*$ are symmetry allowed. No evidence for two overlapping systems was found in this investigation of the spectra of this molecule. It may be that one system is much weaker than the other. Another possibility is that either the n_+ and n_- orbitals lie sufficiently close together to be unresolved at a resolving power of 70,000 (Bausch and Lomb spectrograph) or the n -orbital separation energy is reasonably large.

A summary of the values for the totally symmetric vibrations of the oxalyl halides in the ground and first excited states is given in Tables 6.6 to 6.9. The possible sequences identified are shown in Tables 6.10 and 6.11 where the parentheses denote less certain assignments.

TABLE 6.6

THE a_g VIBRATIONS OF OXALYL BROMIDE

| | 1A_g (RAMAN) | 1A_g (U.V.) | 1A_u | 3A_u |
|---------|-------------------|------------------|-----------|-----------|
| ν_1 | 1784 | 1801? | 1538 | 1537.2 |
| ν_2 | 1032 | 1116 | 953 | 1002.9 |
| ν_3 | 600 | 608 | 621 | 641.9 |
| ν_4 | 415 | 440 | 296 | 312.3 |
| ν_5 | 191 | 185 | 180 | 185.9 |

TABLE 6.7

THE a_g VIBRATIONS OF OXALYL CHLORIDE

| | 1A_g (RAMAN) | 1A_g (U.V.) | 1A_u | 3A_u |
|---------|-------------------|------------------|-----------|-----------|
| ν_1 | 1778 | 1783.3 | 1460 | 1508.4 |
| ν_2 | 1078 | 1217.1 | 970 | 1028.2 |
| ν_3 | 619 | 612.1 | 619.2 | 634.6 |
| ν_4 | 465 | 498.5 | 398.5 | 401.1 |
| ν_5 | 276 | 283.0 | 281.8 | 281.1 |

TABLE 6.8

THE a_g VIBRATIONS OF OXALYL FLUORIDE

| | 1A_g (RAMAN) | 1A_g (U.V.) | 1A_u | 3A_u |
|---------|-----------------|----------------|---------|---------|
| ν_1 | 1872 | - | 1440.4 | 1495.3 |
| ν_2 | 1286 | - | 1145.9 | 1241.6 |
| ν_3 | 809 | 801.7 | 710.3 | - |
| ν_4 | 565 | - | 531.4 | 508.7 |
| ν_5 | 292 | 318.1 | 280.5 | 287.9 |

TABLE 6.9

 a' VIBRATIONS OF OXALYL CHLORIDE FLUORIDE

| | $^1A'$ | $^1A''$ | $^3A''$ |
|---------|--------|---------|---------|
| ν_1 | 1858 | 1280 | 1294 |
| ν_3 | 1197 | 1111 | - |
| ν_4 | 932 | 912 | - |
| ν_7 | 491 | 419 | 418 |
| ν_8 | 287 | 277 | 283 |
| ν_9 | 228 | 180 | 182 |

TABLE 6.10

SEQUENCE INTERVALS (CM^{-1}) IN THE I ${}^1\text{A}_u \leftarrow {}^1\text{A}_g$
SYSTEMS OF THE OXALYL HALIDES

| Normal mode | $(\text{COF})_2$ | $(\text{CO}^{35}\text{Cl})_2$ | $(\text{COBr})_2$ |
|--------------|------------------|-------------------------------|-------------------|
| ν_7 | +97.0 | +78.4 | +65 |
| ν_6 | - | +31.6 | +32 |
| (ν_{11}) | -86.9 | -84.6 | - |
| (ν_{12}) | -41.5 | -11.8 | - |

TABLE 6.11

SEQUENCE INTERVALS (CM^{-1}) IN THE I ${}^3\text{A}_u \leftarrow {}^1\text{A}_g$
SYSTEMS OF THE OXALYL HALIDES

| Normal Mode | $(\text{COF})_2$ | $(\text{CO}^{35}\text{Cl})_2$ | $(\text{COBr})_2$ |
|--------------|------------------|-------------------------------|-------------------|
| ν_7 | +100.5 | +78.3 | +64.6 |
| ν_6 | (+14.8) | +31.6 | +31.5 |
| (ν_{11}) | -78.2 | -71.1 | -74.5 |
| (ν_{12}) | -30.4 | -11.1 | - |

CHAPTER 7

ROTATIONAL BAND ENVELOPES FOR ASYMMETRIC TOP MOLECULES.

7.1 Introduction.

As was mentioned in Section 1.3, each electronic state has vibrational and rotational quantum states associated with it. A change in electronic energy may be accompanied by simultaneous changes in vibrational and rotational energy, giving an electronic-vibration-rotation spectrum. Transitions between the various rotational quantum states of vibronic levels give rotational structure to the vibronic bands of an electronic system.

7.2 Energy Levels of an Asymmetric Rotor.

The principal moments of inertia of a rigid molecule, I_a , I_b and I_c , may be determined by a method outlined by Hirschfelder⁹⁹. The principal axes a, b and c are defined such that $I_a \leq I_b \leq I_c$. Molecules where $I_a \neq I_b \neq I_c$, as is the case for the oxalyl halides, are called asymmetric tops. For a planar molecule, the c-axis is perpendicular to the molecular plane and only two of the principal moments of inertia are independent⁺.

⁺ This relation is strictly true for a rigid molecule only: for a vibrating molecule a small inertial defect, $\Delta = I_c - I_a - I_b$, occurs for moments of inertia calculated from rotational constants.

$$I_c = I_a + I_b \quad (7.1)$$

The rotational constants A, B and C are related to the respective moments of inertia by equations of the type

$$A \text{ (cm}^{-1}\text{)} = \frac{h}{8 \pi^2 c I_a} = \frac{16.852}{I_a \text{ (a.m.u.-\AA}^2\text{)}} \quad (7.2)$$

The rotational energy of an asymmetric rotor is given by

$$F(J, \kappa) = \frac{1}{2}(A+C)J(J+1) + \frac{1}{2}(A-C)E(\kappa) \quad (7.3)$$

where the asymmetry parameter,

$$\kappa = \frac{2B-A-C}{A-C} \quad (7.4)$$

and J is the quantum number associated with total angular momentum. When B=C, $\kappa = -1$, and expression (7.3) becomes that for a prolate symmetric rotor.

$$F(J, K_{-1}) = BJ(J+1) + (A-B)K_{-1}^2 \quad (7.5)$$

when A=B, $\kappa = +1$, and the molecule is an oblate symmetric top with

$$F(J, K_1) = BJ(J+1) + (C-B)K_1^2 \quad (7.6)$$

For a symmetric top, K is the quantum number for the component of the total angular momentum along the top axis.

The calculation of $E(\kappa)$ has been discussed in detail by King, Hainer and Cross¹⁰⁰, (henceforth called

KHC). Briefly, the $E(\kappa)$, for a given J , are eigenvalues of an energy matrix $[E(\kappa)]$ whose elements are of the form

$$\int \psi_{JK_m}^A \xi(\kappa) \psi_{JK_n}^A d\tau$$

where the operator $\xi(\kappa)$ is related to the angular momentum operators \mathcal{P} through

$$\xi(\kappa) = \frac{2}{A-C} \left\{ \frac{\mathcal{P}_a^2}{2I_a} + \frac{\mathcal{P}_b^2}{2I_b} + \frac{\mathcal{P}_c^2}{2I_c} \right\} - \frac{A-C}{A+C} J(J+1) \quad (7.7)$$

and the asymmetric⁺ rotor wave functions ψ_{JK}^A are linear combinations of symmetric rotor wave functions, ψ_{JK}^S .

K_m and K_n can take the values $-J, -J+1, \dots, 0, \dots, J$ and matrix elements are non-zero for

$$K_m - K_n = 0, \pm 2$$

Thus, for each J value, there are $2J+1$ values of $E(\kappa)$.

Following KHC, we label the levels of an asymmetric rotor $J_{K_{-1}K_1}$ where K_{-1} and K_1 and the respective K values of the prolate and oblate limits with which the particular asymmetric rotor level correlates. Levels may be classified ee, eo, oe or oo

⁺ Throughout this chapter, superscript A refers to the asymmetric rotor while superscript S refers to the symmetric rotor.

depending upon whether the K subscripts are even or odd.

Before diagonalizing $[E(\kappa)]$ to find the $E(\kappa)$ values for the expression (7.3) for the energy levels, it is convenient to symmetry factorize the matrix into four submatrices.

$$[E(\kappa)] = [E^+] + [E^-] + [O^+] + [O^-] \quad (7.8)$$

The symmetries of the levels of the submatrices are given in Table 7.1 for near-prolate (KHC, I^r) and near-oblate (III^r) cases. In practice, the reduced energy submatrices of equation (7.8), which are of the general form

$$[E] = \begin{bmatrix} k_0 & b_1^{1/2} & 0 & \dots \\ b_1^{1/2} & k_1 & b_1^{1/2} & \dots \\ 0 & b_2^{1/2} & k_2 & \dots \\ \dots & \dots & \dots & \dots \end{bmatrix}$$

are converted by a similarity transformation into

$$[D_E] = \begin{bmatrix} k_0 & 1 & 0 & \dots \\ b_1 & k_1 & 1 & \dots \\ 0 & b_2 & k_2 & \dots \\ \dots & \dots & \dots & \dots \end{bmatrix}$$

and the eigenvalues $E(\kappa)$ are obtained by diagonalizing the four $[D]$ matrices¹⁰¹. This treatment is completely general for all singlet states.

TABLE 7.1

CLASSIFICATION OF THE LEVELS OF SUBMATRICES

| Submatrix | Prolate | | Oblate | |
|-----------|---------|-------|--------|-------|
| | J even | J odd | J even | J odd |
| E^+ | ee | eo | ee | oe |
| E^- | eo | ee | oe | ee |
| O^+ | oe | oo | oo | eo |
| O^- | oo | oe | eo | oo |

TABLE 7.2

CORRELATION BETWEEN AXES (x,y,z) AND
THE PRINCIPAL AXES (a,b,c)near-prolate

$x \leftrightarrow b$

$y \leftrightarrow c$

$z \leftrightarrow a$

near oblate

$x \leftrightarrow a$

$y \leftrightarrow b$

$z \leftrightarrow c$

7.3 Intensities and Selection Rules for Asymmetric Rotor Transitions.

Gora¹⁰² has shown that exact asymmetric rotor line strengths may be obtained from the appropriate symmetric top intensity formulae. (We restrict ourselves to a discussion of singlet-singlet transitions only.)

If $[T'']$ and $[T']$ are the ground and excited state transformation matrices which diagonalize the reduced energy matrices $[E(\kappa)'']$ and $[E(\kappa)']$ to give ground and excited state eigenvalues ω'' and ω' ,

$$[T]^{-1} [E(\kappa)] [T] = [\omega] \quad (7.9)$$

and $[\Phi^S]$ is the direction cosine matrix whose elements $\int \psi_{J,K}^S \phi^S \psi_{J''K''}^S d\tau$ are given by the Hönl-London formulae¹⁰³, (Table 7.2), then the asymmetric rotor line strengths are given by

$$[\Phi^A] = [T']^{-1} [\Phi^S] [T''] \quad (7.10)$$

Since the $[T]$ matrices are unitary the elements t_{ij} can be found¹⁰². The intensity of a transition from a rotational level described by a set of ground state quantum numbers n'' to an excited state described by n' is given by

$$I_{n'',n'} = C \cdot g_{n''} \cdot \exp \left\{ -E_{n''}/kT \right\} \cdot |\phi^A|^2 \quad (7.11)$$

TABLE 7.2a

SYMMETRIC TOP DIRECTION COSINE

MATRIX ELEMENTS

$$\langle J, K | \phi_x^S | J+1, K^{\pm 1} \rangle = \pm \frac{1}{2} [(J^{\pm K+1})(J^{\pm K+2})]^{\frac{1}{2}}$$

$$\langle J, K | \phi_y^S | J+1, K^{\pm 1} \rangle = \mp \frac{1}{2} [(J^{\pm K+1})(J^{\pm K+2})]^{\frac{1}{2}}$$

$$\langle J, K | \phi_z^S | J+1, K^{\pm 1} \rangle = 0$$

$$\langle J, K | \phi_x^S | J, K^{\pm 1} \rangle = \frac{1}{2} [(J^{\mp K})(J^{\pm K+1})]^{\frac{1}{2}}$$

$$\langle J, K | \phi_y^S | J, K^{\pm 1} \rangle = \frac{1}{2} [(J^{\mp K})(J^{\pm K+1})]^{\frac{1}{2}}$$

$$\langle J, K | \phi_z^S | J, K^{\pm 1} \rangle = 0$$

$$\langle J, K | \phi_x^S | J-1, K^{\pm 1} \rangle = \pm \frac{1}{2} [(J^{\mp K})(J^{\mp K-1})]^{\frac{1}{2}}$$

$$\langle J, K | \phi_y^S | J-1, K^{\pm 1} \rangle = \mp \frac{1}{2} [(J^{\mp K})(J^{\mp K-1})]^{\frac{1}{2}}$$

$$\langle J, K | \phi_z^S | J-1, K^{\pm 1} \rangle = 0$$

with the provision that for $K'' = 0$, $\Delta K = +1$
the value of the integral is multiplied by
 $\sqrt{2}$.

TABLE 7.2a (cont.)

$$\begin{aligned} \langle J, K | \phi_x^S | J+1, K \rangle &= 0 \\ \langle J, K | \phi_y^S | J+1, K \rangle &= 0 \\ \langle J, K | \phi_z^S | J+1, K \rangle &= [(J+1)^2 - K^2]^{\frac{1}{2}} \end{aligned}$$

$$\begin{aligned} \langle J, K | \phi_x^S | J, K \rangle &= 0 \\ \langle J, K | \phi_y^S | J, K \rangle &= 0 \\ \langle J, K | \phi_z^S | J, K \rangle &= K \end{aligned}$$

$$\begin{aligned} \langle J, K | \phi_x^S | J-1, K \rangle &= 0 \\ \langle J, K | \phi_y^S | J-1, K \rangle &= 0 \\ \langle J, K | \phi_z^S | J-1, K \rangle &= -[J^2 - K^2]^{\frac{1}{2}} \end{aligned}$$

C is a constant and $g_{n''}$ is the statistical weight of the ground state rotational level.

The selection rules for an asymmetric rotor depend upon the polarization of the transition moment for the transition. When the transition moment is directed along the a-axis the band is called A-type and if the transition moment has components along the a- and b- axes the band is called an AB hybrid, etc. Table 7.3 summarizes the selection rules governing the strong branches of which each band is composed.

7.4 Band Profiles by Digital Computer.

For large asymmetric molecules where the rotational constants are small, (e.g. oxalyl fluoride: $A'' \approx 0.198 \text{ cm}^{-1}$; $\kappa'' = -0.26$), as many as 60,000 transitions can contribute appreciably to the intensity of a rotational band. To obtain accurate energy levels and intensities for such a molecule may require the diagonalization and manipulation of matrices up to $J'' \approx 120$ and $K'' \approx 80$. It is only recently, with the advent of fast digital computers, that these calculations have been possible.

Using an IBM 7072 (10K storage) computer, Parkin¹⁰⁴ was able to calculate and print out a band contour for naphthalene in just over 25 minutes. He

TABLE 7.3

SELECTION RULES FOR ASYMMETRIC ROTORS*

| Polarization | a | b | c |
|-----------------|-------------------------|-------------------------|-------------------------|
| ΔK_{-1} | 0 | ± 1 | ± 1 |
| ΔK_{+1} | ± 1 | ± 1 | 0 |
| ΔJ | 0, ± 1 | 0, ± 1 | 0, ± 1 |
| Symmetry | ee \leftrightarrow eo | ee \leftrightarrow oo | ee \leftrightarrow oe |
| | eo \leftrightarrow oo | oe \leftrightarrow eo | eo \leftrightarrow oo |

* Where $\Delta K=0$, very weak branches are allowed in the asymmetric rotor for $\Delta K=\pm 2, \pm 4, \dots$ and where $\Delta K=\pm 1$, very weak branches are allowed with $\Delta K=\pm 3, \pm 5, \dots$

calculated exactly, for each K'' value, the energies and intensities for transitions from ten selected J'' values in the range $J'' = 3$ to $J'' = 110$. The energies and intensities of the other transitions were found by interpolation and extrapolation. This procedure has the advantage that the calculation can be done on a medium-sized computer in a reasonably short period of time.

Dr. Parkin has kindly supplied this research group with copies of his near-prolate and near-oblate asymmetric rotor programs. These have been translated into Fortran IV for use on the McMaster University IBM 7040 (32K) computer.

Considerable computational difficulties arise owing to the fact that not all symmetry species ee , eo , oe and oo exist for J'' values where $J'' < 3$. Because of this, Parkin used $J'' = 3$ as his first selected J'' value and found the energies and intensities of transitions from $J'' = 0, 1$ and 2 by extrapolation. Unfortunately, it is precisely for these low J'' values, near the band centre, that the energies and intensities are rapidly changing.

To avoid errors due to extrapolation, the program was modified and analytical expressions for the line strengths of all transitions from $J'' = 0, 1$, and 2 for A, B and C-type bands in near-prolate (KHC, I^r) and

near-oblate (KHC, III^R) approximations, were determined using Gora's method¹⁰². The algebraic formulae derived are given in the Appendix, Table A.8. These expressions together with the $E(\kappa)$ values given in Reference 100, were incorporated into the program so that $J'' \leq 3$ could be treated exactly.

With this modification, the band contours for A, B and C-type bands of ethylene ($\kappa'' = -0.9$) were found to be identical to the experimental and calculated contours of Christoffersen and Hollas¹⁰⁵. Calculations of the profiles of the 3821 Å band of propynal and the 4550 Å band of glyoxal were also in excellent agreement with those observed^{58,30}.

The oblate program was tested by calculating A and B-type bands for $\kappa \approx +0.9$. The agreement with those reported¹⁰⁶ is shown in Figures 7.1 and 7.2. (N.b. the spectra of Reference 106 are for $J'' \leq 10$.)

In the original programs of Parkin there is provision made for the separate print out of individual $\Delta K \Delta J$ branches if required. When all branches are calculated together, no computational errors occur. However, tests have shown that, when the R_P branch alone is calculated, B and C-type prolate and A and B-type oblate contours are calculated incorrectly if the first selected J'' value is 3. For the above band

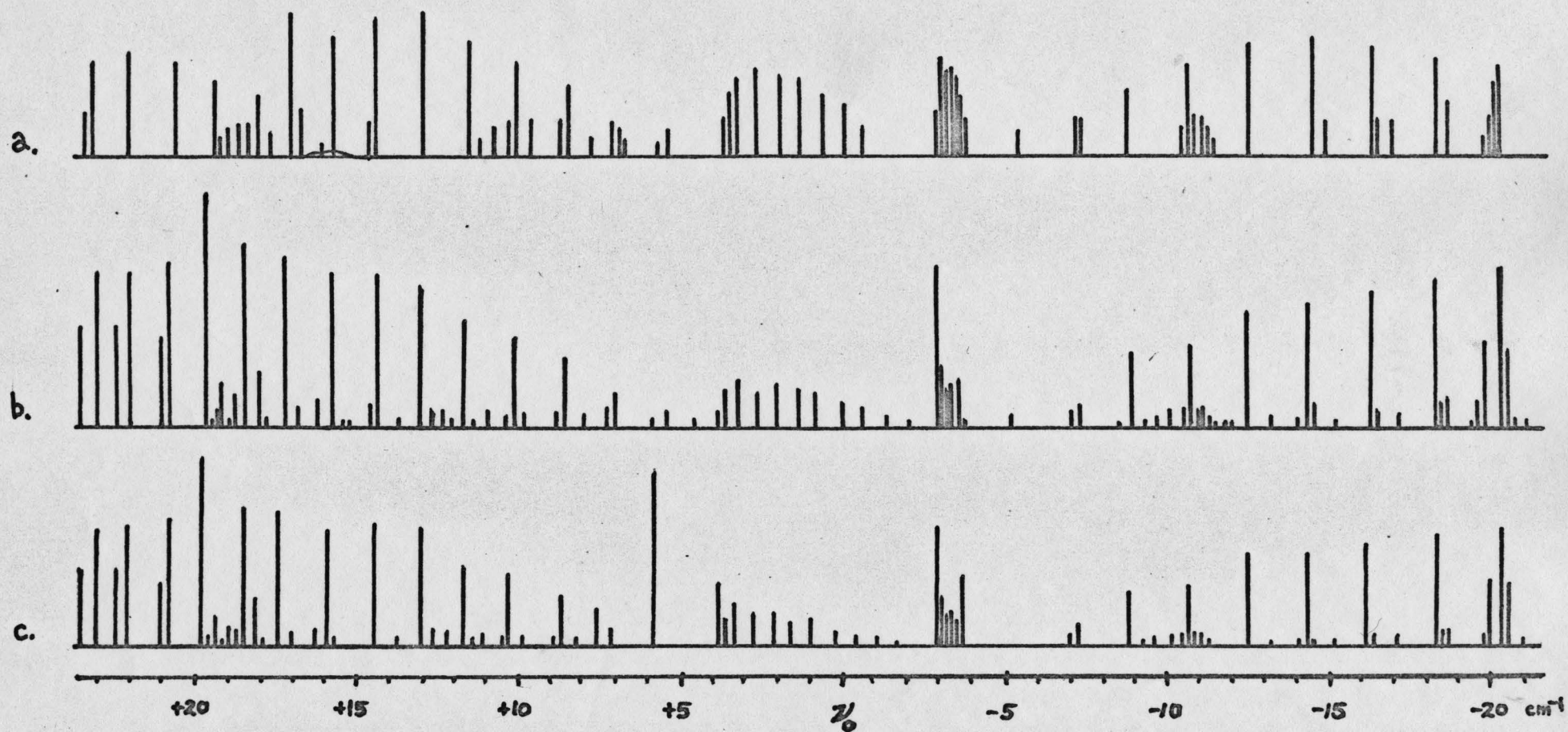


FIGURE 7.1 A-TYPE NEAR OBLATE $\kappa = +0.9$.

a. Reference 106, p. 185 ;

b. $0 < J'' < 20$, $J'' < 3$ exact ;

c. $0 < J'' < 20$, $J'' < 3$ not exact

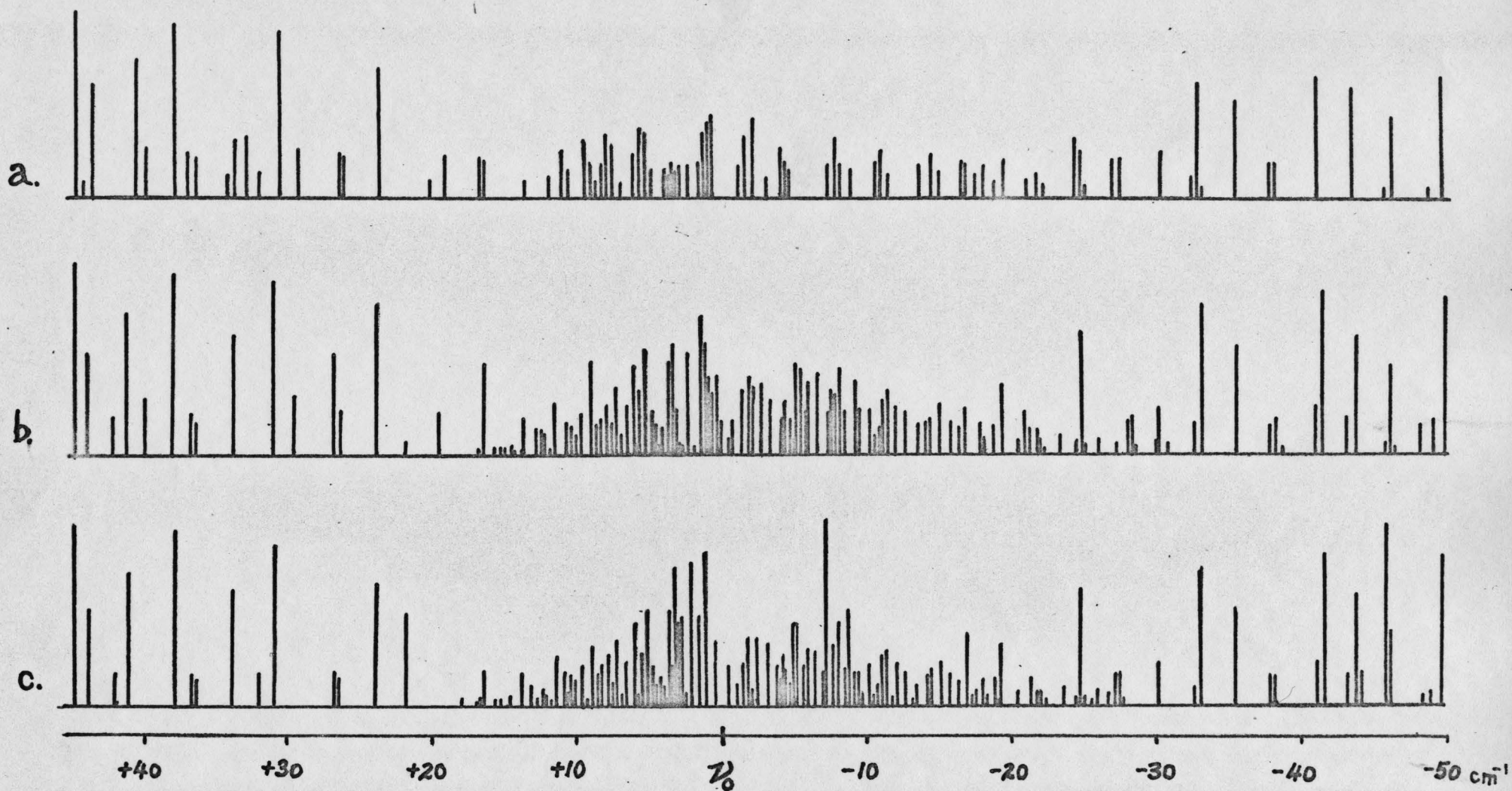


FIGURE 7.2 B-TYPE NEAR OBLATE $k = +0.9$.

a. Reference 106, p.216 ;

b. $0 \leq J'' \leq 20$, $J'' < 3$ exact ;

c. $0 \leq J'' \leq 20$, $J'' < 3$ not exact .

types an error occurs in indexing the calculated transitions due to the fact that there is no allowed transition from the symmetry $e_e (3_{22})$ for $J'' = 3$ in an R_P branch. The routine for this part of the calculation has been rewritten.

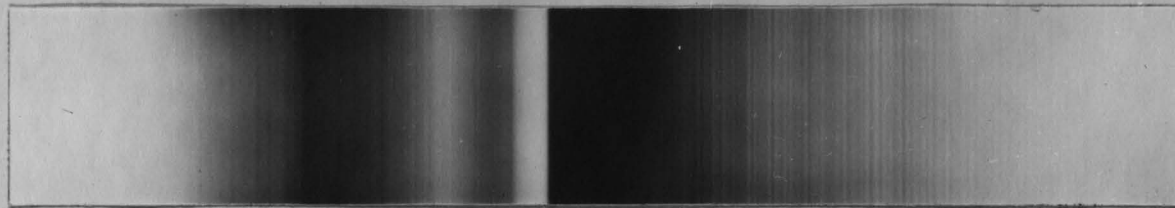
No attempt was made to calculate the energies and intensities of all transitions exactly and it should be kept in mind that the interpolation procedure used can lead to errors in the calculated energies and intensities especially if rotational branches "double back" within the region of interpolation.

7.4 Band Contour Calculations for Oxalyl Fluoride.

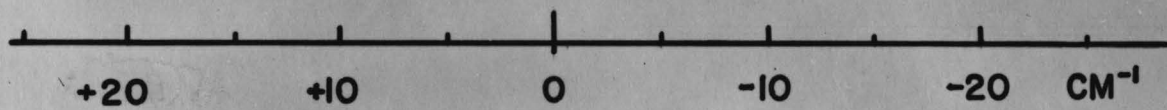
Photographs of the origin bands of the I $^1A_u \leftarrow ^1A_g$ and I $^3A_u \leftarrow ^1A_g$ systems of oxalyl fluoride taken at a resolving power of $\sim 300,000$ are shown in Figure 7.3. The asymmetric rotor band contour program has been used to calculate the profile of the (0,0) band of the oxalyl fluoride singlet-singlet system assuming the ground state geometry given in Table 1.2a and the corresponding rotational constants.

As expected, the origin band was found to be C-type (perpendicular). Figure 7.4 shows several C-type contours calculated for various values of r'_{CO} and r'_{CC} . On the assumption of zero inertial defect, the ground

A.



B.



THE ORIGIN BANDS OF OXALYL FLUORIDE

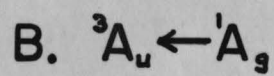
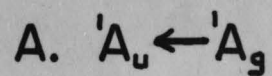


Figure 7.3

state parameters in Table 1.2a give rotational constants; $A'' = 0.1975 \text{ cm}^{-1}$, $B'' = 0.1202 \text{ cm}^{-1}$ and $C'' = 0.0747 \text{ cm}^{-1}$. The best fit with the experimental contour is obtained for $\Delta A = A' - A'' = -0.0132 \text{ cm}^{-1}$, $\Delta B = +0.0023 \text{ cm}^{-1}$ and $\Delta C = -0.0011 \text{ cm}^{-1}$. (Figure 7.5) The computation was carried out using the selected J'' values 3, 6, 10, 16, 23, 30, 40, 50, 65 and 85 and took just over 12 minutes. The symmetric top approximation was used for $J'' > 45$ and $K'' > 30$.

Within limits, the calculated contour is relatively insensitive to the exact values of the rotational constants and, consequently, without much higher experimental resolution, it is not possible to obtain accurate values for A, B and C in the two combining states.

If the CF bond length (1.34 Å) and \widehat{CCF} (111°) do not alter on electronic excitation, then the observed contour of the (0,0) band of oxalyl fluoride can be explained by an increase in the CO bond length of 0.10 Å, a decrease in the CC bond length of 0.08 Å and an opening of the \widehat{CCO} by $\sim 2^\circ$.

The B-type band at 1870 cm^{-1} in oxalyl fluoride has two maxima separated by $\sim 12 \text{ cm}^{-1}$. Milligan *et al.*¹⁰⁷ suggest this "doubling" is due to the occurrence of cis and trans isomers but a calculation of the band contour with $A' = A'' = 0.1975 \text{ cm}^{-1}$, $B' = B'' = 0.1202 \text{ cm}^{-1}$

GROUND STATE

$$r'_{CO} = 1.17 \text{ \AA}$$

$$r'_{CC} = 1.50 \text{ \AA}$$

$$r'_{CF} = 1.32 \text{ \AA}$$

$$\widehat{CCO}' = 123^\circ$$

$$\widehat{CCF}' = 112^\circ$$

EXCITED STATE

$$r'_{CF} = 1.32 \text{ \AA}$$

$$\widehat{CCO}' = 126^\circ$$

$$\widehat{CCF}' = 112^\circ$$

$$r'_{CO} = 1.27 \text{ \AA}$$

$$r'_{CC} = 1.42 \text{ \AA}$$

$$r'_{CO} = 1.27 \text{ \AA}$$

$$r'_{CC} = 1.43 \text{ \AA}$$

$$r'_{CO} = 1.26 \text{ \AA}$$

$$r'_{CC} = 1.41 \text{ \AA}$$

$$r'_{CO} = 1.26 \text{ \AA}$$

$$r'_{CC} = 1.42 \text{ \AA}$$

$$r'_{CO} = 1.26 \text{ \AA}$$

$$r'_{CC} = 1.43 \text{ \AA}$$

$$r'_{CO} = 1.25 \text{ \AA}$$

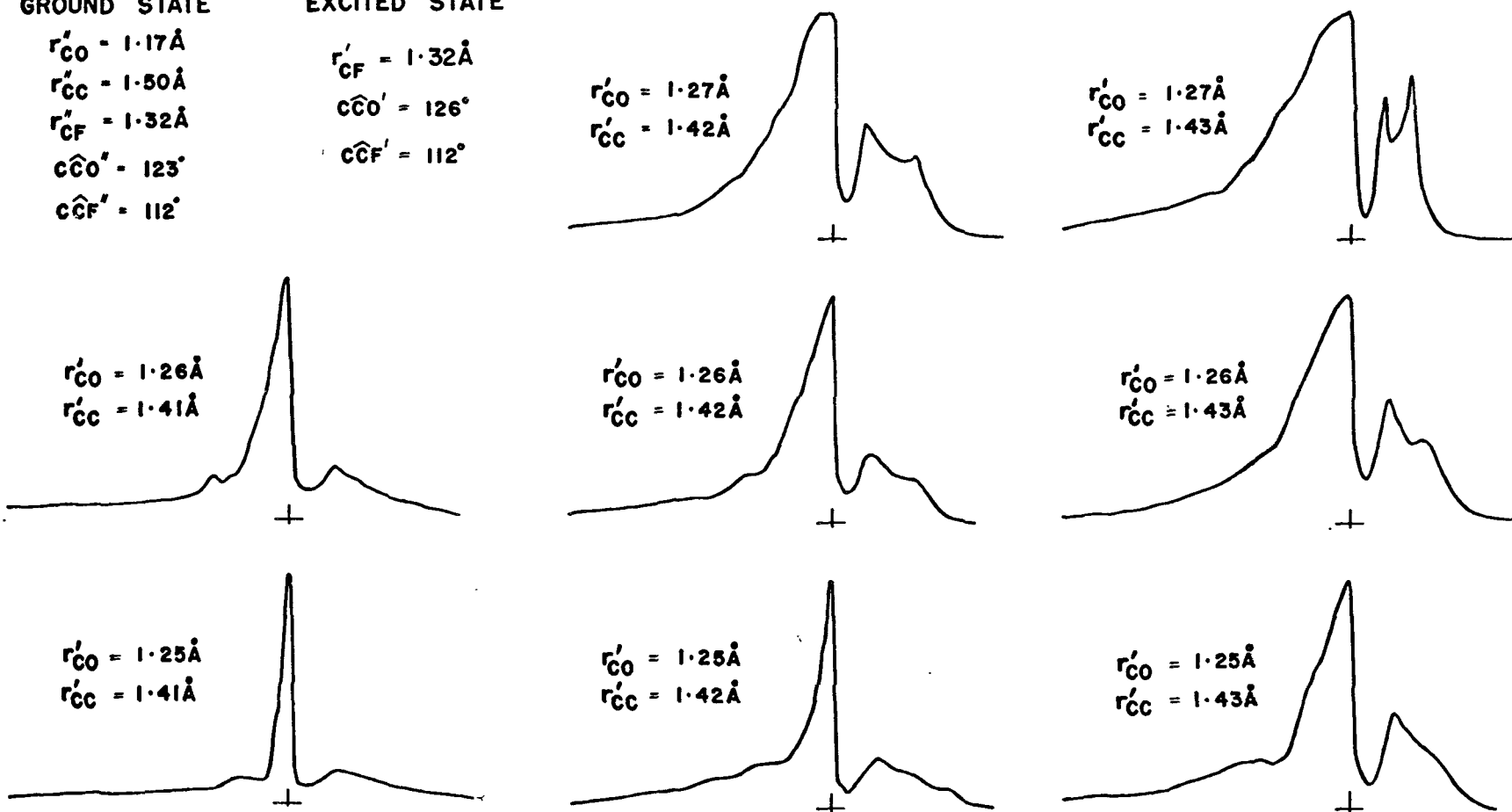
$$r'_{CC} = 1.41 \text{ \AA}$$

$$r'_{CO} = 1.25 \text{ \AA}$$

$$r'_{CC} = 1.42 \text{ \AA}$$

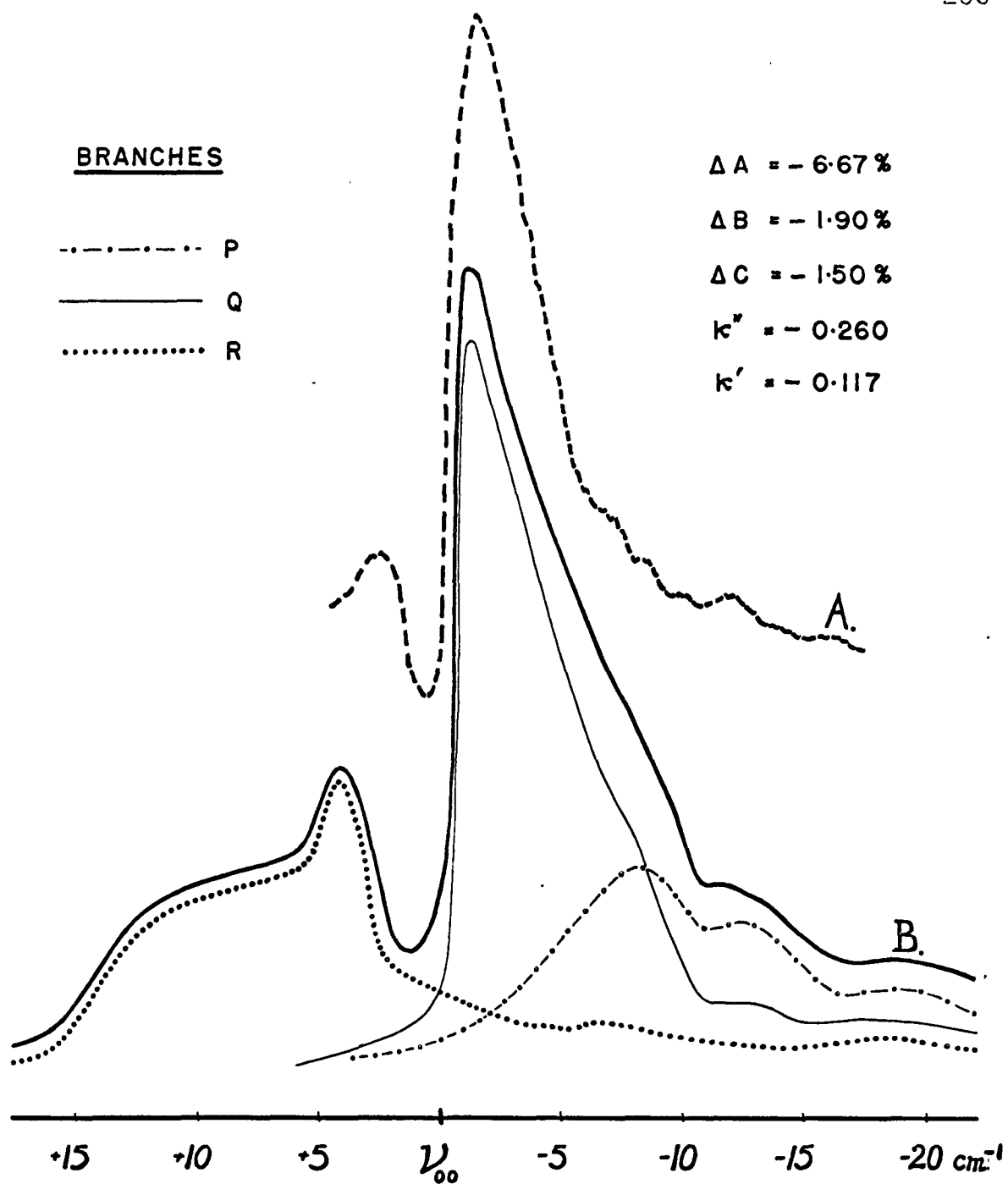
$$r'_{CO} = 1.25 \text{ \AA}$$

$$r'_{CC} = 1.43 \text{ \AA}$$



PROLATE C-TYPE CONTOURS FOR OXALYL FLUORIDE

Figure 7.4 (N.b. Energy increasing \rightarrow)



$0_g (A_u \leftarrow A_g)$ BAND OF OXALYL FLUORIDE

CURVE A : OBSERVED CURVE B : CALCULATED

Figure 7.5

and $C' = C'' = 0.0747 \text{ cm}^{-1}$ shows that the two maxima are P and R branches. The calculated P-R separation is $\sim 13 \text{ cm}^{-1}$.

The (0,0) band of the singlet-singlet system of oxalyl fluoride was chosen for rotational analysis because it is very sharp whereas the origin band of oxalyl bromide is diffuse and that of oxalyl chloride is complicated by the presence of different isotopic species.

Preliminary calculations on the (0,0) band of oxalyl chloride fluoride ($I \ ^1A'' \leftarrow \ ^1A'$ system) indicate that the contour is C-type. However, high resolution photographs of this spectrum will be required before these calculations can be refined.

CHAPTER 8

CONCLUSIONS

Hencher and King^{16,17} concluded that the infrared and Raman spectra of oxalyl fluoride, oxalyl chloride fluoride and oxalyl chloride could be explained on the basis of a planar-trans structure. The investigation of the near ultraviolet spectra of these molecules is in full agreement with this interpretation of the ground state.

For all the oxalyl halides studied, the spectral evidence strongly favours a planar and trans structure for the I 1A_u and I $^3A_u(n, \pi^*)$ excited states also. If the molecules were bent out-of-plane in the excited state (as in the case with formaldehyde), we would expect the CO out-of-plane bending modes to be strongly active and this is not found.

The torsional frequencies of the excited states are apparently almost harmonic and, although the energies of the ground state torsional levels are not known, an extreme value as low as 20 cm^{-1} for ν_t'' would lead to a trans \rightarrow cis barrier V^* (equation 6.1) in excess of $15,000 \text{ cm}^{-1}$ in the I $^1A_u(n, \pi^*)$ and I $^3A_u(n, \pi^*)$ states

of the oxalyl halides studied. No cis or gauche forms have been detected¹⁰⁸ in the ground state of glyoxal where the torsional barrier is only 4810 cm^{-1} ⁹⁷.

The vibrational structure of each spectrum is in good agreement with that expected for $n \rightarrow \pi^*$ electron promotion. The most prominent vibrations observed are those associated with the carbonyl group, namely the CO stretching and the two CCO bending symmetric modes.

The majority of the spectral bands have been satisfactorily analyzed. All the totally symmetric vibrations in the excited state are active in the spectra of oxalyl chloride and oxalyl bromide and most of the totally symmetric modes have been found for oxalyl fluoride and oxalyl chloride fluoride. However, apart from the symmetric carbonyl stretching vibration in the excited state, no long progressions are found and this suggests, on Franck-Condon grounds, that the geometric changes on excitation are fairly small. The rotational analysis of the O_0^0 (${}^1A_u \leftarrow {}^1A_g$) band of oxalyl fluoride confirms this, showing the largest changes in geometry to be an extension of the CO bond length by $\sim 0.1 \text{ \AA}$, accompanied by a shortening of the CC bond by $\sim 0.08 \text{ \AA}$ and an increase in the $\hat{C}CO$ of $\sim 2^\circ$.

BIBLIOGRAPHY

1. M. Born and J. R. Oppenheimer, Ann. Physik 84, 457 (1927).
2. L. Pauling and E. B. Wilson, Jr., "Introduction to Quantum Mechanics", New York: McGraw-Hill Book Co., Inc., (1935) section 40.
3. R. Wierl, Physik. Z. 31, 366 (1930).
4. J. E. LuValle, reported in Acta Cryst. 3, 49 (1950).
5. P. Groth and O. Hassel, Acta Chem. Scand. 16, 2311 (1962).
6. P. Groth and O. Hassel, Proc. Chem. Soc. 343 (1961).
7. K. W. F. Kohlrausch and A. Pongratz, Ber. deut. chem. Ges. 67, 976 (1934).
8. V. N. Thatte and M. S. Joglekar, Phil. Mag. 23, 1067 (1937).
9. B. D. Saksena, Proc. Indian Acad. Sci. 12A, 416 (1940).
10. J. S. Ziomek, F. F. Cleveland, and A. G. Meister, J. Chem. Phys. 17, 669 (1949).
11. K. W. F. Kohlrausch and H. Wittek, Z. physik. Chemie B48, 177 (1941).
12. B. D. Saksena and R. E. Kagarise, J. Chem. Phys. 19, 987 (1951).
13. B. D. Saksena, R. E. Kagarise, and D. H. Rank, J. Chem. Phys. 21, 1613 (1953).
14. R. E. Kagarise, J. Chem. Phys. 21, 1615 (1953).
15. J. S. Ziomek, A. G. Meister, F. F. Cleveland and C. E. Decker, J. Chem. Phys. 21, 90 (1953).

16. J. L. Hencher and Gerald W. King, J. Mol. Spectry 16, 158 (1965).
17. J. L. Hencher and Gerald W. King, J. Mol. Spectry 16, 168 (1965).
18. Y. Kanda, R. Shimada, H. Shimada, H. Kaseda and T. Matumura, in "Proceedings of the International Symposium on Molecular Structure and Spectroscopy", p. B304-1. Science Council of Japan, (1962).
19. K. B. Krauskopf and G. K. Rollefson, J. Amer. Chem. Soc. 58, 443 (1936).
20. J. E. Tuttle and G. K. Rollefson, J. Amer. Chem. Soc. 63, 1525 (1941).
21. B. D. Saksena and R. E. Kagarise, J. Chem. Phys. 19, 999 (1951).
22. J. W. Sidman, J. Amer. Chem. Soc. 78, 1527 (1956).
23. B. D. Saksena and G. S. Jauhri, J. Chem. Phys. 36, 2233 (1962).
24. Z. G. Szabó, D. Király and I. Bárdi, Z. Physik. Chemie (Frankfurt) 27, 127 (1961).
25. G. T. O. Martin and J. R. Partington, J. Chem. Soc. 1178 (1936).
26. B. D. Saksena and R. E. Kagarise, J. Chem. Phys. 19, 994 (1951).
27. K. Noack and R. N. Jones, Z. Elektrochem. 64, 707 (1960).
28. D. R. Lide, Jr. and M. Jen, J. Chem. Phys. 40, 252 (1964).
29. G. I. M. Bloom and L. E. Sutton, J. Chem. Soc. 727 (1941).
30. J. Paldus and D. A. Ramsay, Can. J. Phys. 45, 1389 (1967).
31. R. W. Kilb, C. C. Lin and E. B. Wilson, Jr., J. Chem. Phys. 26, 1695 (1957).
32. L. Pierce and L. C. Krisher, J. Chem. Phys. 31, 875 (1959).

33. K. M. Sinnott, J. Chem. Phys. 34, 851 (1961).
34. L. C. Krisher, J. Chem. Phys. 33, 1237 (1960).
35. R. F. Miller and R. F. Curl, Jr., J. Chem. Phys. 34, 1847 (1961).
36. G. A. Boulet, Diss. Abs. 25, 3283 (1964).
37. "Handbook of Chemistry and Physics" (45th Edition) The Chemical Rubber Co. (1964) p. D90.
38. S. Soundararajan and R. Raman, Indian Inst. Sci. Golden Jubilee Research Volume (1909-1959) Publ. 1959, p. 1.
39. C. W. Tullock and D. D. Coffman, J. Org. Chem. 25, 2016 (1960).
40. J. L. Hencher, Ph.D. Thesis, McMaster University, (1964), p. 17.
41. C. W. Tullock, reported in J. Chem. Phys. 42, 3187 (1965).
42. R. N. Haszeldine and F. Nyman, J. Chem. Soc. 1084 (1959).
43. J. Bacon and R. J. Gillespie, J. Chem. Phys. 38, 781 (1963).
44. Gerald W. King, J. Sci. Instr. 35, 11 (1958).
45. H. J. Bernstein and G. Herzberg, J. Chem. Phys. 16, 30 (1948).
46. G. R. Harrison, ed., "M.I.T. Wavelength Tables", The M.I.T. Press, Cambridge, Massachusetts. (1963)
47. B. Edlén, J. Opt. Soc. Amer. 43, 339 (1953).
48. G. W. Robinson, in L. Marton: "Methods of Experimental Physics Vol. 3", section 2.4.2.4.2., Academic Press, New York, (1962).
49. Gerald W. King, "Spectroscopy and Molecular Structure", Holt, Rinehart and Winston, Inc., Toronto, (1964) Chapter 7.

50. M. Tinkham, "Group Theory and Quantum Mechanics" McGraw-Hill Book Co., Inc., New York, (1964).
51. R. S. Mulliken, J. Chem. Phys. 3, 564 (1935).
52. M. Kasha, Disc. Faraday Soc. 9, 14 (1950).
53. J. R. Platt, J. Chem. Phys. 19, 101 (1951).
54. M. A. El Sayed and G. W. Robinson, Mol. Phys. 4, 273 (1961).
55. H. E. White, "Introduction to Atomic Spectra", McGraw-Hill Book Co., Inc., New York (1934), p. 90.
56. J. C. D. Brand, J. Chem. Soc. 858 (1956).
57. W. T. Raynes, J. Chem. Phys. 44, 2755 (1966).
58. J. C. D. Brand, J. H. Callomon and J. K. G. Watson, Disc. Faraday Soc. 35, 175 (1963).
59. Gerald W. King and D. C. Moule, J. Mol. Spectry 20, 331 (1966).
60. J. C. D. Brand, Trans. Faraday Soc. 50, 431 (1954).
61. W. H. Eberhardt and H. Renner, J. Mol. Spectry 6, 483 (1961).
62. J. W. Sidman and D. S. McClure, J. Amer. Chem. Soc. 77, 6461 (1955).
63. J. A. Pople, Proc. Phys. Soc. 68A, 81 (1955).
64. C. C. J. Roothaan, Rev. Mod. Phys. 23, 69 (1951).
65. Y. Kanda, H. Kaseda and T. Matumura, Spectrochim. Acta 20, 1387 (1964).
66. R. F. Borkman and D. R. Kearns, J. Chem. Phys. 46, 2333 (1967).
67. A. D. Walsh, Trans. Faraday Soc. 42, 66 (1946).
68. V. R. Ells, J. Amer. Chem. Soc. 60, 1864 (1938).
69. I. Zanon, G. Giacometti and D. Picciol, Spectrochim. Acta 19, 301 (1963).

70. J. R. Lombardi, D. Campbell and W. Klemperer, J. Chem. Phys. 46, 3482 (1967).
71. M. Adelhelm, Private communication, (1967).
72. J. Franck, Trans. Faraday Soc. 21, 536 (1925-26).
73. E. U. Condon, Phys. Rev. 28, 1182 (1926); 32, 858 (1928).
74. D. P. Craig, J. Chem. Soc. 2146 (1950).
75. C. K. Ingold and Gerald W. King, J. Chem. Soc. 2725 (1963).
76. J. A. Howe and J. H. Goldstein, J. Amer. Chem. Soc. 80, 4846 (1958).
77. C. H. D. Clark, Phys. Rev. 47, 238 (1938).
78. R. M. Badger, J. Chem. Phys. 2, 128 (1934); 3, 710 (1935).
79. E. M. Layton, Jr., R. D. Kross and V. A. Fassel, J. Chem. Phys. 25, 135 (1956).
80. J. C. D. Brand and D. G. Williamson, Disc. Faraday Soc. 35, 184 (1963).
81. J. M. Hollas, Spectrochim. Acta 19, 1425 (1963).
82. J. C. D. Brand and J. K. G. Watson, reported in J. Mol. Spectry 10, 166 (1963).
83. J. C. D. Brand, J. H. Callomon, D. C. Moule, J. Tyrrell and T. H. Goodwin, Trans. Faraday Soc. 61, 2365 (1965).
84. A. O. Nier and E. E. Hanson, Phys. Rev. 50, 722 (1936).
85. R. K. Harris, Spectrochim. Acta 20, 1129 (1964).
86. J. M. Hollas, Spectrochim. Acta 20, 1563 (1964).
87. I. G. Ross, J. M. Hollas and K. K. Innes, J. Mol. Spectry 20, 312 (1966).
88. B. S. Ray, Z. Physik 78, 74 (1932).
89. G. Herzberg and E. Teller, Z. physik. Chem. B21, 410 (1933).

90. H. Spöner and E. Teller, Rev. Mod. Phys. 13, 75 (1941).
91. R. K. Harris and R. E. Witkowski, Spectrochim. Acta 20, 1651 (1964).
92. J. L. Hencher, Ph.D. Thesis, McMaster University (1964), Chapter 5.
93. J. B. Coon, R. E. DeWames, and C. M. Loyd, J. Mol. Spectry 8, 285 (1962).
94. G. W. Robinson and V. E. DiGiorgio, Can. J. Chem. 36, 31 (1958).
95. D. S. McClure, J. Chem. Phys. 17, 665 (1949).
96. D. A. Ramsay and J. Tyrrell, private communication, (1967).
97. W. G. Fateley, R. K. Harris, F. A. Miller and R. E. Witkowski, Spectrochim. Acta 21, 231 (1965).
98. K. S. Pitzer, J. Chem. Phys. 14, 239 (1946).
99. J. O. Hirschfelder, J. Chem. Phys. 8, 431 (1940).
100. Gilbert W. King, R. M. Hainer and P. C. Cross, J. Chem. Phys. 11, 27 (1943).
101. J. M. Bennett, I. G. Ross and E. J. Wells, J. Mol. Spectry 4, 342 (1960).
102. E. K. Gora, J. Mol. Spectry 2, 259 (1958).
103. G. Herzberg, "Molecular Spectra and Molecular Structure, II Infrared and Raman Spectra of Polyatomic Molecules", Van Nostrand, Inc., Princeton, N. J., (1945) pp. 422 and 426.
104. J. E. Parkin, J. Mol. Spectry 15, 483 (1965).
105. J. Christoffersen and J. M. Hollas, private communication (1966).
106. H. C. Allen and P. C. Cross, "Molecular Vibrators", Wiley and Sons, Inc., New York, (1963).
107. D. E. Milligan, M. E. Jacox, A. M. Bass, J. J. Comeford, and D. E. Mann, J. Chem. Phys. 42, 3187 (1965).
108. E. A. Cherniak and C. C. Costain, J. Chem. Phys. 45, 104 (1966).

APPENDIX

TABLE A.1

THE OBSERVED BAND HEADS OF THE ${}^1A_u \leftarrow {}^1A_g$
SYSTEM OF $(CO^{35}Cl)_2$.

The intensities of all bands not assigned in Table 5.1 are extremely weak unless otherwise specified.

| Frequency (cm^{-1} vac.) | Frequency (cm^{-1} vac.) | Frequency (cm^{-1} vac.) | Frequency (cm^{-1} vac.) |
|--------------------------------|--------------------------------|--------------------------------|--------------------------------|
| 25405.6 | 25962.0 | 26 250.0 | 26 450.1 |
| 484.6 | 971.8 | 257.3 | 477.4 |
| 519.2 | 985.0 vw | 263.0 | 543.8 |
| 535.7 | 992.9 vw | 273.1 | 576.8 |
| 566.9 | 26007.2 | 287.0 | 589.8 |
| 760.6 w | 011.3 | 292.0 | 596.6 vw |
| 862.9 | 054.7 | 307.5 | 605.3 |
| 893.0 | 087.5 | 318.3 | 628.7 |
| 911.4 | 093.4 | 327.9 | 634.5 w |
| 925.2 vw | 095.2 | 352.7 | 643.0 |
| 925.7 vw | 107.8 | 360.2 | 652.7 |
| 934.0 | 108.5 | 370.4 | 672.0 |
| 937.0 | 139.0 | 406.8 | 678.3 |
| 940.5 | 178.6 | 414.2 | 684.8 mw |
| 943.8 | 236.6 | 447.6 | 690.4 |

| | | | |
|-------------|----------|----------|--------|
| 26 705.8 vw | 27 170.0 | 27 617.6 | 28 292 |
| 711.4 | 177.1 | 624.5 | 505 s |
| 722.7 | 182.8 | 663.9 | 597 |
| 751.0 | 188.9 | 724.5 | 649 |
| 767.7 vw | 220.5 | 728.6 vw | 662 |
| 769.2 | 252.8 | 739.9 | 728 |
| 783.7 | 267.3 | 750.1 | 736 |
| 802.5 | 299.6 | 757.7 | 802 |
| 842.9 | 316.2 | 808.1 | 845 |
| 848.2 | 335.7 w | 815.3 | 896 |
| 883.1 | 345.7 | 854.0 | 924 |
| 890.7 | 364.7 | 864.3 | 929 |
| 896.4 | 387.6 | 871.9 | 968 |
| 905.9 | 392.5 | 947.3 | 999 |
| 924 | 418.0 | 985.3 | 29009 |
| 966.1 vw | 423.2 | 28061.9 | 041 |
| 973.8 | 468.4 | 100 | 060 |
| 27012.1 | 470.7 | 112 | 125 |
| 051.6 | 499.3 | 131 | 203 |
| 088.6 | 503.2 | 144 | 271 |
| 104.3 | 540.9 vw | 159 | 280 |
| 126.5 | 545.1 vw | 172 | 410 |
| 137.8 | 547.6 | 212 | 473 |
| 142.3 vw | 564.4 | 239 | 551 vw |
| 153.4 | 575.9 | 258 mw | 602 |
| 165.3 | 587.4 | 263 m | 675 |

29727 31765

810 32910

891

997

30038 vw

084

162

237

274

356

432

482

543

612 w

706

793

874

958

31011

088

138 mw

213

447

488

561

633

TABLE A.2

THE OBSERVED BAND HEADS OF THE ${}^1A_u \leftarrow {}^1A_g$
SYSTEM OF OXALYL BROMIDE

The intensities of bands not assigned in Table 5.2 are very weak unless otherwise specified.

| Frequency (cm^{-1} vac.) | Frequency (cm^{-1} vac.) | Frequency (cm^{-1} vac.) | Frequency (cm^{-1} vac.) |
|---------------------------------------|---------------------------------------|---------------------------------------|---------------------------------------|
| 23571.0 | 25020 | 25371 | 25847 |
| 602.2 | 028 | 403 | 914 |
| 640.7 | 047 vw | 436 | 925 |
| 750.3 | 067 | 470 | 952 |
| 865.4 | 100 vw | 475 | 960 |
| 24254.3 | 129 | 493 w | 992 |
| 286.4 | 142 | 502 | 26024 |
| 316.3 | 158 | 536 | 061 |
| 435.9 | 172 | 551 | 145 w |
| 552 | 185 | 568 | 168 |
| 763 | 199 w | 600 | 214 mw |
| 858 | 216 mw | 616 | 250 mw |
| 886 vw | 227 | 667 | 285 |
| 930 | 304 | 700 | 324 |
| 961 | 321 | 735 | 398 |
| 998 | 337 mw | 780 | 432 |

| | | |
|--------|-------|-------|
| 26468 | 27927 | 29930 |
| 501 | 983 | 959 |
| 532 | 28048 | 30020 |
| 566 | 160 | 067 |
| 657 | 289 | 140 |
| 698 m | 330 | 196 |
| 724 | 353 | 259 |
| 777 | 412 | 297 w |
| 845 w | 451 | 31351 |
| 865 ms | 478 | 419 |
| 886 w | 519 | |
| 909 | 545 | |
| 944 | 592 | |
| 979 | 655 | |
| 27087 | 707 | |
| 158 | 757 | |
| 216 | 777 | |
| 255 | 821 | |
| 282 | 883 | |
| 314 | 960 | |
| 347 | 29026 | |
| 389 | 364 | |
| 462 | 460 | |
| 519 | 784 | |
| 795 | 842 w | |
| 861 | 895 | |

TABLE A.3

THE OBSERVED BAND HEADS OF THE ${}^1A_u \leftarrow {}^1A_g$
SYSTEM OF OXALYL FLUORIDE.

Most measurements refer to the Q branch head. (See Figure 7.5) However, in bands to high frequencies, the R heads are intense and it is often difficult to locate the Q heads accurately. In such cases the R heads are listed, denoted by an asterisk.

| Frequency (cm^{-1} vac.) | Frequency (cm^{-1} vac.) | Frequency (cm^{-1} vac.) | Frequency (cm^{-1} vac.) |
|---------------------------------------|---------------------------------------|---------------------------------------|---------------------------------------|
| 31526.4 | 31841.6 | 32272.1 | 32572.5 |
| 530.8 | 923.7 | 278.6 | 598.0 |
| 556.5 | 934.4 | 310.7 <i>mw</i> | 627.3 |
| 601.1 | 32012.3 | 328.2 | 638.6 |
| 609.5 | 019.8 | 358.1 | 652.2 |
| 643.3 | 091.4 | 403.5 | 683.1 |
| 655.0 | 112.6 | 445.0 | 712.2 |
| 698.0 | 123.5 | 456.2 | 724.2* |
| 740.3 | 126.9 | 500.4 | 725.5* |
| 753.6 | 173.8 | 519.4 | 727.8 |
| 797.6 | 213.1 | 542.0 | 735.2 |
| 837.2 | 225.8 | 553.8 | 744.9 |

| | | | |
|----------|---------|----------|-----------|
| 32773.0 | 33100.7 | 33420.1* | 33828.0 |
| 794.9 | 105.6 m | 427.3* | 852.4 m |
| 815.3 | 111.2 | 433.1 | 885.2 |
| 831.5 | 155.3 | 440.7* | 895.7 |
| 839.0 w | 158.7* | 452.7* | 929.3 mw |
| 866.0 | 167.5 | 491.7 | 982.2 |
| 874.3 | 177.9 | 500.9* | 996.8 |
| 888.1 | 189.9* | 521.4 | continuum |
| 895.5* | 199.5* | 546.1* | |
| 907.8 | 219.8* | 552.2* | |
| 912.9* | 243.3* | 590.9 | |
| 917.0 | 249.0 | -- + | |
| 919.2 | 252.5* | 625.9 | |
| 931.4 | 257.7 | 631.3 w | |
| 976.4 | 264.3* | 634.9 w | |
| 996.9 | 280.0 | 638.9 | |
| 33002.1* | 287.9* | 643.8 | |
| 003.8 | 326.7 | 665.3 mw | |
| 010.9 mw | 335.3* | 666.2 mw | |
| 030.1 | 345.4 | 681.7 | |
| 055.9 | 352.9* | 687.8 | |
| 065.2* | 355.2 | 723.6 mw | |
| 071.8 | 359.1* | 755.9 w | |
| 077.8* | 373.4 | 810.6 mw | |
| 081.2* | 376.8* | 823.5 | |
| 096.6 | | | |

+ The spectrum is extremely complex beyond this point; only the stronger, less diffuse bands are listed.

TABLE A.4

THE OBSERVED BAND HEADS OF THE ${}^1A'' \leftarrow {}^1A'$
SYSTEM OF OXALYL CHLORIDE FLUORIDE.

| Frequency (cm^{-1} vac.) | Frequency (cm^{-1} vac.) | Frequency (cm^{-1} vac.) | Frequency (cm^{-1} vac.) |
|---------------------------------------|---------------------------------------|---------------------------------------|---------------------------------------|
| 28098 | 28 747 | 29183 | 29540 mw |
| 183 | 808 | 212 w | 562 |
| 269 | 832 | 229 | 582 |
| 279 | 866 | 267 | 599 |
| 298 | 893 | 281 | 620 ms |
| 333 | 904 | 314 | 636 |
| 375 | 927 | 316 w | 701 mw |
| 414 | 959 | 319 mw | 715 |
| 434 | 989 | 324 | 742 |
| 460 | 29001 | 340 | 761 |
| 506 | 024 | 354 | 800 |
| 514 | 042 | 366 | 835 |
| 518 | 073 | 380 | 939 mw |
| 519 | 086 | 385 | 30004 |
| 556 | 108 | 401 w | 089 |
| 610 | 125 w | 421 | 174 |
| 655 w | 143 | 440 w | 199 |
| 724 | 158 | 462 mw | 249 mw |
| 738 | 170 | 489 w | 282 |

30355 ms

366

404

437 ms

477

489

509 mw

538 mw

561

578 m

667 ms

680

698 m

724 m

770 m

806 (vb) s

892 (vb) s

31112

195

275

357

~ 32360

~ 530

TABLE A.5

THE OBSERVED BAND HEADS OF THE ${}^3A_u \leftarrow {}^1A_g$
SYSTEM OF $(CO^{35}Cl)_2$.

The intensities of all bands not listed in Table 6.2
are extremely weak unless otherwise noted.

| Frequency (cm^{-1} vac.) | Frequency (cm^{-1} vac.) | Frequency (cm^{-1} vac.) | Frequency (cm^{-1} vac.) |
|--------------------------------|--------------------------------|--------------------------------|--------------------------------|
| 24201.2 | 24370.2 | 24574.7 | 24785.5 |
| 218.7 | 378.9 | 583.0 | 794.6 |
| 223.9 | 393.3 w | 616.9 | 797.4 |
| 232.2 | 401.6 | 651.3 | 801.9 |
| 253.3 | 408.1 w | 661.5 | 806.0 |
| 266.8 | 414.0 w | 670.5 | 838.9 |
| 276.7 | 417.6 | 682.2 | 848.8 |
| 290.1 | 435.6 | 693.9 | 852.5 |
| 299.1 | 448.5 | 696.3 | 863.3 |
| 312.0 | 458.4 | 698.7 | 880.0 |
| 316.1 w | 480.5 | 728.5 | 883.0 |
| 323.2 mw | 498.2 | 735.5 | 896.4 |
| 330.2 | 514.1 | 739.8 | 925.6 |
| 333.8 | 526.6 | 760.9 | 928.7 |
| 356.5 | 559.4 | 771.3 | 932.5 |
| 359.1 | 566.4 | 777.0 | 940.2 w |

| | | |
|---------|---------|-----------|
| 24956.1 | 25210.9 | 25660.1 w |
| 959.5 | 214.4 | 667.5 w |
| 970.6 | 233.8 | 677.0 |
| 985.4 | 248.6 | 692.6 w |
| 991.8 | 276.4 | 714.4 w |
| 25000.2 | 277.9 | 749.3 |
| 004.8 | 290.1 | 795.7 |
| 010.3 | 323.4 | 877.7 |
| 012.8 | 333.4 | 26158.8 |
| 017.6 | 350.6 | 275.0 |
| 030.4 | 361.0 w | |
| 036.6 | 366.2 | |
| 051.6 | 395.9 w | |
| 061.8 | 398.4 | |
| 080.6 | 430.8 | |
| 108.6 | 445.0 | |
| 113.3 | 469.5 | |
| 126.7 | 473.1 | |
| 130.9 | 519.2 | |
| 138.2 | 543.7 | |
| 156.2 | 548.1 | |
| 156.8 | 593.2 w | |
| 171.3 | 617.6 | |
| 201.5 | 628.7 | |
| 202.0 | 640.9 w | |

TABLE A.6

THE OBSERVED BAND HEADS OF THE ${}^3A_u \leftarrow {}^1A_g$
SYSTEM OF OXALYL BROMIDE

The intensities of all bands not assigned in Table 6.3 are very weak unless otherwise specified.

| Frequency (cm^{-1} vac.) | Frequency (cm^{-1} vac.) | Frequency (cm^{-1} vac.) | Frequency (cm^{-1} vac.) |
|---------------------------------------|---------------------------------------|---------------------------------------|---------------------------------------|
| 22368 | 22855.3 | 23049.1 | 23347.0 |
| 413.7 | 863.5 | 065.2 | 359.1 |
| 497 | 872.0 | 066.6 | 364.8 |
| 587.0 | 885.2 | 098.6 | 379.3 |
| 602.7 | 893.7 | 123.9 | 385.0 |
| 633.7 | 898.1 | 156.9 | 412 |
| 646.4 | 910.8 m | 163.6 | 436 |
| 652 | 938.0 | 187.7 | 447 mw |
| 677.7 | 969.5 | 205.0 | 473 m |
| 706.3 | 974.8 | 220.2 | 512.2 |
| 726.0 | 980.1 | 226.9 | 516.6 w |
| 752.7 | 23002.6 | 250.3 | 531.4 |
| 782.2 | 004.4 m | 281.5 | 539.8 w |
| 789.2 | 034.3 | 289.8 | 563.7 |
| 819.8 | 041.2 | 313.3 | 579.9 |

| | | |
|---------|---------|---------|
| 23611.8 | 24004.2 | 24359.1 |
| 651.5 | 030.7 | 397.8 |
| 684.3 | 035.0 | 428.3 |
| 689.1 | 037.7 | 441.9 w |
| 697.3 | 042.0 | 475.2 |
| 722.8 | 067 | 506.7 |
| 756.3 | 083.9 | 539.6 |
| 763.1 | 107.9 | 571.3 |
| 780.5 | 118.4 | 581 |
| 788.7 | 128.0 | 603.4 |
| 792.0 | 153.2 | 624.8 |
| 814.4 | 162.0 | 637.2 |
| 834.1 | 163.9 | 660 |
| 846.1 w | 178.3 | 670 |
| 855.4 | 199.6 | 700 |
| 887.6 | 211.8 | 726 mw |
| 903.9 | 216.9 | 731 |
| 921.9 | 222.0 | 738 m |
| 927.0 | 236.3 | 783 |
| 940.9 | 246.3 | |
| 958.7 | 250.0 | |
| 971.3 | 270.5 | |
| 974.6 | 289.4 | |
| 984.2 | 303.6 | |
| 997.3 | 328.8 | |

TABLE A.7

THE OBSERVED BAND HEADS OF THE ${}^3A_u \leftarrow {}^1A_g$
SYSTEM OF OXALYL FLUORIDE.

Under low resolution, (70,000; Bausch and Lomb spectrograph), the spectral bands of the singlet-triplet system of oxalyl fluoride appear almost atomic in sharpness. At a resolving power of 300,000, it is seen that the bands are degraded towards the red and form an intense head on the high energy side. Most bands show a second weak, red-degraded head about 14-17 cm^{-1} to higher frequencies of the intense head. These may be part of the rotational structure of the band or, alternatively, due to sequences. Both heads are included in the table. Rotational features, resulting from a super-position of rotational lines and which are not heads in the true sense, are not listed.

| Frequency (cm^{-1} vac.) | Frequency (cm^{-1} vac.) | Frequency (cm^{-1} vac.) | Frequency (cm^{-1} vac.) |
|---------------------------------------|---------------------------------------|---------------------------------------|---------------------------------------|
| 29081.3 | 29489.2 | 29681.1 | 29779.4 |
| 139.0 | 527.7 | 689.2 | 785.0 |
| 321.2 | 566.3 w | 705.8 | 802.2 |
| 398.8 w | 626.3 | 713.3 | 805.0 |
| 416.5 | 654.7 | 770.8 | 813.9 |

| | | | |
|-----------|---------|---------|----------|
| 29827.3 w | 30152.6 | 30528.4 | 30 954.9 |
| 839.4 w | 160.0 | 539.4 | 979.9 |
| 843.0 | 176.5 | 552.8 | 992.0 |
| 854.7 mw | 184.1 | 574.1 | 31020.4 |
| 862.0 mw | 198.6 | 578.8 w | 035.7 |
| 863.7 | 229.8 | 586.6 | 088.3 |
| 882.7 | 243.7 | 600.9 | 183.5 |
| 888.9 | 247.9 | 613.3 | 272.3 w |
| 907.3 mw | 253.7 | 624.2 | 283.3 |
| 911.5 | 284.9 w | 629.4 | 293.3 w |
| 941.9 | 298.0 | 638.3 | 302.3 mw |
| 956.7 | 306.7 | 653.5 | 350.7 |
| 966.2 | 329.3 | 674.3 | 391.1 mw |
| 977.3 | 330.7 | 711.3 | 393.1 mw |
| 985.8 | 354.7 | 739.9 | 437.2 |
| 992.5 | 381.4 | 771.8 | 457.2 m |
| 999.4 | 398.1 | 779.6 | 473.0 |
| 30012.1 | 410.8 w | 809.4 | 530.8 |
| 042.4 | 428.7 | 821.3 | 685.2 |
| 047.2 | 433.1 m | 825.5 | 722.5 |
| 058.6 | 450.6 | 844.1 | 815.9 |
| 068.3 | 467.7 | 855.6 | |
| 080.8 | 476.3 | 862.4 | |
| 133.5 | 499.7 | 907.9 | |
| 143.1 | 515.2 | 926.3 | |

TABLE A.8

LINE STRENGTHS FOR ASYMMETRIC ROTOR TRANSITIONS

| Symmetric Limit | J | Sym. | REM | d |
|-----------------|---|------|----------------|---|
| prolate | 2 | ee | E ⁺ | $[1+3(\kappa+1)^2/(\kappa-3)^2]^{-1/2}$ |
| | 3 | oo | O ⁺ | $[1+15(\kappa+1)^2/(15-\kappa)^2]^{-1/2}$ |
| | 3 | eo | E ⁺ | $[1+15(\kappa+1)^2/(3-\kappa)^2]^{-1/2}$ |
| | 3 | oe | O ⁻ | $[1+15(\kappa+1)^2/(9-7\kappa)^2]^{-1/2}$ |
| oblate | 2 | ee | E ⁺ | $[1+3(\kappa-1)^2/(\kappa+3)^2]^{-1/2}$ |
| | 3 | oo | O ⁻ | $[1+15(\kappa-1)^2/(15+\kappa)^2]^{-1/2}$ |
| | 3 | eo | O ⁺ | $[1+15(\kappa-1)^2/(9+7\kappa)^2]^{-1/2}$ |
| | 3 | oe | E ⁺ | $[1+15(\kappa-1)^2/(3+\kappa)^2]^{-1/2}$ |

REM = Reduced Energy Matrix

κ = asymmetry parameter

d = Gora's d-parameter¹⁰² used in the intensity expressions contained in the following pages.

| G.S. | E.S. | LINE STRENGTH, $(\phi^A)^2$, FOR NEAR-PROLATE A-TYPE BAND |
|----------|----------|--|
| 0_{00} | 1_{01} | 1 |
| 1_{01} | 2_{02} | $1+d'$ |
| 1_{11} | 1_{10} | $3/2$ |
| 1_{11} | 2_{12} | $3/2$ |
| 1_{10} | 2_{11} | $3/2$ |
| 2_{02} | 3_{03} | $\{ [5/12(1-d')(1-d'')]^{1/2} + [3/4(1+d')(1+d'')]^{1/2} \}^2$ |
| 2_{12} | 2_{11} | $5/6$ |
| 2_{12} | 3_{13} | $4/3(1+d')$ |
| 2_{11} | 3_{12} | $4/3(1+d')$ |
| 2_{21} | 2_{20} | $5/3(1+d')$ |
| 2_{21} | 3_{22} | $5/3$ |
| 2_{20} | 3_{21} | $1/12 \{ [5(1+d')(1+d'')]^{1/2} + [9(1-d')(1-d'')]^{1/2} \}^2$ |

| G.S. | E.S. | LINE STRENGTH, $(\phi^A)^2$, FOR NEAR PROLATE B-TYPE BAND |
|----------|----------|--|
| 0_{00} | 1_{11} | 1 |
| 1_{01} | 1_{10} | $3/2$ |
| 1_{01} | 2_{12} | $3/2$ |
| 1_{11} | 2_{02} | $1/8 \{ [6(1-d')]^{1/2} + [2(1+d')]^{1/2} \}^2$ |
| 1_{11} | 2_{20} | $1/8 \{ [6(1+d')]^{1/2} - [2(1-d')]^{1/2} \}^2$ |
| 1_{10} | 2_{21} | $3/2$ |
| 2_{02} | 2_{11} | $5/24 \{ [6(1+d'')]^{1/2} - [2(1-d'')]^{1/2} \}^2$ |
| 2_{02} | 3_{13} | $1/24 \{ [12(1+d')(1+d'')]^{1/2} + [(1+d')(1-d'')]^{1/2} + [15(1-d')(1-d'')]^{1/2} \}^2$ |
| 2_{12} | 2_{21} | $5/6$ |
| 2_{12} | 3_{03} | $1/12 \{ [6(1+d')]^{1/2} + [10(1-d')]^{1/2} \}^2$ |
| 2_{11} | 2_{20} | $5/24 \{ [2(1+d')]^{1/2} - [6(1-d')]^{1/2} \}^2$ |
| 2_{11} | 3_{22} | $5/3$ |
| 2_{12} | 3_{21} | $1/12 \{ [6(1-d')]^{1/2} - [10(1+d')]^{1/2} \}^2$ |
| 2_{21} | 3_{12} | $1/12 \{ (1+d')^{1/2} + [15(1-d')]^{1/2} \}^2$ |
| 2_{21} | 3_{30} | $1/12 \{ (1-d')^{1/2} - [15(1+d')]^{1/2} \}^2$ |
| 2_{20} | 3_{13} | $1/24 \{ [12(1+d')(1-d'')]^{1/2} - [(1+d')(1+d'')]^{1/2} - [15(1-d')(1+d'')]^{1/2} \}^2$ |
| 2_{20} | 3_{31} | $1/24 \{ [15(1+d')(1+d'')]^{1/2} - [(1-d')(1+d'')]^{1/2} + [12(1-d')(1-d'')]^{1/2} \}^2$ |

| G.S. | E.S. | LINE STRENGTH, $(\phi^A)^2$, FOR NEAR PROLATE C-TYPE BAND |
|-----------------|-----------------|--|
| 0 ₀₀ | 1 ₁₀ | 1 |
| 1 ₀₁ | 1 ₁₁ | 3/2 |
| 1 ₀₁ | 2 ₁₁ | 3/2 |
| 1 ₁₁ | 2 ₂₁ | 3/2 |
| 1 ₁₀ | 2 ₀₂ | $1/4 \{ [3(1-d')]^{1/2} - (1+d')^{1/2} \}^2$ |
| 1 ₁₀ | 2 ₂₀ | $1/4 \{ [3(1+d')]^{1/2} + (1-d')^{1/2} \}^2$ |
| 2 ₀₂ | 2 ₁₂ | $5/24 \{ [6(1+d'')]^{1/2} + [2(1-d'')]^{1/2} \}^2$ |
| 2 ₀₂ | 3 ₁₂ | $1/24 \{ [12(1+d')(1+d'')]^{1/2} + [15(1-d')(1-d'')]^{1/2} - [(1+d')(1-d'')]^{1/2} \}^2$ |
| 2 ₁₂ | 2 ₂₀ | $5/24 \{ [2(1+d')]^{1/2} - [6(1-d')]^{1/2} \}^2$ |
| 2 ₁₂ | 3 ₂₂ | 5/3 |
| 2 ₁₁ | 2 ₂₁ | 5/6 |
| 2 ₁₁ | 3 ₀₃ | $1/6 \{ [3(1+d')]^{1/2} - [5(1-d')]^{1/2} \}^2$ |
| 2 ₁₁ | 3 ₂₁ | $1/6 \{ [5(1+d')]^{1/2} + [3(1-d')]^{1/2} \}^2$ |
| 2 ₂₁ | 3 ₁₃ | $1/12 \{ (1+d')^{1/2} - [15(1-d')]^{1/2} \}^2$ |
| 2 ₂₁ | 3 ₃₁ | $1/12 \{ [15(1+d')]^{1/2} + (1-d')^{1/2} \}^2$ |
| 2 ₂₀ | 3 ₁₂ | $1/24 \{ [(1+d')(1+d'')]^{1/2} + [12(1+d')(1-d'')]^{1/2} - [15(1-d')(1+d'')]^{1/2} \}^2$ |
| 2 ₂₀ | 3 ₃₀ | $1/24 \{ [15(1+d')(1+d'')]^{1/2} + [(1-d')(1+d'')]^{1/2} + [12(1-d')(1-d'')]^{1/2} \}^2$ |

| G.S. | E.S. | LINE STRENGTH, $(\phi^A)^2$, FOR NEAR OBLATE A-TYPE BAND |
|-----------------|-----------------|--|
| 0 ₀₀ | 1 ₀₁ | 1 |
| 1 ₀₁ | 2 ₀₂ | $1/4 \{ [3(1+d')]^{1/2} + (1-d')^{1/2} \}^2$ |
| 1 ₀₁ | 2 ₂₀ | $1/4 \{ (1+d')^{1/2} - [3(1-d')]^{1/2} \}^2$ |
| 1 ₁₁ | 2 ₁₂ | 3/2 |
| 1 ₁₁ | 1 ₁₀ | 3/2 |
| 1 ₁₀ | 2 ₁₁ | 3/2 |
| 2 ₀₂ | 2 ₂₁ | $5/12 \{ (1+d'')^{1/2} - [3(1-d'')]^{1/2} \}^2$ |
| 2 ₀₂ | 3 ₀₃ | $1/24 \{ [15(1+d')(1+d'')]^{1/2} + [(1-d')(1+d'')]^{1/2} + [12(1-d')(1-d'')]^{1/2} \}^2$ |
| 2 ₀₂ | 3 ₂₁ | $1/24 \{ [(1+d')(1+d'')]^{1/2} + [12(1+d')(1-d'')]^{1/2} - [15(1-d')(1+d'')]^{1/2} \}^2$ |
| 2 ₁₂ | 2 ₁₁ | 5/6 |
| 2 ₁₂ | 3 ₃₁ | $1/12 \{ (1+d')^{1/2} - [15(1-d')]^{1/2} \}^2$ |
| 2 ₁₂ | 3 ₁₃ | $1/12 \{ [15(1+d')]^{1/2} + (1-d')^{1/2} \}^2$ |
| 2 ₁₁ | 3 ₁₂ | $1/6 \{ [5(1+d')]^{1/2} + [3(1-d')]^{1/2} \}^2$ |
| 2 ₁₁ | 3 ₃₀ | $1/6 \{ [3(1+d')]^{1/2} - [5(1-d')]^{1/2} \}^2$ |
| 2 ₂₁ | 2 ₂₀ | $5/12 \{ [3(1+d')]^{1/2} + (1-d')^{1/2} \}^2$ |
| 2 ₂₁ | 3 ₂₂ | 5/3 |
| 2 ₂₀ | 3 ₀₃ | $1/24 \{ [12(1-d')(1+d'')]^{1/2} - [15(1+d')(1-d'')]^{1/2} - [(1-d')(1-d'')]^{1/2} \}^2$ |
| 2 ₂₀ | 3 ₂₁ | $1/24 \{ [12(1+d')(1+d'')]^{1/2} - [(1+d')(1-d'')]^{1/2} + [15(1-d')(1-d'')]^{1/2} \}^2$ |

| G.S. | E.S. | LINE STRENGTH, $(\phi^A)^2$, FOR NEAR OBLATE B-TYPE BAND |
|-----------------|-----------------|--|
| 0 ₀₀ | 1 ₁₁ | 1 |
| 1 ₀₁ | 1 ₁₀ | 3/2 |
| 1 ₀₁ | 2 ₁₂ | 3/2 |
| 1 ₁₁ | 2 ₀₂ | $1/4 \{ [3(1+d')]^{1/2} - (1-d')^{1/2} \}^2$ |
| 1 ₁₁ | 2 ₂₀ | $1/4 \{ (1+d')^{1/2} + [3(1-d')]^{1/2} \}^2$ |
| 1 ₁₀ | 2 ₂₁ | 3/2 |
| 2 ₀₂ | 2 ₁₁ | $5/12 \{ (1+d'')^{1/2} + [3(1-d'')]^{1/2} \}^2$ |
| 2 ₀₂ | 3 ₁₃ | $1/24 \{ [15(1+d')(1+d'')]^{1/2} + [12(1-d')(1-d'')]^{1/2} - [(1-d')(1+d'')]^{1/2} \}^2$ |
| 2 ₀₂ | 3 ₃₁ | $1/24 \{ [(1+d')(1+d'')]^{1/2} + [15(1-d')(1+d'')]^{1/2} - [12(1+d')(1-d'')]^{1/2} \}^2$ |
| 2 ₁₂ | 2 ₂₁ | 5/6 |
| 2 ₁₂ | 3 ₀₃ | $1/12 \{ [15(1+d')]^{1/2} - (1-d')^{1/2} \}^2$ |
| 2 ₁₂ | 3 ₂₁ | $1/12 \{ (1+d')^{1/2} + [15(1-d')]^{1/2} \}^2$ |
| 2 ₁₁ | 2 ₂₀ | $5/12 \{ [3(1+d')]^{1/2} - (1-d')^{1/2} \}^2$ |
| 2 ₁₁ | 3 ₂₂ | 5/3 |
| 2 ₂₁ | 3 ₁₂ | $1/6 \{ [5(1+d')]^{1/2} - [3(1-d')]^{1/2} \}^2$ |
| 2 ₂₁ | 3 ₃₀ | $1/6 \{ [3(1+d')]^{1/2} + [5(1-d')]^{1/2} \}^2$ |
| 2 ₂₀ | 3 ₁₃ | $1/24 \{ [15(1+d')(1-d'')]^{1/2} - [12(1-d')(1+d'')]^{1/2} - [(1-d')(1-d'')]^{1/2} \}^2$ |
| 2 ₂₀ | 3 ₃₁ | $1/24 \{ [12(1+d')(1+d'')]^{1/2} + [(1+d')(1-d'')]^{1/2} + [15(1-d')(1-d'')]^{1/2} \}^2$ |

| G.S. | E.S. | LINE STRENGTH, $(\phi^A)^2$, FOR NEAR OBLATE C-TYPE BAND |
|-----------------|-----------------|---|
| 0 ₀₀ | 1 ₁₀ | 1 |
| 1 ₀₁ | 1 ₁₁ | 3/2 |
| 1 ₀₁ | 2 ₁₁ | 3/2 |
| 1 ₁₁ | 2 ₂₁ | 3/2 |
| 1 ₁₀ | 2 ₀₂ | 1-d' |
| 1 ₁₀ | 2 ₂₀ | 1+d' |
| 2 ₀₂ | 2 ₁₂ | 5/3(1+d'') |
| 2 ₀₂ | 3 ₁₂ | 1/12 { [5(1+d')(1+d'')] ^{1/2} + [9(1-d')(1-d'')] ^{1/2} } ² |
| 2 ₀₂ | 3 ₃₀ | 1/12 { [9(1+d')(1-d'')] ^{1/2} - [5(1-d')(1+d'')] ^{1/2} } ² |
| 2 ₁₂ | 2 ₂₀ | 5/3(1-d') |
| 2 ₁₂ | 3 ₂₂ | 5/3 |
| 2 ₁₁ | 2 ₂₁ | 5/6 |
| 2 ₁₁ | 3 ₀₃ | 4/3(1-d') |
| 2 ₁₁ | 3 ₂₁ | 4/3(1+d') |
| 2 ₂₁ | 3 ₁₃ | 4/3(1-d') |
| 2 ₂₁ | 3 ₃₁ | 4/3(1+d') |
| 2 ₂₀ | 3 ₁₂ | 1/12 { [9(1-d')(1+d'')] ^{1/2} - [5(1+d')(1-d'')] ^{1/2} } ² |
| 2 ₂₀ | 3 ₃₀ | 1/12 { [9(1+d')(1+d'')] ^{1/2} + [5(1-d')(1-d'')] ^{1/2} } ² |